Title
Heat Recovery at Wastewater Treatment Plants Using Heat Pipe Heat Exchangers

Author
MANDIZADEH, MARZIEH

Publication Date
2018

Peer reviewed|Thesis/dissertation

UNIVERSITY OF CALIFORNIA

Los Angeles

Heat Recovery at Wastewater Treatment Plants Using Heat Pipe Heat Exchangers

A dissertation submitted in partial satisfaction of the requirements for the degree Doctor of Philosophy in Mechanical Engineering

by

Marzieh Mandizadeh

2018

ABSTRACT OF THE DISSERTATION

Heat Recovery at Wastewater Treatment Plants

Using Heat Pipe Heat Exchangers

by

Marzieh Mandizadeh

Doctor of Philosophy in Mechanical Engineering

University of California, Los Angeles, 2018

Professor Adrienne G. Lavine, Co-Chair

and

Professor Michael K. Stenstrom, Co-Chair

An anaerobic digester is a part of a wastewater treatment technology and its role is to digest the wastewaters to treat biosolids. Anaerobic digesters typically operates at either 35°C to 37°C or 45°C, and biosolids must be heated from ambient temperature (10-20°C). To heat the sludge in anaerobic digesters steam injection is used which dilute the sludge and the requirement of electricity to heat steam is not economically favorable. Conventional heat exchangers have been used in wastewater treatment plants (WWTP) but there are many difficulties regarding the maintenance, clogging and cleaning, which discourages their use, especially for heat recovery.

Methane gas (CH_4) is produced in digesters which is combusted and used for heating the buildings. In the case of large WWTPs, combusted methane is also used for power generation; but it is usually combusted to the air. There are largely unused opportunities for heat recovery and it is not practiced due to the low potential heat recovery as well as maintenance problems with heat exchangers.

Heat pipes are an interesting technology and have not been used in WWTPs. In this dissertation heat pipes for wastewater treatment (low temperature heat recovery) and combusted biogas products' applications are evaluated. Then heat pipe heat exchanger (HPHE) is designed and the simulations of heat pipe heat exchanger (HPHE) for different fluid pairs at $C_r<<1$ and $C_r\approx1$ is demonstrated and then compared with a conventional heat exchanger (spiral heat exchanger). Then a method to justify when using HPHE is favorable for any design and application is introduced.

Finally parametric study on the key parameters in the heat pipe design is done and then the heat pipe design is refined to decrease the HPHE length. The last step is HPHE design optimization to shorten the space needed for the designed HPHE.

The dissertation of Marzieh Mandizadeh is approved.

Jennifer A. Jay

Sanjay K. Mohanty

Adrienne G. Lavine, Committee Co-Chair

Michael K. Stenstrom, Committee Co-Chair

University of California, Los Angeles

2018

I would like to dedicate this dissertation to my husband, *Amir* who has been a constant source of support and encouragement during the challenges of graduate school and life. I am truly thankful and lucky for having you in my life.

This work is also dedicated to my little son *Nickon* who motivated me with filling my heart with his pure love, and my newborn baby boy *Yara* who gave me another chance to be a mom, completed our little family and fulfilled our joy.

I would also like to dedicate it to my parents who taught me the first lessons in my life; to work hard for what I aspire to achieve as well as my beautiful sister, *Sara* and my parents in-law who always encouraged me.

Love

Marzieh

TABLE OF CONTENTS

LIST OF FIGURES

LIST OF TABLES

GLOSSARY

COP	Coefficient of Performance
eff	Effective
Eq	Equation
HP	Heat pipe
HPHE	Heat pipe heat exchanger
HTP	Hyperion Treatment Plant
HX	Heat exchanger
WWTP	Wastewater treatment plant

NOMENCLATURE

$A_{s,tot}$	Total surface area
A_v	Vapor cross-sectional area
A_w	Wick cross-sectional area
C	Heat capacity $(\dot{m}c_p)$ (W/K)
C_{min}	Minimum $(\dot{m}c_p)$ in a heat exchanger
C_{max}	Maximum $(\dot{m}c_p)$ in a heat exchanger
c_p	Specific heat constant
C_r	Heat capacity ratio
d_i	Heat pipe inside diameter
d_o	Heat pipe outside diameter
d_v	Heat pipe vapor core diameter
d_{sw}	Screen wire diameter
F_l	Liquid frictional factor
F_v	Vapor frictional factor
f_l	Liquid coefficient of drag
(fRe)	Coefficient of drag for laminar flow in annuli pipe
h_c	Convective heat transfer coefficient in the condenser side of HPHE
h_e	Convective heat transfer coefficient in the evaporator side of HPHE
k_{eff}	Effective thermal conductivity of the liquid-wick combination
k_l	Liquid thermal conductivity
k_p	Thermal conductivity of the heat pipe wall
k_w	Thermal conductivity of the wick
K	Permeability
L_a	Length of the adiabatic region
L_c	Length of the condenser
L_e	Length of the evaporator
L_{eff}	Effective length of the heat pipe

L_{tot}	Overall length of the heat pipe
M_v	Vapor Mach number
$\dot{m}$	Mass flow rate
N	Wire screen mesh number (1/in) or (1/m)
N_L	Number of columns
N_T	Number of rows
NTU	Number of transferred units
Nu	Nusselt number
P_c	Capillary pressure
P_{cm}	Maximum capillary pressure
$\Delta P_{c,max}$	Maximum capillary head along the evaporator
P_l	Liquid pressure
P_v	Vapor pressure
ΔP_{II}	Axial hydrostatic pressure drop
$\Delta P_{\perp}$	Normal hydrostatic pressure drop
Q	Volumetric flow rate (m^3/s)
$q_{b,max}$	Boiling heat transfer rate limit (W)
q	Heat transfer rate (W)
$q_{c,max}$	Maximum capillary heat transfer rate
$(qL)_{c,max}$	Maximum capillary heat transport factor
$q_{e,max}$	Entrainment heat transfer rate limit
q_{limit}	Maximum heat transfer capacity of a heat pipe
$q_{s,max}$	Sonic heat transfer rate limit
R	Thermal resistance
Re	Reynolds number
$Re_{d,max}$	Maximum Reynolds number in bank of tubes
R_c	Resistance of the external flow in the condenser side of HPHE
R_e	Resistance of the external flow in the evaporator side of HPHE
R_{HP}	Total resistance inside a heat pipe

$R_{p,c}$	Thermal resistance of the heat pipe wall at the condenser
$R_{p,e}$	Thermal resistance of the heat pipe wall at the evaporator
R_v	Gas constant of the vapor (in axial heat flux equation in a heat pipe) OR thermal resistance of the vapor flow from the evaporator to the condenser
$R_{w,c}$	Thermal resistance of the liquid-saturated wick at the condenser
$R_{w,e}$	Thermal resistance of the liquid-saturated wick at the evaporator
$R_{tot\,1\,HP}$	Total resistance of one heat pipe in HPHE (external flow resistances are included)
r_c	Effective capillary radius
r_h	Hydraulic radius
$r_{h,l}$	Liquid hydraulic radius
$r_{h,w}$	Hydraulic radius of wick surface pores
r_i	Inner radius of heat pipe $= d_o - (2 \times t_p) - (2 \times t_w)$
r_n	Nucleation site radius
r_o	Outer radius of heat pipe $= d_v + (4 \times t_p) + (2 \times t_w)$
r_v	Vapor space radius $d_v/2$
S	Wick crimping factor OR cylinder-to-cylinder spacing in banks of tubes model
$\tilde{S}$	Dimensionless spacing $\tilde{S} = \frac{S}{d_o}$
S_T	Transverse pitch (m)
S_L	Longitudinal pitch (m)
$T_{c,i}$	Inlet temperature of cold flow (°C or °F)
$T_{c,o}$	Outlet temperature of cold flow (°C or °F)
$T_{h,i}$	Inlet temperature of hot flow (°C or °F)
$T_{h,o}$	Outlet temperature of hot flow (°C or °F)

T_{sat}	Saturation temperature of the liquid
T_v	Temperature of vapor
T_w	Wall temperature
T_∞	Ambient temperature
t_p	Thickness of heat pipe wall
t_{sw}	Screen wire thickness of wrapped screen mesh
t_w	Thickness of wick
U	Heat transfer coefficient
U_s	U_{HP} based on surface area of a heat pipe
(UA)	Thermal conductance
v	Velocity
V	Volume
We	Webber number

Greek Letters:

β	Momentum correction factor
γ_v	Vapor specific ratio
ε	Effectiveness of a heat exchanger OR void fraction
ε_p	Effectiveness of one row of heat pipes in the HPHE
ϵ	Wick porosity
λ	Latent heat of vaporization
μ_v	Dynamic viscosity of the vapor
μ_l	Dynamic viscosity of the liquid
ρ	Density
ρ_l	Density of liquid
ρ_v	Density of vapor
σ	Surface tension

τ_l	frictional shear stress at liquid-solid interface
ψ	Heat pipe inclination

Subscripts:

a	adiabatic
c	condenser / capillary / cold
e	evaporator
eff	effective
HPHE	Heat pipe heat exchanger
HP	Heat pipe
i	inner
l	liquid
L	Longitudinal
o	outer OR stagnation state
p	Pipe
s	surface
T	Transverse
v	vapor OR void
w	wick or wall

ACKNOWLEGEMENT

First, I must thank my beloved husband who completed my second half. *Amir*, I learned a lot from you, I learned I can do everything even it seems impossible, I learned how to be focused and independent. I learned that what matters in our life is love and to be loved only, and the rest are just small things that we can handle when we are standing together. I also appreciate the time you spent to format my dissertation chapters to be prepared on time.

Secondly, I would like to thank my co-chair and adviser in Civil and Environmental Engineering Department, *Dr. Michael Stenstrom* who inspired me with his research subject and never hesitated to spend time with me discussing the research and resolving the problems. I always felt so comfortable to contact you whenever I needed your help.

I am truly thankful to my co-chair and adviser in Mechanical and Aerospace Engineering Department, *Dr. Adrienne Lavine* who devoted her precious time to see my progress and read my documents. Professor Lavine, replying back my emails quickly and constantly available 24 hours, means a lot to me. I just don't know how you managed your time to do everything perfectly. Without you, I would have never been able to go through the obstacles in my research. I appreciate all of your support and understanding from bottom of my heart and thank you for inspiring me with your genius ideas all the time.

Thank you to my candidacy/defense committee *Dr. Jennifer Jay* and *Dr. Sanjay Mohanty* for accepting to be on my committee.

I found very smart and supportive friends in UCLA who never hesitated to encourage me or help me get out of the obstacles: *Ladan Amouzegar*, *Sheida Saeidi*, *Armin Karimi*, *Qi Yao*, *Maryam Ghavamloo Ghajar*, and my friends who never left me alone: *Hasti Mojarradzadeh*, *Homa* and

Sima Feizi, *Salmeh Dehghan*, *Ryan Farahani* and my wonderful helper *Faranak Bakhtiari*; I am so thankful for having you all in my life.

In MAE department there are very supportive staffs who helped me when I needed them. Thank you, *Angie Castilo* and *Abel Lebon*, for helping me to find funding to support myself at school, and also *Evgenia Grigorova* and *Lance Kono*.

I am also thankful to *Mr. Peter Dussinger*, vice-president of Energy Recovery Systems and *Mr. Bryan Muzyka*, sales manager in Advanced Cooling Technologies, Inc. who provided consultations in the heat pipe design.

My supportive mentor at Mechanical Engineering Department at California State University, Northridge (CSUN), *Dr. Sidney Schwartz*, thank you for always encouraging me and supporting me to step into higher educations.

I would also like to acknowledge the support of California State University (CSU) Chancellor's Doctoral Incentive Program (CDIP) for selecting me as a CDIP scholar.

And the last but not the least thank you to *Dr. Mohamed Abdou*, director of Fusion Science & Technology Center at UCLA, who trusted me and gave me the opportunities to assist teaching his classes. I achieved wonderful teaching experience and I learned a lot from you, I do appreciate for always supporting me.

Marzieh Mandizadeh

Spring 2018

VITA

Education

Graduate Student Researcher/ Teaching Fellow– **Mechanical Engineering/ Heat and Mass Transfer, UCLA** (University of California, Los Angeles)

M.S.– Mechanical Engineering /Heat and Mass Transfer, **CSUN** (California State University, Northridge)

B.S.– Mechanical Engineering/ Fluid Mechanics**, IUST** (Iran University of Science and Technology)

Research Experience

Lab and Research Assistant, Intern Nov. 2014- May 2015

NASA, Jet Propulsion Laboratory (JPL)

Graduate Research Assistant Nov. 2013- Spring 2018

University of California Los Angeles (UCLA) – Mechanical & Aerospace Engineering (MAE) Department

Lab and Research Assistant

California State University, Northridge (CSUN) May 2009 – Aug. 2012
–Mechanical Engineering (ME) Department

PhD Research

Heat Recovery at Wastewater Treatment Plants Using Heat Pipe Heat Exchangers

Master Research

Experimental Study of the Thermal Performance and Flow Characteristics of Metal Foams

Honors And Awards

- **UCLA Conference Travel Grant** and **CSU Chancellor Travel Grant**, Fall 2016
- California State University (CSU) **Chancellor's Doctoral Incentive Program Scholar,** Spring 2011
- **Exceptional Student** in Annual Graduation Commencement of the "College of Engineering and Computer Sciences", California State University Northridge (CSUN), Spring 2010
- **Honor Student** in Annual Honors Convocation, CSUN**,** Spring 2010
- **Award**, CSUN Thesis Support Program, Fall 2009
- Research **Grant**, **Pratt and Whitney Rocketdyne**, Spring 2009
- Holder of the **Pratt and Whitney Rocketdyne** Annual **Scholarship**, Spring 2009
- **Grant and Special Award** "1st Iranian National Robotic Contest", Spring 2002
- **Full Scholarship** for undergraduate study in mechanical engineering, Iran University of Science and Technology (IUST)

Publications

Mandizadeh, M., Lavine, A.G. and Stenstrom M.K., 2016, '*Opportunities for Low Value Heat Recovery at Wastewater Treatment Plants*', Water Environment Federation's Annual Technical Exhibition and Conference (WEFTEC), 2016

Mandizadeh, M., Tadayoni, A., Ebrahimi, M., Emami, V., Shams, M., Nayerloo, M., Tabatabayi, Y. Habibnejad, M, '*Tennis ball collector robot, national robotic contest*', ASME conference, Semnan, Iran, 2003 (in Farsi)

CHAPTER 1

1. Introduction

Wastewater treatment plants produce methane in anaerobic digesters and use the methane for heating; in the case of large treatment plants, methane is also used for power generation. There are a number of places in the process where heat is not recovered because of its low economic value. With increasing cost of energy and emphasis on sustainability and energy conservation, there are greater incentives to recover energy.

To conserve or recover energy from devices and systems, heat exchangers are commonly used. Heat exchangers are widely used to recover energy from the systems working at high or low temperatures.

In this research our focus is on wastewater treatment plants (WWTPs) and innovative ways are needed to recover heat. Heat exchangers have been previously used in WWTPs and specifically in influent and rarely in effluent pipes to anaerobic digesters (Figure 1-2) but there are many difficulties regarding the maintenance, clogging and cleaning, which discourages their use, especially for heat recovery.

There are many areas for opportunities in wastewater treatment process but the greatest opportunity for heat recovery in WWTPs is in anaerobic digesters which treat biosolids and produce methane gas. Anaerobic digesters typically operate at either 35 to 37°C (mesophilic) or 45°C (thermophilic), and biosolids must be heated from ambient temperature (10 to 20°C). Heating systems are a mature technology and few studies focus on new and improved ways of heating and energy recovery from the burning methane gas or effluent from the digesters. The new

emphasis on energy recovery and the lack of new research encourages us to study more efficient or practically suitable heat exchangers.

Heat pipes are an interesting technology and have never been used in WWTPs. Heat pipes have been used in other applications such as in aerospace for spacecraft cooling and temperature stabilization, as well as to dissipate heat generated by electronic components in satellites (Shukla, 2015), and for cooling of electronic devices, such as cooling CPUs. This study is innovative since we propose to evaluate heat pipes as used in other industries for new applications for wastewater treatment applications. To the best of our knowledge this is the first time and the only research that aims to use heat pipes to recover energy from anaerobic digesters.

The purpose of this study is to identify heat recovery opportunities at WWTPs and evaluating new ways of recovering energy.

Figure 1-1 shows a schematic of a WWTP and also the areas that have potential for heat recovery. Figure 1-2 shows existing technology to heat influent feed from ambient temperature to digester temperature (either 37°C or 45°C) and then to recover heat from the digested sludge. Few if any treatment plants currently recover heat from digested sludge, exhaust gases and heat from methane gas combustion.

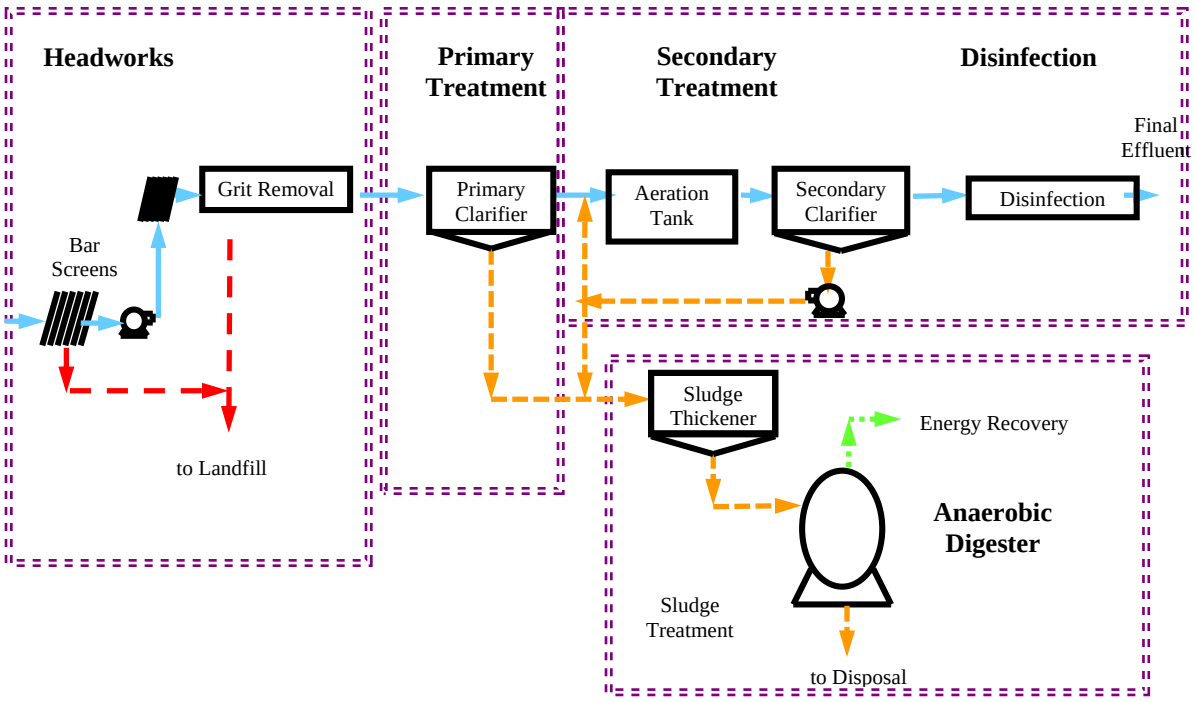

Figure 1-1: A schematic of a wastewater treatment plant (WWTP). The double dotted lines show the areas that have opportunities for heat recovery (Copyright 2000-2010 Michael Stenstrom)

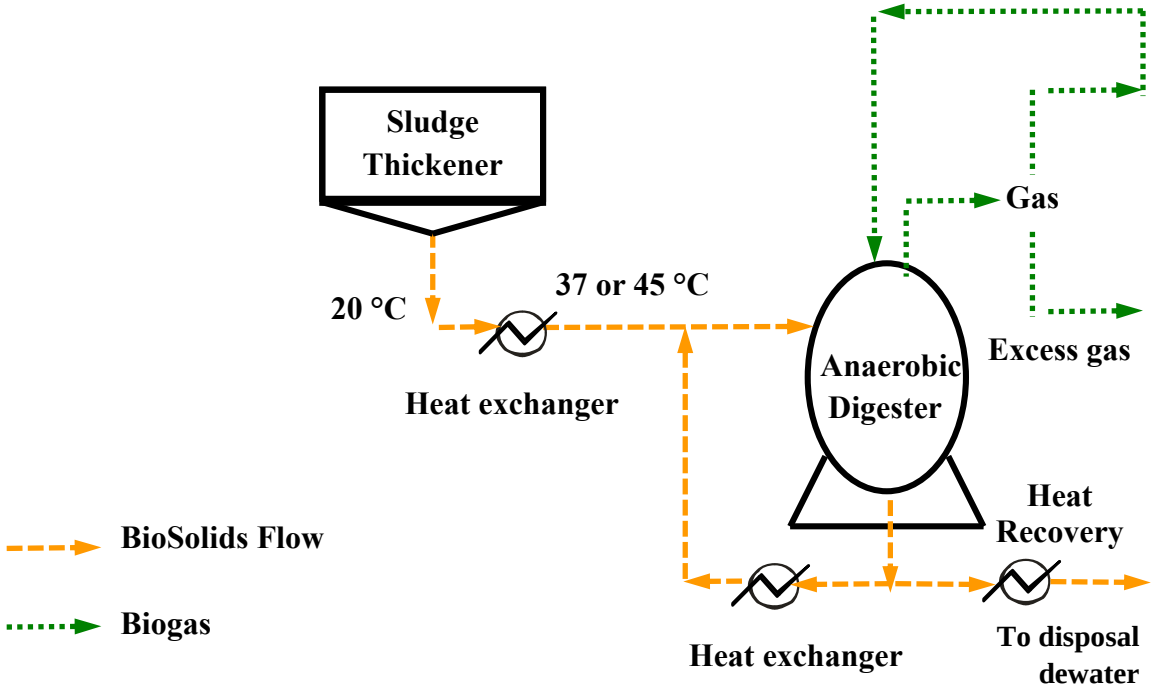

Figure 1-2: Digesters treatment and possible energy recovery diagram

Most researchers who work on heat recovery in WWTPs, study the feasibility of using wastewater as a heat source and recovering energy. Unfortunately there is still not a good alternative for the existing heat exchangers in WWTPs (as previously discussed).

Considering the maintenance and clogging, a better substitution for the conventional heat exchangers is evaluated in this research, thus the feasibility of bundles of heat pipes (heat pipe heat exchanger) is investigated to recover energy in WWTPs, specifically in digesters. Important applications include heating raw and secondary sludge prior to digestion, heating digesters in cold climates to maintain optimum temperature, recovering heat from digested sludge, especially thermophilically digested sludge and moreover recovering heat from the methane gas combustion.

In this study, first a heat pipe is designed and then a heat pipe heat exchanger (HPHE) and both designs are validated with literature references. Then the concept extends for a design of a HPHE to be replaced or installed in Oceanside WWTP in northern California to recover heat from warm sludge and combusted methane gas.

Currently the best technology is used to recover heat in treatment plants is spiral heat exchanger. To understand under what conditions HPHE works with shorter length compared to the spiral heat exchanger, all of the inlet and exit temperatures as well as the width and the height of the heat exchangers are fixed and then the fluid pairs in the evaporator and the condenser side is varied.

Under the same conditions (same inlet temperatures and flow rates for the external flows) first the exit temperatures for the spiral heat exchanger are evaluated and then the number of rows of heat pipes to achieve the same temperatures at the exit are adjusted. At the end the two heat exchangers are compared to see which one could work with shorter length.

For each comparison three different fluids pair are tried: water-water, air-air and air-water and in all of them cold flow is the minimum fluid (has minimum $\dot{m}c_p$) because maximum change in the cold flow temperature by recovering energy from the hot flow is desired. Most of the input values in these comparisons are realistic values and we will talk in detail in CHAPTER 6.

From thermal resistance analyzing, we found an insight when using HPHE is favorable. This insight helps us to decide either substitute the existing heat exchangers with HPHE or not. There is no doubt using HPHE is more convenient regarding maintenance and clogging, but we have to consider other factors such as the needed space and the costs. Refer to Spirax Sarco case study list (see CHAPTER 5), HPHE return the capital quickly but all of the conditions to use them should be considered carefully.

This dissertation is arranged with the following topics:

- Literature review to characterize the potential value of heat recovery in WWTPs
- Description of wastewater treatment technologies to identify the opportunities
- Anaerobic digester systems
- Current practice using heat exchangers in WWTPs
- Heat pipes, theory and applications
- Sample design of a heat pipe
- Heat pipe heat exchanger (HPHE) design and then comparison with the spiral heat exchanger to allocate the best place for heat recovery in WWTPs
- Heat pipe design refinement
- HPHE optimization
- Economical overview

CHAPTER 2

2. Literature review of heat recovery from WWTPs

In this section, the work of the researchers who investigated or modeled the opportunities to recover heat from digesters in WWTP will be referred first, and then their results are summarized in Table 2-1.

Very little research has been conducted to find better ways to recover low value (low temperature) energy from WWTPs, specifically from anaerobic digesters. Some researchers (Abdel-Aal, 2014) tried to model and measure wastewater temperature along a sewer pipe to assess the viability of recovering heat from wastewaters, which are typically a few degrees warmer than ambient temperature. They were satisfied that there is a potential for heat recovery in sewers.

Other researchers (Dürrenmatt et al., 2014) investigated the effect of heat recovery on the wastewater temperature in the sewer since reducing wastewater temperatures may cause problems for the biological processes used in WWTPs and also for the receiving waters. After running the model in the simulation program called TEMPEST (TEMPEST is a new interactive simulation program for the estimation of the wastewater temperature in sewers, Dürrenmatt et al., 2008), they concluded the temporary storage of heat in the pipe wall and the exchange of heat between wastewater and the pipe wall are the most important processes for heat transfer. The researchers think that the model can be used as a tool to determine the optimal site for heat recovery in treatment systems and the maximal amount of extractable heat.

In another study, the Korean researchers (Baek and Shin, 2004) investigated the feasibility of wastewater as a heat source for a heat pump heating system. They found that the yearly mean Coefficient of Performance (COP) of such a heat pump was approximately 4.8 and a heat pump

can supply 100% of the hot water load except on weekends in winter. They pointed out that the important factor that should be considered for the system design is to decrease the temperature difference between condenser and evaporator working fluids during the heat charging process by the heat pump.

A summary of the studies on heat recovery from digesters in WWTPs is given in Table 2-1.

Table 2-1: Heat recovery observed by researchers

References	Model/Simulation	Important factor(s)	Remarks
Dürrenmatt and Wanner – Switzerland (2014)	TEMPEST	Temporary storage of heat in the pipe wall and the exchange of heat between wastewater and the pipe wall.	The planning of new facilities requires predictions of the effect of heat recovery on the wastewater temperature in the sewer. Wastewater temperatures may cause problems for the biological processes used in wastewater treatment plants and receiving waters.
Baek and Shin- (2004)	Heat pump system using off-peak electricity as a water heating system designed and analyzed to heat low-temperature (about 301K) hot spring water during night time hours (22:00–08:00)	Decreasing the temperature difference between condenser and evaporator working fluids during the heat charging process by the heat pump	The yearly mean COP (Coefficient of Performance) of heat pump is about 4.8 and heat pump can supply 100% of hot water load except weekend of winter season.
Abdel-Aal, Smits, Mohamed, De Gussem, Schellart and Tait. (2014)	Modeling of wastewater temperatures along a sewer pipe using energy balance equations and assuming steady-state conditions		Long sewers may prove to be more viable for heat recovery, as heat lost can be reclaimed before wastewater reaches the WWTP.

Limited research has been conducted on possibilities of recovering energy from exhaust gas from combustion of digester biogas. One of them is a case study (Bruno et al., 2008) on integration of an absorption cooling system into a micro gas turbine using biogas. The study investigated several configurations and concluded the best configuration would be to completely replace the existing system with a trigeneration plant that uses all available biogas produced in the plant. In Table 2-1 of the paper, the electrical efficiency of a biogas-run system which is comparable to the efficiency of a system using natural gas is shown.

CHAPTER 3

3. Wastewater treatment technology

First an introduction on wastewater treatment and then the part of the treatment process which we are interested to study the heat recovery possibilities (anaerobic digesters) will be provided. Then the heat recovery technology which is currently available in treatment plants and their cons will be addressed. At the end of this chapter the product information provided by the spiral heat exchanger manufacturer, the real data from a sample treatment plant which runs that heat exchanger and my calculations for the existing spiral heat exchanger will be shown.

In a wastewater treatment plant, domestic wastewater is treated to be discharged back into a watercourse. The wastewater produced by private households is polluted largely by dissolved biodegradable substances.

A wastewater treatment plant is essentially divided into the following sections:

- Mechanical treatment
- Biological treatment
- Sludge or biosolids treatment

The largest part of the plant treats the liquid flow (and the flow should be warm enough) and it is never heated due to the cost. When the sludge temperature is warm enough, then a large portion of the biodegradable material is converted to waste biomass (sludge) which is disposed in a solids processing train. The volumetric flow rate of the waste biomass is small compared to the liquid flow rate (typically less than 1%) which means that it can be heated economically if anaerobic digesters are used. In treatment plants of good design in temperate climates, there is always excess methane, which is usually recovered, especially at the larger treatment plants.

Figure 3-1 shows the typical processes in sludge treatment and disposal. Heating is always used with anaerobic digestion but heat recovery of digested sludge is rarely practiced. Heat recovery options are associated with the stabilization, heat drying and thermal reduction steps. The diagram shows many possible alternatives and no plant would employ all of the alternatives.

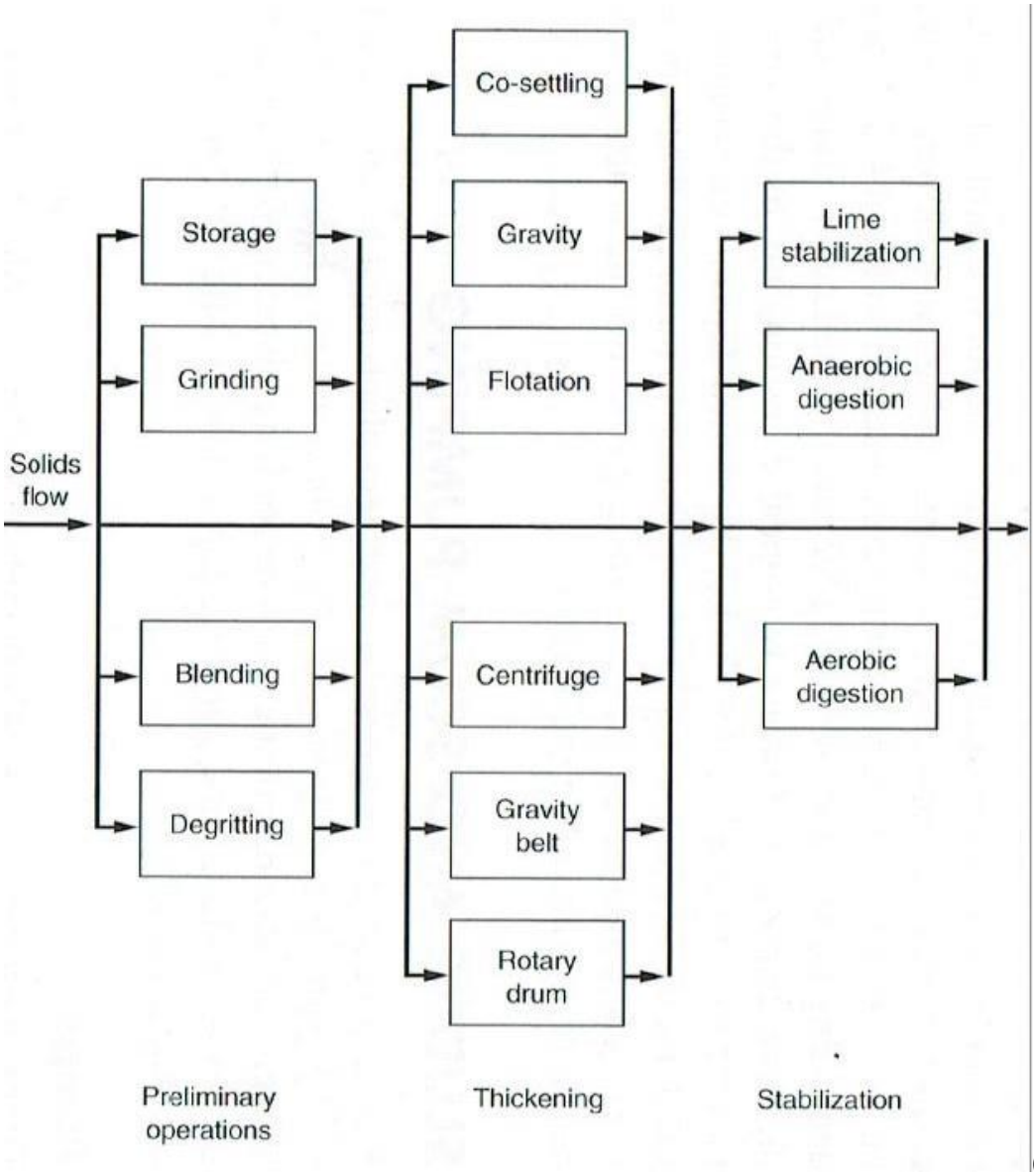

(To be cont'd)

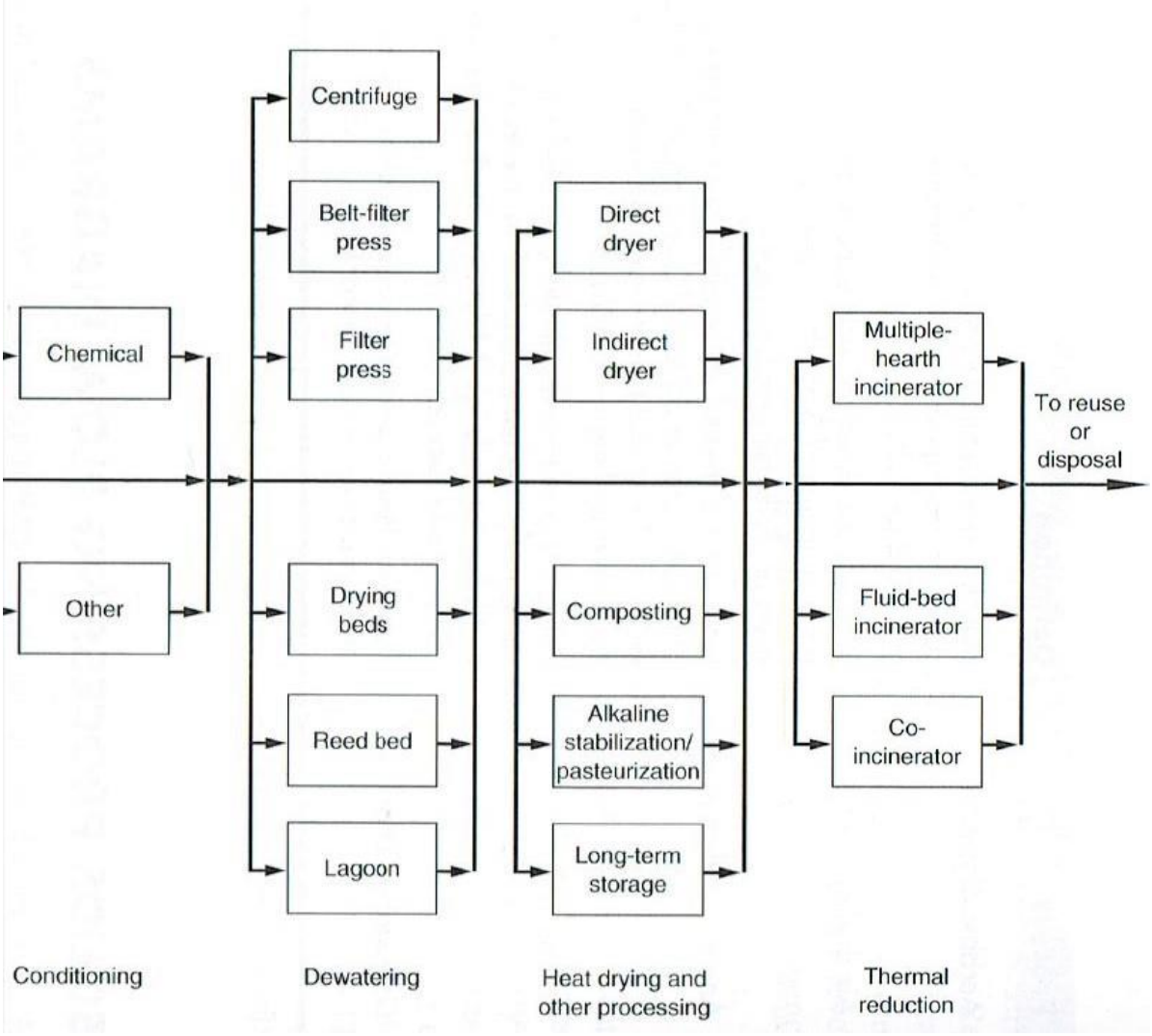

Figure 3-1: Generalized sludge-processing flow diagram (Metcalf and Eddy, 2003, Figure 14-2)

3.1. Anaerobic digestion

Anaerobic digestion is a part of a wastewater treatment loop and is a collection of processes by which microorganisms break down biodegradable material in the absence of oxygen. The anaerobic process products are used either to manage waste water and/or as an alternative to fossil fuels.

The "anaerobic activity" process is the term referred to anaerobic degradation which naturally occurs in some types of soils, lakes and also in the oceanic basin sediments. This is the source of marsh gas methane as discovered by Volta in 1776. (Zehnder, Alexander J. B. (1978). "Ecology of methane formation").

Anaerobic digestion is particularly well suited to concentrated organic material, and is commonly used for effluent and sewage treatment (Cakir and Stenstrom, 2005). It is a simple process which can greatly reduce the amount of organic matter which might otherwise be destined to be dumped at sea, dumped in landfills, or burnt in incinerators.

In Figure 3-2 is graphically shown how digesters work.

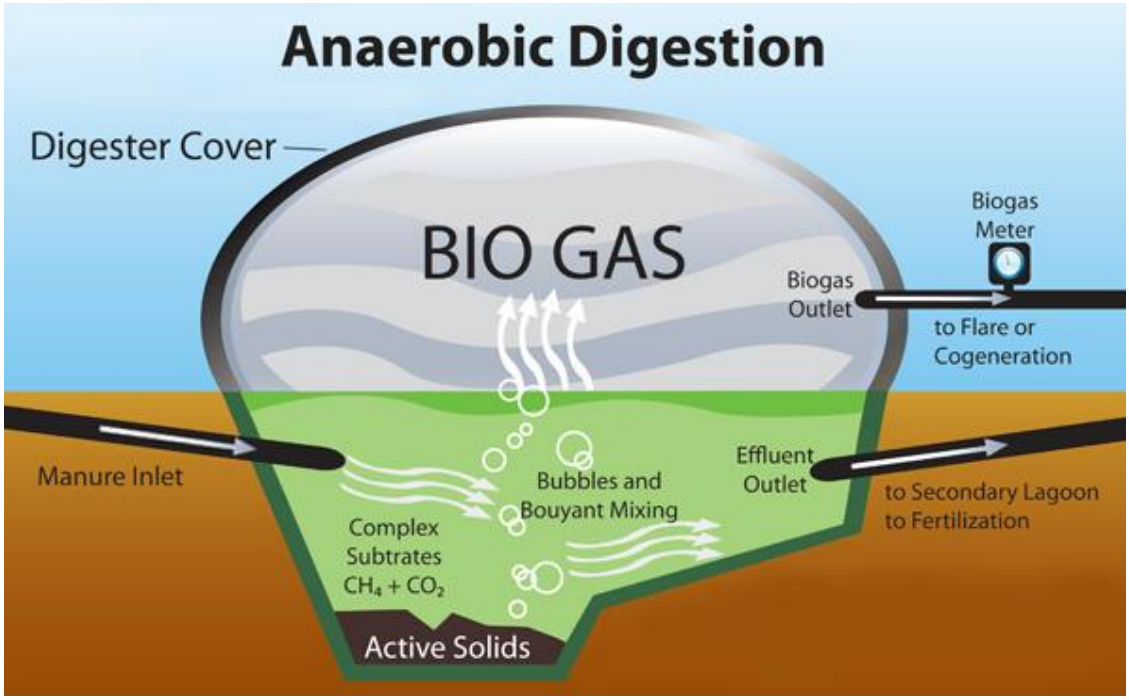

Figure 3-2: Anaerobic digestion diagram (The Renewable Energy Hub webpage, March. 2018)

www.renewableenergyhub.co.uk/blog/anaerobic-digesters-future-renewable-energy/

Anaerobic digesters contain biosolids, liquid and gas which makes it a good area for heat recovery opportunities.

3.2. Heat recovery opportunities from digesters in WWTPs

3.2.1. Energy recovery opportunity from digesters using methane gas

In the recent years, anaerobic digestion systems have been recognized and used as a source of renewable energy (even for domestic or industrial treatment plants). The products of anaerobic digestion are biogas (65% methane gas), carbon dioxide (CO_2) and other "contaminant" gases as well as digested sludge. The combusted methane gas can be used as an alternative to fossil fuels in gas engines such as turbines or can be upgraded to natural gas-quality as bio-methane. Also, the digesters' effluent sludge can be used as fertilizer.

Anaerobic digestion has received higher attention among countries such as United Kingdom (2011), Germany and Denmark (2011) recently, because of the re-use capability of waste as an energy resource which with appropriate technological approaches can reduce capital costs.

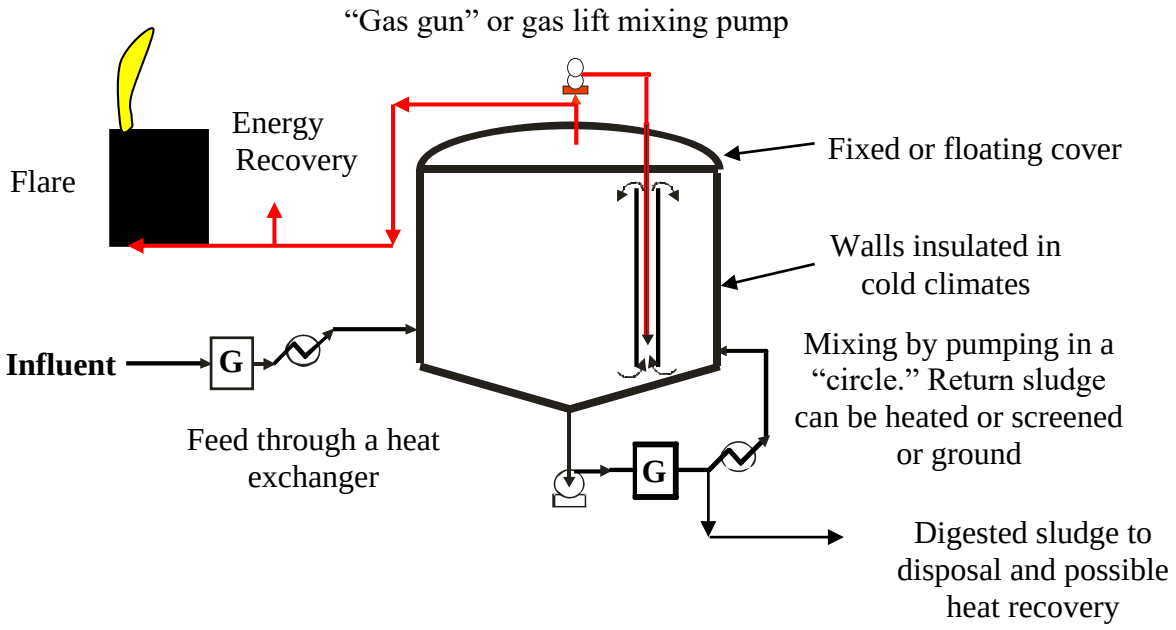

Figure 3-3: Traditional Digester (Copyright 2000-2010 Michael Stenstrom, UCLA)

As mentioned earlier, methane gas (CH_4) combustion in anaerobic digestion facilities can be a good replacement for the alternative fossil fuels energy. It also reduces greenhouse gases emissions, because the carbon in methane gas (CH_4) is a biodegradable material and is part of a carbon cycle.

3.2.2. Heat recovery from digesters using heat exchangers

Wastewater treatment plants have traditionally wasted a lot of heat due to insufficient economic incentives. Among the technologies for heat recovery, the most important devices used widely are heat exchangers.

Digester heat exchangers are installed in the influent and/or effluent of anaerobic digesters to preheat the influent and/or transfer the energy from warm effluent.

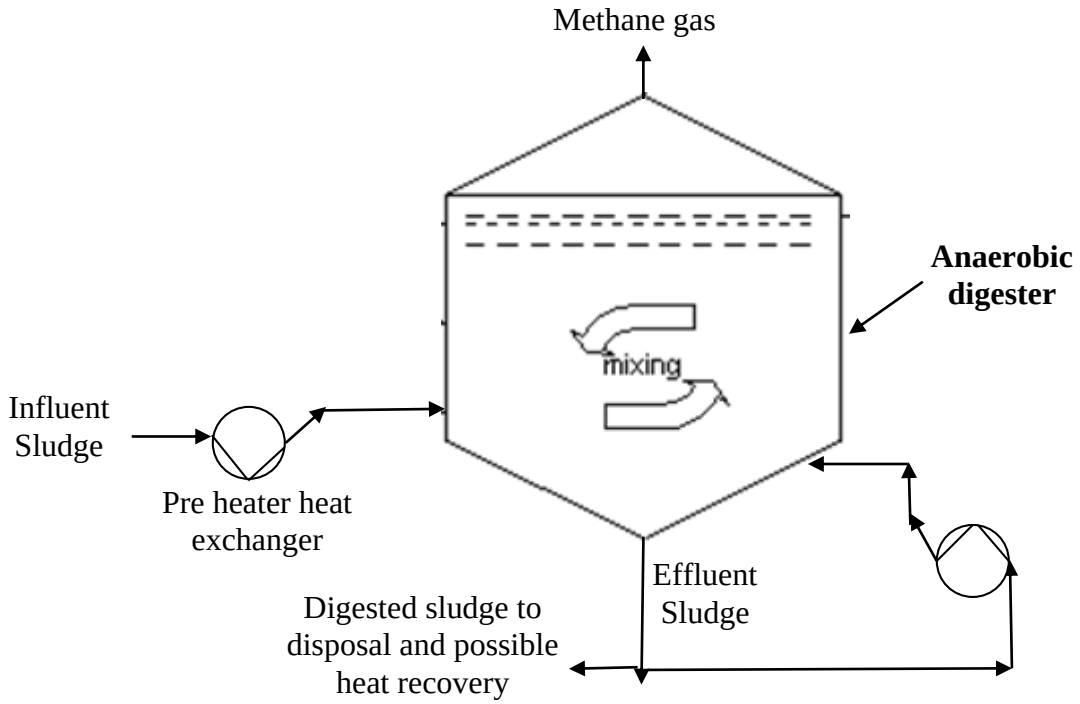

Figure 3-4: Anaerobic digester, possible energy recovery diagram

Heat exchangers are widely used to heat anaerobic digesters but their uses have some pros and cons:

Pros: preheats the influent to the digester to increase the methane production rate and improves digester's efficiency.

Cons: maintenance is costly and inconvenient.

An alternative to heat exchangers is steam injection, which does not require an exchanger but has efficiency disadvantages and dilutes the digesting sludge. Also on the requirement of electricity to heat steam is not economically favorable.

Nowadays the most common heat exchangers used in WWTPs are double pipe and spiral (or so-called "jelly roll") heat exchangers. Figure 3-5 and Figure 3-6 show these two heat exchanger types schematically.

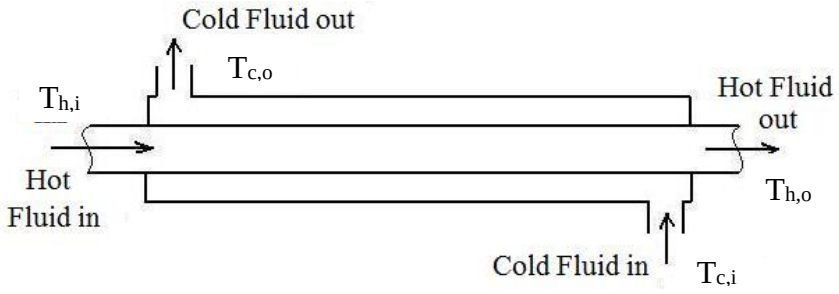

Figure 3-5: Double pipe heat exchanger

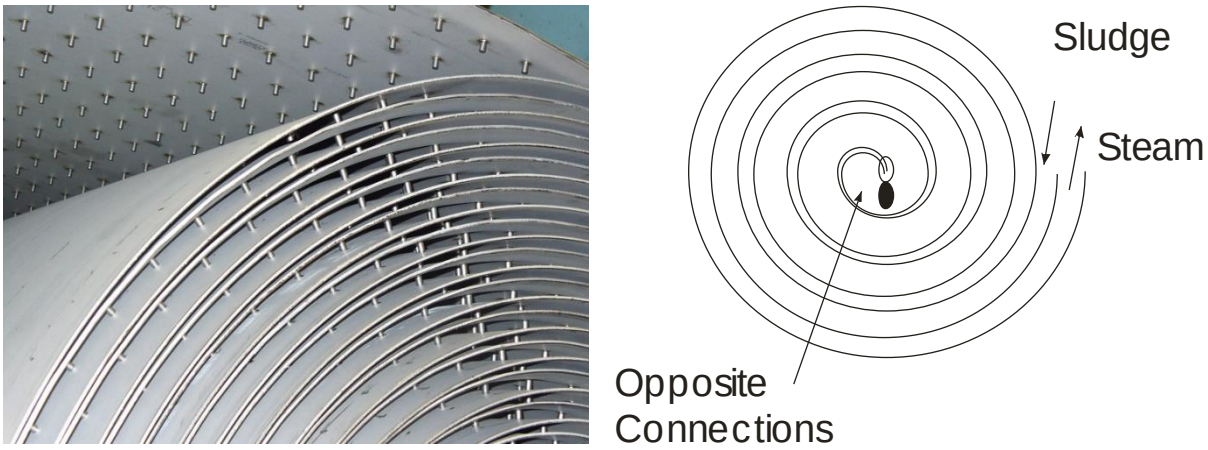

Figure 3-6: Spiral heat exchanger (Copyright 2000-2010 Michael Stenstrom)

3.3. Reviewing Oceanside WWTP data and heat recovery possibilities

3.3.1. Spiral heat exchanger in Oceanside WWTP, Northern California

In Figure 1-1 and Table 3-1 and Table 3-2, the specifications and calculated effectiveness for the existing spiral heat exchanger in Oceanside WWTP in San Francisco (Northern California area) are presented.

Alfa Laval Spiral Heat Exchanger Specification

Customer : San Francisco PUC
Model : 1H-SW-1W
Quote No. : Sludge Heating HX
Item : OS43M34-1 thru 4
Date: 11/15/2012

		Hot side	*Cold side*
Fluid		Water	Sludge - 3% - 5%
Density	lb/ft³	61.12	62.40
Specific heat capacity	Btu/lb,°F	0.998	1.00
Thermal conductivity	Btu/ft,h,°F	0.381	0.360
Viscosity.inlet	cP	0.412	3.4
Viscosity.outlet	cP	0.436	3.2
Volume flow rate	GPM	500.0	500.0
Inlet Temperature	°F	155.0	125.0
Outlet Temperature	°F	147.8	132.0
Pressure Drop	psi	6.6	3.9
Heat Exchanged	kBtu/h	1750	
Rel. directions of fluids		Countercurrent	
L.M.T.D.	°F	22.9	
Total area	ft²	285.0	
Fouling factor	ft²,h,°F/Btu	0.0003	
Plate Material		CARBON STEEL	
Connection Size		6->6	6->6
Channel Closure		Bar-Bar	Open-Bar
Design According to		ASME	
Flange Standard		ANSI	
Design Overpressure	psig	70.0	70.0
Design Temperature	°F	200	200
Fluid Volume	ft³	10.50	12.99

Performance is conditioned on the accuracy of customer's data and customer's ability to supply equipment and products in conformity therewith.

Figure 3-7: Specifications by Alfa Laval Co. for existing spiral heat exchanger in Oceanside WWTP in San Francisco, California

Table 3-1: Specifications provided by Alfa Laval Corporate for spiral heat exchanger in Oceanside WWTP

Description	**Symbol**	**Unit**	**Hot side (Water)**	**Cold side (Sludge)**
Density	**ρ**	kg/m^3	979.1	999.6
Volumetric flow rate	**Q**	m^3/s	0.032	0.032
Mass flow rate	$\dot{m}$	kg/s	30.9	31.5
Hot fluid inlet temperature	$\mathbf{T_{h,i}}$	° C	68.3	-
Hot fluid outlet temperature	$\mathbf{T_{h,o}}$	° C	64.3	-
Cold fluid inlet temperature	$\mathbf{T_{c,i}}$	° C	-	51.7
Cold fluid outlet temperature	$\mathbf{T_{c,o}}$	° C	-	55.6
Specific heat at constant pressure	c_p	kJ/kg·K	4.2	4.2
Heat capacity rate, $C = \dot{m} c_p$	**C**	kW/K	129.0	132.0
Heat transfer between two fluid streams in heat exchanger	**q**	kW	513	
Fluid volume	**V**	m^3	0.3	0.4

The Alfa Laval spiral heat exchanger located in Oceanside WWTP has two rectangular channels (see Figure 3-6), one for the water and another one for the sludge.

The water channel is 0.75 inches high by 30 inches wide and 57 feet long. The sludge channel is 1 inch high, 30 inches wide and 57 feet long.

The reported total surface area is 285 ft^2 and the total area for heat transfer is 233.5 ft^2.

Table 3-2: Data provided by Oceanside WWTP for the existing Alfa Laval spiral heat exchanger

Data	Unit	Hot side (Water)	Cold side (Sludge)
Q	m^3/s	0.033	0.035
$T_{h,i}$	° C	61.2	-
$T_{h,o}$	° C	-	-
$T_{c,i}$	° C	-	55.0
$T_{c,o}$	° C	-	57.2

Table 3-3: Our calculations for the spiral heat exchanger in Oceanside WWTP based on data in Table 3-2

q_{max} (Watts)	4.3×10^5
ε (effectiveness)	0.52

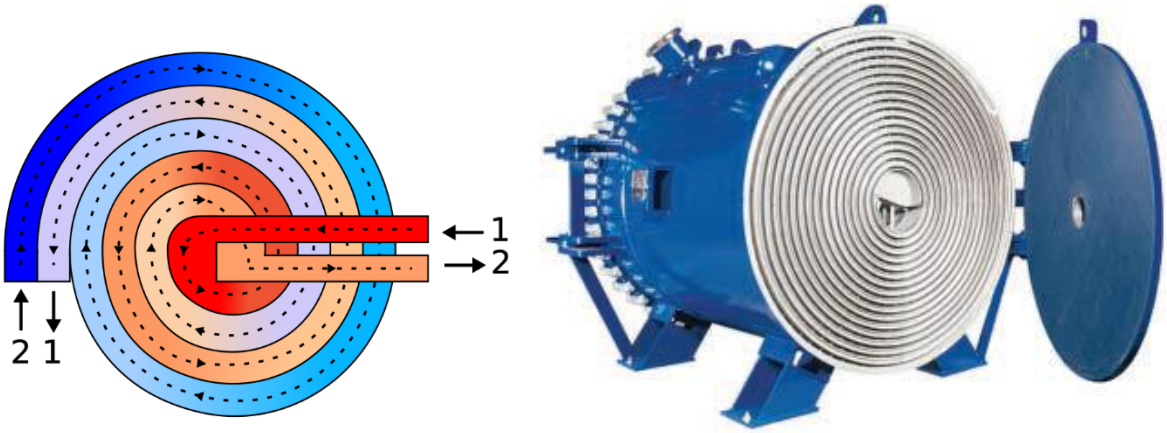

(a) (b)

Figure 3-8: Spiral heat exchanger picture

(a) source: By Michael Schmid [GFDL (gnu.org/copyleft/fdl.html, March 2018), CC-BY-SA-3.0 (creativecommons.org/licenses/by-sa/3.0/) b) Alfa Laval spiral heat exchanger catalog

As shown in Section 3.2.2, currently the treatment plant engineers found spiral heat exchangers are the best device to recover energy from digesters. With the existing spiral heat exchanger with the detailed properties mentioned in this section, there is an opportunity to transfer 430 kW from hot fluid to cold fluid.

3.4.Summary of the section

- Methane (CH_4) gas is produced in anaerobic digester in wastewater treatment plants.
- CH_4 is a good source of energy and can generate heat and electricity if used properly.
- Nowadays heat exchangers such as double tube and spiral types are used to heat sludge being fed to digesters, although they are troublesome because of costly and time consuming maintenance. They also need enough space to be located outside the digesters.
- The need of a good replacement for the convectional heat exchangers is necessary (the proposed heat exchanger is introduced in CHAPTER 5).
- Within the existing spiral heat exchanger data provided from Oceanside WWTP in San Francisco area, we could validate the spiral heat exchanger design for Oceanside WWTP where the calculations and the results are in agreement with Alfa Laval reported specifications in Table 3-1.

CHAPTER 4

4. Heat pipe introduction and applications

In this chapter first information about heat pipe characteristics, applications, the governing equations that are used from the references to design a heat pipe will be provided, and then the conditions the heat pipes would work successfully are referred. Later the heat pipe design approach is validated with the literatures, and finally the designed heat pipe characteristics and parameters for wastewater treatment application are shown.

A heat pipe is an evacuated closed-end tube, which usually has circular cross-sectional area. These simple devices are widely used in many industries, i.e. in personal computers. The heat pipes are known as a new generation of heat exchangers when they are lined up in rows and columns and are exposed to external flows. Moreover, they are reliable and less complicated devices to transmit or dissipate heat. The heat pipe principle was first proposed by Gaugler in 1944 and again in 1962 by Trefethen (Chi, 1976). A working fluid in the heat pipe is carefully selected based on working temperature as well as heat pipe wall and wick material. In this hollow cylinder, the inner portion is a passage for vapor flow and a porous capillary wick structure on the inside walls to assist the liquid movement to the opposite end of the heat pipe. Generally the liquid movement is gravity assisted by the orientation of the heat pipe.

Heat pipes have the ability to transport a large amount of thermal energy in a small unit size and to recover heat even at low temperature differences (low value heat recovery) between evaporator and condenser. For these reasons, heat pipes are considerably better devices to transport heat as compared to solid conductors.

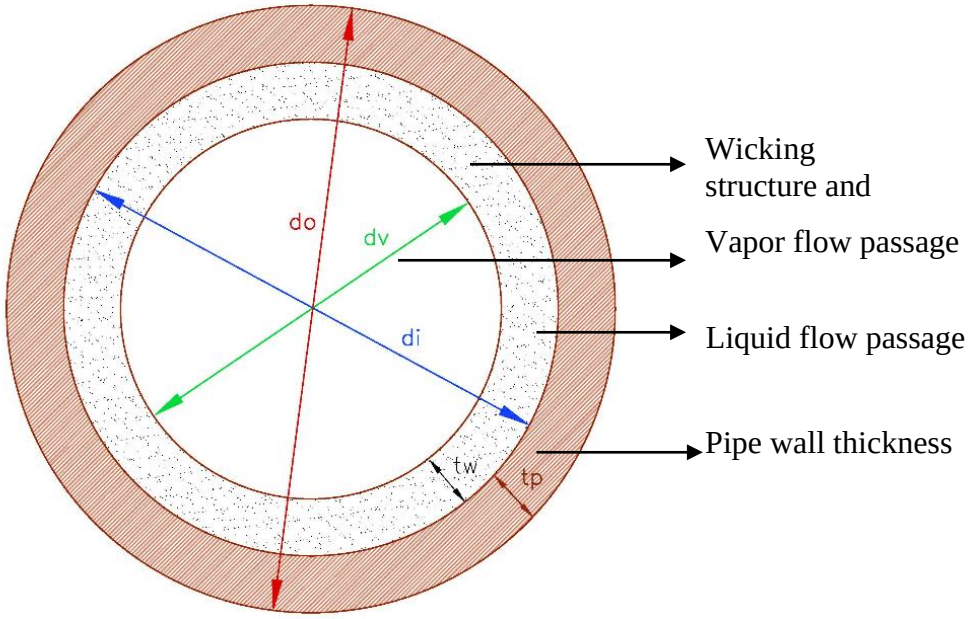

Figure 4-1: Heat pipe cross-sectional area

Note: There is no wall between the vapor in the core and the liquid in the wick; those are in direct contact.

At one end of the heat pipe, heat is applied from an external source or a hot flow; this end is called the evaporator side. The liquid inside the pipe evaporates and moves to the other end via the inner passage (vapor passage). At the opposite end, the heat is removed by a heat sink or by applying colder flow outside of the heat pipe; this end is called the condenser side. As the vapor liquefies, the liquid returns to the evaporator section with the help of a wick structure. In this way, heat is transported from one side to another without any moving mechanical device. The amount of heat transported is the latent heat of vaporization and it is usually several orders of magnitude larger than the heat that can be transferred by a solid conductor (such as copper).

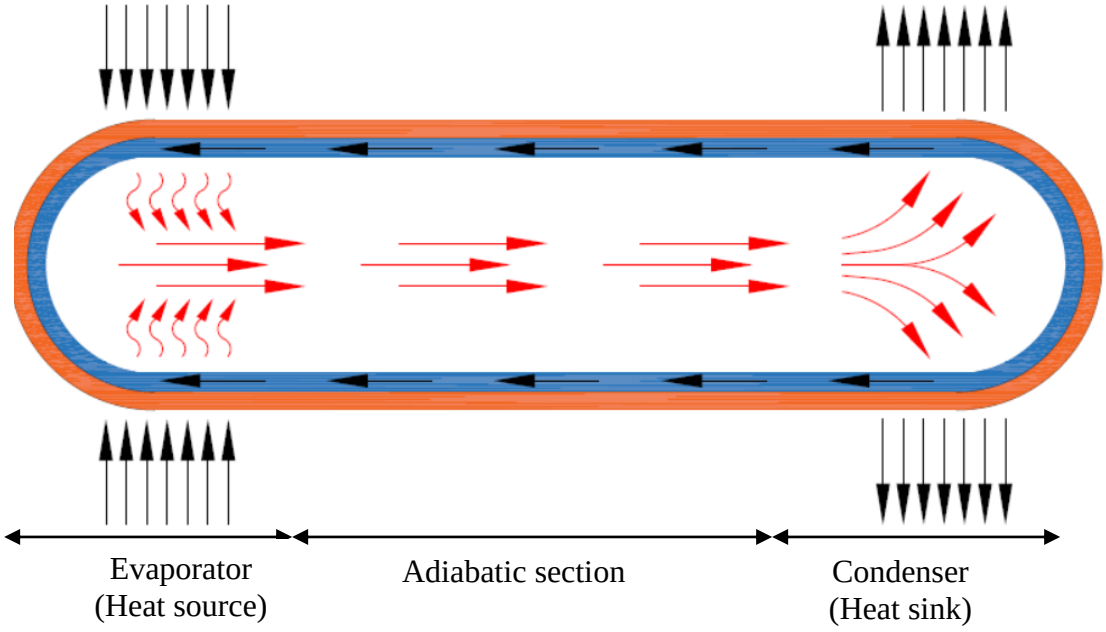

Figure 4-2: Schematic of a heat pipe. The red arrows are the vapor and the black arrows show the condensed liquid

Heat pipes can work horizontally or vertically. If a heat pipe is installed vertically, the condenser can be either above or below the evaporator. The former is called gravity-assisted heat pipe or thermosyphon. Figure 4-2 shows horizontal installation of a heat pipe for convenience. In this research the mounting is taken to be vertical with the condenser on the top and the evaporator on the bottom. There is a pressure difference from the evaporator to the condenser and then results in capillary pressure which pumps the condensed liquid back to the evaporator side of the heat pipe.

There are some limitations in heat pipe design; the most common one is heat pipe dry-out, which is due to high input heat on the evaporator side and consequently higher vapor velocity in the vapor passage (inner hollow of heat pipe). Then the vapor shears the liquid from the surface of the wick and liquid enters the vapor. Finally it results in evaporator wick dry-out which is called heat pipe entrainment phenomenon.

There are some universal benefits of using a heat pipe:

1. **High Effective Thermal Conductivity:** Heat pipes can transfer heat over long distances, where temperature drop is not considerable.
2. **Passive operation:** Heat pipes can operate passively meaning they require no energy input other than heat to operate.
3. **Long lifetime with almost no maintenance:** There are no moving parts inside heat pipes that could wear out. The heat pipes are also vacuum sealed, which prevents liquid/vapor losses. The outside of heat pipes is covered with protective coatings which protects against corrosion.
4. **Heat pipes can recover heat** even for small temperature gradients (low temperature heat recovery).

Figure 4-3: Heat pipe application: CPU cooler using 6 embedded copper heat pipes (www.cdrinfo.com/Sections/Reviews/Print.aspx?ArticleId=22229, March 2018)

4.1. Heat pipe literature and governing equations

To be able to design a heat pipe, it is necessary to understand the theory behind it. In this text definitions, theory and the equations has been used to design heat pipe in this study are shown and those are adopted from Chi (1976) and Peterson (1985).

4.1.1. Surface Tension and Wettability

In operation of a heat pipe, surface tension of the liquid inside the heat pipe has a very important role to create capillary pressure and so that the heat pipe can operate. (For more information about surface tension mechanism, please read APPENDIX). Liquid-surface interface behavior which is the result of interaction between surface tension, wettability and contact angle, makes a pressure imbalance occurring at or near the interface and then it provides the capillary pumping for heat pipe priming and operation. In the case of the interface between the liquid and a vapor, the interface is as a meniscus and the meniscus has a key role to make a heat pipe work. In other words, the non-equilibrium conditions between the evaporator and condenser liquid-vapor interfaces are responsible for the operation of heat pipes.

4.1.2. Capillary pressure

Capillary pressure is the working force that moves the fluid inside the heat pipe from one end to another. The surface tension of the liquid and the vapor interface forms meniscus at the liquid-vapor interface (Figure 4-4), and then results in the pressure difference at the interface. This pressure difference forms the capillary pressure which is the result of (P_v - P_l), and it can be calculated by the Laplace-Young equation (Chi, 1976):

$$P_c = \sigma\left(\frac{1}{R_1} + \frac{1}{R_2}\right) \tag{4-1}$$

The above expression shows that the capillary pressure difference occurring across the meniscus separates the liquid and vapor regions and it is a function of the two principal radii of curvature, R_1 and R_2.

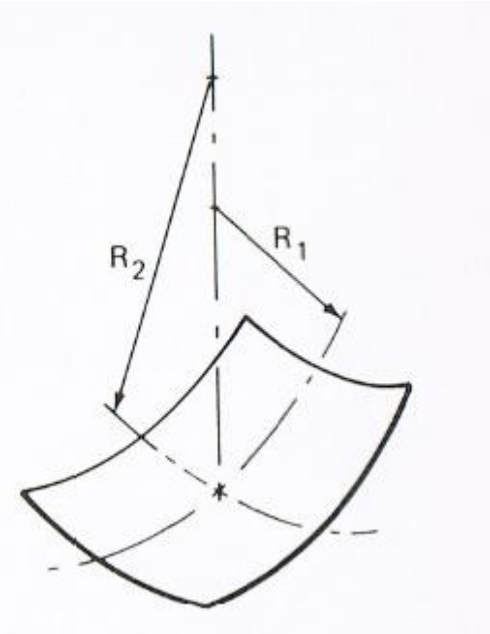

Figure 4-4 : Geometry of meniscus at liquid-vapor interface (Chi, 1976)

During the vaporization process molecules escaping from the liquid surface must overcome an attraction force exerted by the other molecules in the liquid. If the liquid wets the wick or solid surface, then interfacial shape is concave. The molecular attraction in concave interface is greater than that occurring at a plane surface in equilibrium. As a result, the energy of the surface is greater than that required for a plane surface and hence the pressure and density over the concave curved liquid surface are less than for a flat liquid surface. As another case a convex liquid surface requires an energy level which is slightly higher than that required for a plane surface. This results in a vapor pressure that is slightly greater for a convex surface than for a plane surface.

As shown in Figure 4-5, the capillary pressure gradient across a liquid-vapor interface is equal to the pressure difference between the liquid and vapor phases at any given axial position. For a

heat pipe to function properly, the net capillary pressure difference between the wet and dry points, (see Figure 4-5 b) must be greater than the summation of all the pressure losses occurring throughout the liquid and vapor flow paths.

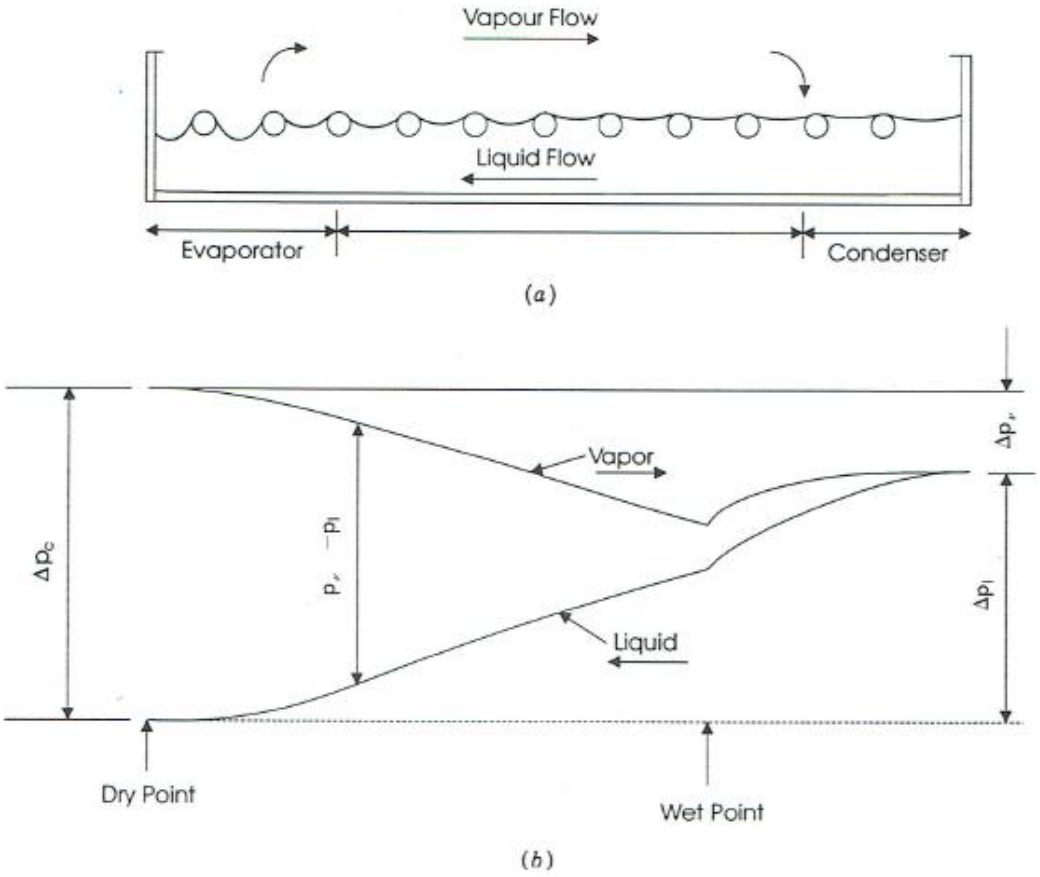

Figure 4-5: (a) Variation of meniscus curvature as a function of axial position. (b) Typical liquid and vapor pressure distributions in a heat pipe (Peterson, 1994).

We are interested in finding the maximum capillary pressure for various types of wick structures. For convenience in heat pipe applications, the Eq. (4-1) is written as:

$$P_c = \frac{2\sigma}{r_c} \tag{4-2}$$

where r_c is called the capillary radius.

4.2. Pressure gradients in a heat pipe

Pressure drop hinders the heat pipe performance if it is larger than the working force, therefore its evaluation is important. Evaluating the vapor pressure drop is also essential because Reynolds and Mach number of vapor are considerable and affect the maximum capillary heat limit. In this section we show the details and correlations for vapor flow pressure drop and the theory behind liquid flow pressure drop could be found in APPENDIX . The other types of pressure drops, normal and axial, which impact the maximum heat transfer are evaluated for the heat pipe.

4.2.1. One-dimensional Vapor pressure drop

The vapor pressure drop varies in the axial direction of a heat pipe which is the result of the viscous pressure drop occurring along the vapor flow path.

In the evaporator, the viscous pressure drop may be coupled with the momentum changes required to accelerate the vapor molecules escaping from the liquid meniscus, which further decreases the pressure. For very high vapor flow rates, these momentum or inertial effects may be the dominant factor on determining the pressure gradient and can amount to as much as 80% of the total vapor pressure drop.

In the adiabatic section of the heat pipe, the vapor pressure gradient is typically linear and results only from the viscous friction occurring between the flowing vapor and pipe walls and wicking structure.

In the condenser region, the inertial effects caused by deceleration of the vapor molecules can be recovered (although not completely) because of the decreasing mass flow rate caused by condensation of some of the vapor. This condensation results in some pressure recovery and effectively decreases the rate at which the pressure decreases.

Because determination of the vapor pressure drop in heat pipes is complicated by the mass addition and removal in the evaporator and condenser, respectively, and by the compressibility of the vapor phase, an alternative procedure has been developed. Both Chi (1976) and Dunn and Reay (1982) have studied this problem. Based on Chi's work, he found that upon integration of the vapor pressure gradient which is the solution of conservation of momentum equation, the dynamic pressure effects cancel. The result is an expression for the pressure drop in the evaporator section:

$$\Delta P_v = \left(\frac{C(fRe)_v \mu_v}{2(r_{h,v}^2) A_v \rho_v \lambda} \right) L_{eff} q \tag{4-3}$$

and q is defined as

$$q = M_v A_v \rho_v \lambda \sqrt{\gamma_v R_v T_v} \tag{4-4}$$

where q is the maximum heat transfer rate in the heat pipe, R_v is the gas constant of the vapor which is equal to $\frac{\bar{R}}{M} = \frac{\text{Universal Gas Constant}}{\text{Molecular Weight of Vapor}}$ and γ_v is called vapor specific heat ratio which is equal to 1.67, 1.4, 1.33 for monatomic, diatomic and polyatomic vapors respectively (Chi, 1976). In Eq. (4-3), $r_{h,v}$ is the hydraulic radius of the vapor space, C is a constant that depends on the Mach number (M_v) and L_{eff} is the effective length of the heat pipe and defined as:

$$L_{eff} = 0.5L_e + L_a + 0.5L_c \tag{4-5}$$

The rest of the variables can be found in the Nomenclature.

It is useful to relate the vapor flow regime (Reynolds and Mach number) to the heat transfer rate:

$$Re_v = \left(\frac{2r_{h,v}}{A_v \mu_v \lambda} \right) q \tag{4-6}$$

According to the reported results of Kraus and Bar-Cohen (1983), the following combinations of these conditions can be used with reasonable accuracy:

1. $\mathrm{Re}_v < 2300$ and $\mathrm{M}_v < 0.2$: $(\mathrm{fRe})_v = 16$, C=1.00

2. $\mathrm{Re}_v < 2300$ and $\mathrm{M}_v > 0.2$: $(\mathrm{fRe})_v = 16$, $\mathrm{C} = 1/\sqrt{\left[1+\left(\frac{\gamma_v - 1}{2}\right)\mathrm{M}_v^2\right]}$

3. $\mathrm{Re}_v \geq 2300$ and $\mathrm{M}_v \leq 0.2$: $(\mathrm{fRe})_v = 0.038\left(\frac{2(r_{h,v})q_{c,max}}{A_v \mu_v \lambda}\right)^{3/4}$, $\mathrm{C} = 1.00$

The above correlations match with the equations introduced by Chi (1976), i.e. for the case of $\mathrm{Re}_v \geq 2300$ and $\mathrm{M}_v \leq 0.2$, vapor frictional coefficient which is $\mathrm{F}_v = \frac{\Delta P_v}{L_{eff} q_{c,max}}$ and F_v have been defined by Chi as follows:

$$\mathrm{F}_v = \frac{0.019\,\mu_v}{A_v r_{h,v}^2 \rho_v \lambda}\left(\frac{2 r_{h,v} q_{c,max}}{A_v \lambda \mu_v}\right)^{3/4} \tag{4-7}$$

For the case of turbulent vapor flow and $\mathrm{M}_v \leq 0.2$, since the equations to evaluate both the Reynolds number and the Mach number are functions of the heat transport capacity, it is first necessary to assume the conditions of the vapor flow. Then an iterative procedure must be used to determine the maximum heat capacity, $q_{c,max}$. Once the $q_{c,max}$ is known, it can be substituted into the expressions of the vapor Reynolds number and Mach number to determine the accuracy of the original assumption (Peterson, 1994). The details for the turbulent vapor flow and $\mathrm{M}_v \leq 0.2$ and how to calculate $q_{c,max}$ are given in APPENDIX .

In Figure 4-6 the effective length is shown by a sketch.

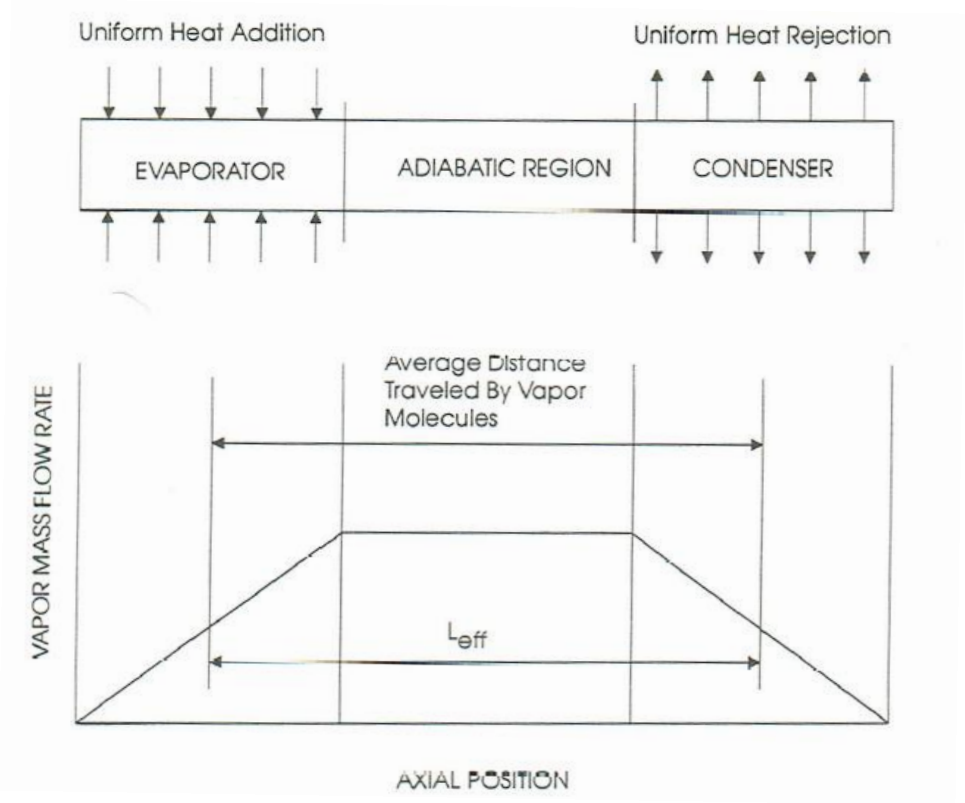

Figure 4-6: Schematic of the effective length (L_{eff}) for constant heat addition and heat rejection in a heat pipe (Peterson, 1994)

In this study wick permeability equation is used to calculate the maximum possible rate of heat transfer that could be transferred in our designed heat pipe (see APPENDIX), and the correlations are shown in Table 4-1 as below.

Table 4-1: Wick permeability (K) for several wick structures (Chi, 1976)

Structure	K	Data
Circular cylinder (artery or tunnel wick)	$r^2/8$	r = radius of liquid flow passage
Open rectangular grooves	$2\epsilon(r_{h,l})^2/(f_l \mathrm{Re}_l)$	ϵ = wick porosity ω = groove width s = groove pitch δ = groove depth $(r_{h,l}) = 2\omega\delta/(\omega + 2\delta)$
Circular annular wick	$2(r_{h,l})^2/(f_l \mathrm{Re}_l)$	$(r_{h,l}) = r_1 - r_2$
Wrapped screen wick	$\frac{d^2\epsilon^3}{122(1-\epsilon)^2}$	d_ω = wire diameter $\epsilon = 1 - (1.05\pi N d_w/4)$ N = mesh number
Packed sphere	$\frac{r_s^2\epsilon^3}{37.5(1-\epsilon)^2}$	r_s = sphere radius ϵ = porosity dependent on packing mode)

4.2.2. Normal hydrostatic pressure

In addition to pressure drop in liquid and vapor phases of a heat pipe, a hydrostatic pressure gradient exists in a heat pipe which is the result of gravitational or body forces of the vapor and liquid phases. Thermosyphons use gravitational forces alone and for the gravity-assisted heat pipes (the evaporator is below the condenser), the gravitational body force linearly increases contribution to the pressure in the liquid phase and linearly decreases contribution to the pressure in the evaporator phase.

In heat pipes with circumferential communication effect of the liquid in the wick (in non-zero gravity environment), the normal hydrostatic pressure drop $\Delta P_\perp$ occurs. It is the result of the component of the body force (gravitational force) in the direction perpendicular to the axis of the heat pipe and is defined as

$$\Delta P_{\perp} = \rho_l g d_v \cos\psi \tag{4-8}$$

where ρ_l is liquid density, d_v is the vapor core diameter and ψ is the angle of the heat pipe with respect to the horizontal.

4.2.3. Axial hydrostatic pressure

The axial hydrostatic pressure drop results from the component of the body forces parallel to the axis of the heat pipe within the vapor and liquid phases and is defined as

$$\Delta P_{II} = \rho_l g L_{eff} \sin\psi \tag{4-9}$$

It is very important to notice that for a heat pipe operating in a gravitational field, the axial hydrostatic pressure term may either assist or impede the capillary pumping and it depends on the orientation of the heat pipe. If the evaporator lies below the condenser, gravity assists the liquid back to the evaporator, otherwise it impedes.

Later in the governing equation for the maximum effective pumping pressure (refer to Chi 1976 to see examples), we should be very careful to use positive or minus sign for axial hydrostatic pressure.

In a zero-gravity environment (in space), both the normal and axial hydrostatic pressure drop terms are negligible due to absence of the gravitational body force.

4.3. Heat pipe operating limits

Several limits and physical situations control the axial heat transport capacity of a heat pipe. These limits are called viscous, sonic, entrainment and boiling limits.

When we evaluate the maximum heat transfer capacity for each limitation, we have to choose the smallest value among all heat transport limits and then call it the maximum heat transfer

capacity of the heat pipe (q_{limit}). These limitations can be found in detail in APPENDIX of this dissertation.

4.4. Thermal resistances inside the heat pipe

In this section we show the different types of thermal resistances inside a heat pipe and their equations. The heat pipe design is not complete without understanding the thermal resistances inside. Learning from the heat pipe limitations, we need the effective thermal conductivity (k_{eff}) of the liquid-saturated wick to calculate the boiling heat transfer limit (refer to Table A-1 for k_{eff} correlations). Therefore the effective heat transfer coefficient for the heat pipe based on the pipe cross-sectional area should also be determined.

To obtain the effective heat transfer coefficient inside the heat pipe, we should first collect information about different types of thermal resistances within the heat pipe.

$$q = \frac{1}{\left(\sum R\right)}\left(\Delta T\right) \tag{4-10}$$

Based on the order of magnitudes comparison of the resistances inside a heat pipe, the heat pipe can be modeled as in Figure 4-7 and Figure 4-8. Therefore there are five resistances within the heat pipe:

$R_{p,c}$: Radial resistance of the heat pipe wall at the condenser

$R_{w,c}$: Resistance of the liquid-wick combination (liquid saturated wick) at the condenser

$R_{p,e}$: Radial resistance of the heat pipe wall at the evaporator

$R_{w,e}$: Resistance of the liquid-wick combination (liquid saturated wick) at the evaporator

R_v : Resistance of the vapor flow from the evaporator to the condenser

Figure 4-7 shows the simplified thermal resistances inside a heat pipe.

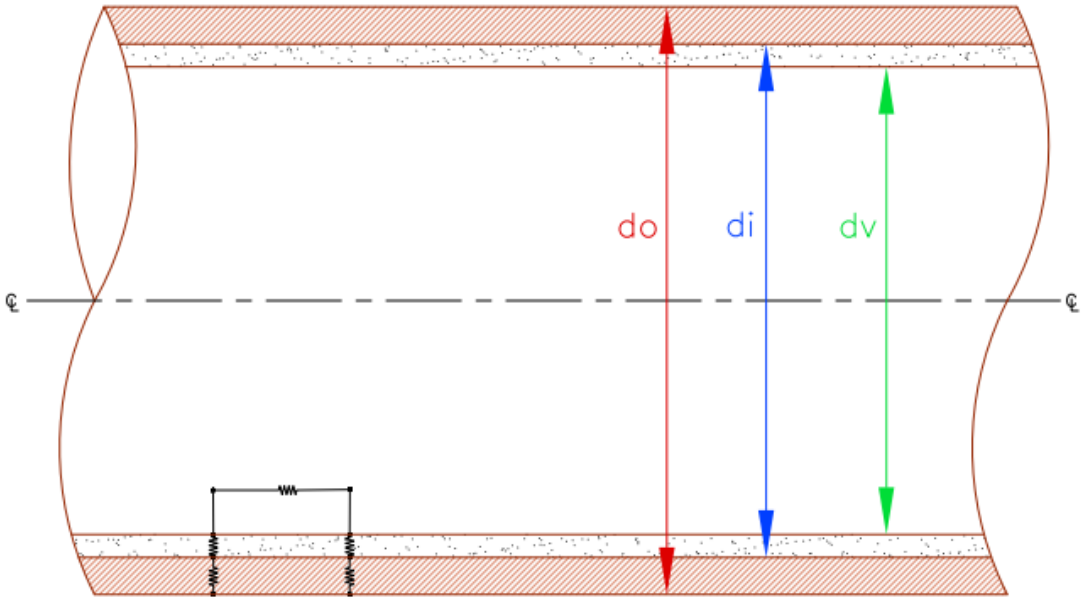

Figure 4-7: Heat pipe side-view showing thermal resistance

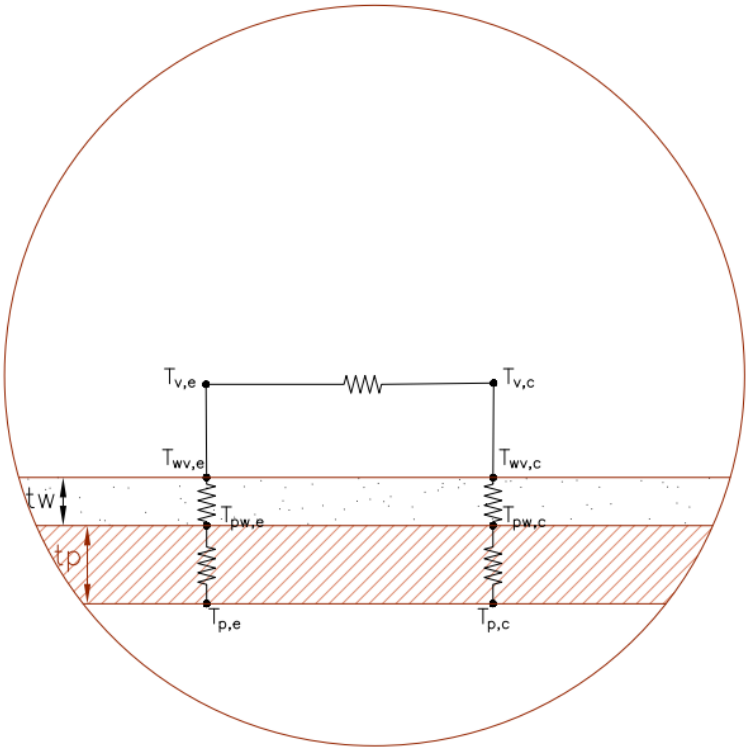

Figure 4-8: Heat pipe thermal resistances without considering external thermal resistances

The expressions for the most significant resistances inside the heat pipe are as follows. All resistances are based on the heat pipe cross-sectional area (Chi, 1976):

Thermal resistance of the heat pipe wall:

$$R_{p,e} = \frac{t_p}{2\pi r_o L_e k_p}\left(\frac{K}{W}\right) \tag{4-11}$$

Thermal resistance of the liquid saturated wick at the evaporator:

$$R_{w,e} = \frac{t_w}{2\pi L_e r_i k_{eff,e}}\left(\frac{K}{W}\right) \tag{4-12}$$

Thermal resistance of the liquid-saturated wick at the condenser:

$$R_{w,c} = \frac{t_w}{2\pi L_c r_i k_{eff,c}}\left(\frac{K}{W}\right) \tag{4-13}$$

Thermal resistance of the heat pipe wall at the condenser:

$$R_{p,c} = \frac{t_p}{2\pi r_o L_c k_p}\left(\frac{K}{W}\right) \tag{4-14}$$

Thermal resistance of the vapor flow from the evaporator to the condenser:

$$R_v = \frac{T_v F_v\left(\frac{L_e}{6} + L_a + \frac{L_c}{6}\right)}{\rho\lambda}\left(\frac{K}{W}\right) \tag{4-15}$$

In this study the above equations have been used to calculate the overall thermal resistance inside the heat pipe ($R = R_{p,e} + R_{w,e} + R_{p,e} + R_{w,e} + R_v$) which is the inverse of the overall conductance $(UA)_{HP}$. Then in a heat pipe heat exchanger (HPHE) system which would have two unmixed external flows passing over the row and columns of the heat pipes, we combine the $(UA)_{HP}$ with the heat conductance of the external flows (see CHAPTER 5 for more details) to calculate the heat conductance of the HPHE for one row of heat pipes and then evaluate the effectiveness for a row of heat pipes in the condenser and evaporator sections. At the final step we can calculate the HPHE effectiveness for n rows of heat pipes in the HPHE system.

4.5. Heat pipe design validation with literature

To confirm the method and the calculations to design the heat pipe in this dissertation, some values from other researchers are regenerated. In Huang and Tsuei (1985), we found some useful details for their designed heat pipe. We used their data for a built heat pipe to calculate overall heat conductance inside the heat pipe.

In the Huang and Tsuei (1985) paper, five heat pipes out of 32 heat pipes in their laboratory were randomly selected and then they had been separately tested. All these heat pipes had the same specifications as in Table 4-2 below:

Table 4-2: A single heat pipe specifications from Huang and Tsuei (1985) paper

L_{eff} (m)	d_o (m)	t_p (m)	Wall material	Wick structure	Wick material	Heat pipe working fluid
0.610	0.0337	0.0016	Carbon steel	Wrapped screen (15 layers)	100- mesh bronze	Distilled water (115 g)

Note: In above table (Table 4-2) N=100 mesh and unit is not given in the literature. In heat pipe design usually imperial unit is used then we assumed they mean 100 1/in (and confirmed this assumption with a heat pipe manufacturer); meaning 100 meshes per inch of wrapped screen.

Other specifications of their heat pipe were not given in the paper and we assumed values either by inspection in Chi (1976) textbook or by investigating the parameter in the heat pipe design which is more sensitive.

Figure 4-9 shows the experimental set up of Huang and Tsuei (1985) to measure the wall temperatures and the energy transfer.

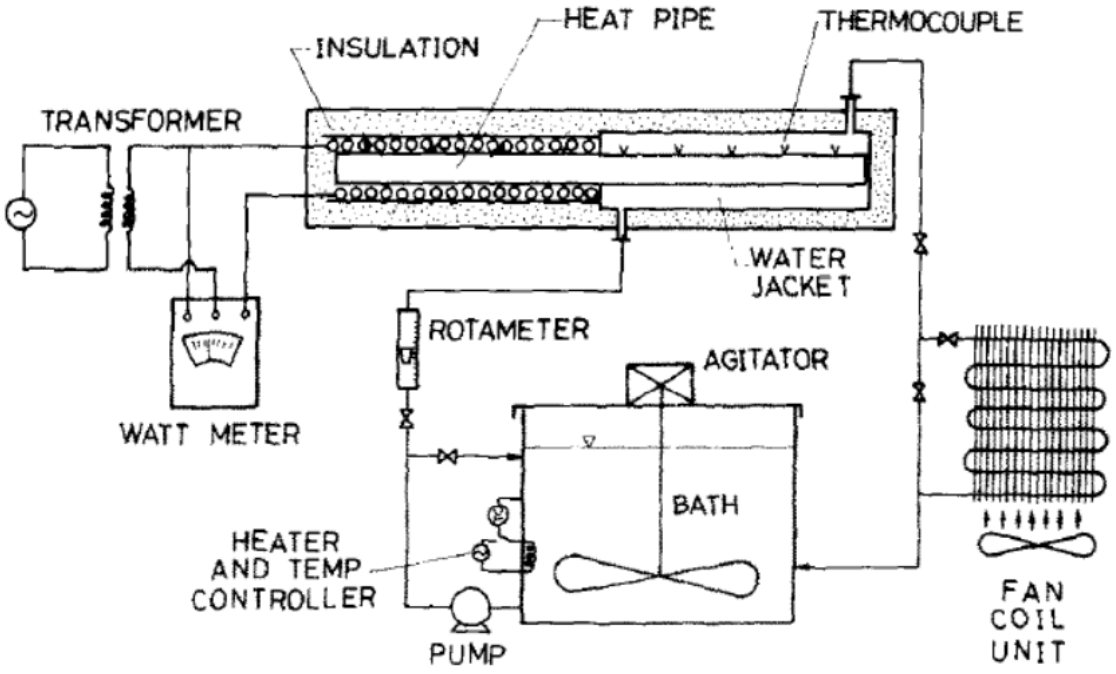

Figure 4-9: Heat pipe setup experiment- Huang and Tsuei (1985)

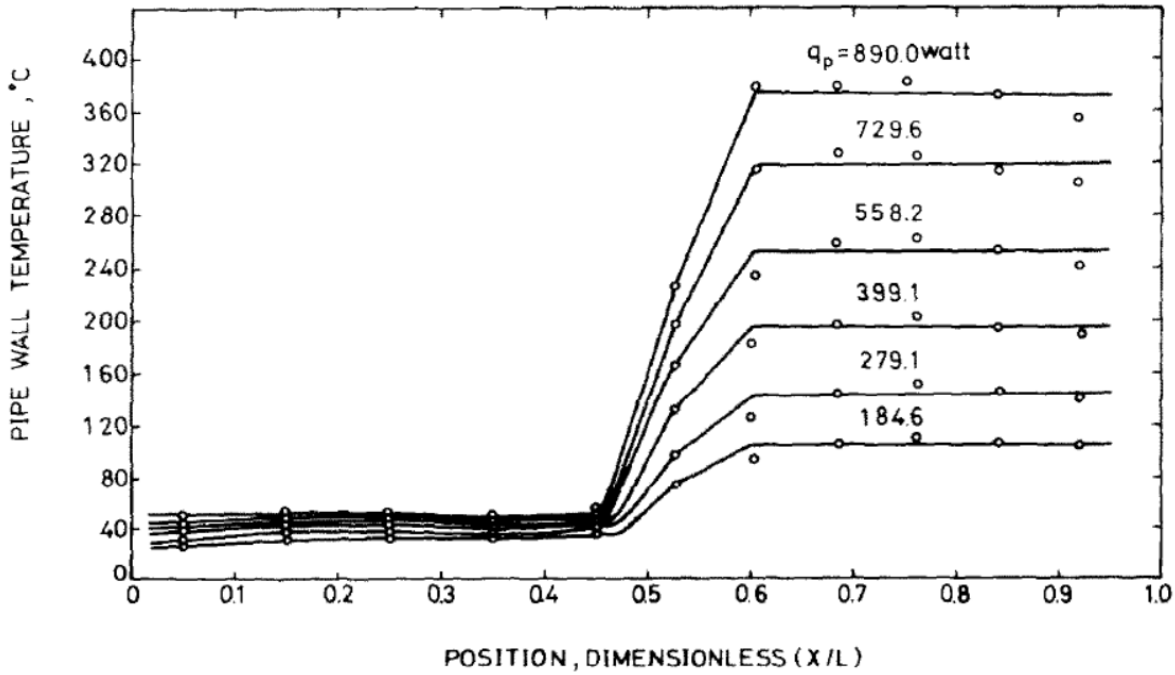

Figure 4-10: Fig.2 of Huang and Tsuei (1985) - Heat pipe wall temperature distributions versus energy transfer rates

The other information we gathered to design a heat pipe similar to Huang and Tsuei (1985) are given as below:

- For the working temperature of heat pipes we used Fig.2 of Huang and Tsuei (1985) (Figure 4-11) paper to assume the temperature in condenser: T_l=40 °C. The temperature in evaporator side of heat pipe was given in the paper T_v =360 °C.
- Wick thickness= 5 mm (by inspection in Chi (1976) textbook, wrapped screen wick and water examples, i.e. Example 2-2).
- Screen wire diameter= 0.0045 inch= 1.14 x 10^{-4} (m) (for 100 1/in mesh this is the diameter of screen (this information has been provided by Advanced Cooling Technologies, Inc.). This parameter is more sensitive in the heat pipe design.

- Heat pipe working angle to horizon= 0 (based on experiment setup picture in the paper)
- Crimping factor S= 1.05 (Chi, 1976)
- Critical nucleation radius $r_n = 10^{-5}$ inch = 2.54 x 10^{-7} m (Peterson, 1994)

With above information gathered, we calculated the heat pipe conductance and then compared to Huang and Tsuei (1985) measured conductance.

Table 4-3: Single heat pipe validation with Huang and Tsuei (1985)

	$(UA)_{HP}$ (W/K)
Huang and Tsuei (1985)	3.36
Our calculation	3.80

As Table 4-3 shows, our calculated $(UA)_{HP}$ is very close to the measured conductance in the literature.

In addition to validate the design of heat pipe with an experimental data (Huang and Tsuei, 1985) we also validated the method by redoing the example 2-2 in Chi 1976 textbook and some more examples in other heat pipe design textbooks such as Peterson, 1985.

4.6. Heat pipe optimization literature review

In Jafari, Shamsi, Filippeschi et al. (2017), they ran an optimization algorithm as well as experimental analysis and found that optimum L_e/L_c is around 1 which improves the heat transfer capability per heat pipe and decreases the thermal resistance inside a heat pipe.

Also in Tan, Liu and Wong (1991) paper, with analytical modeling, the authors found that the optimum ratio of a heat pipe evaporator length to the total length is $\frac{1}{2}$.

In our efforts for heat pipe design optimization, I used the former authors (Jafari, Shamsi, Filippeschi et al., 2017) result is used and let L_e=L_c. And from the latter authors (Tan et al., 1991) results $\frac{L_e}{L_t} \approx 0.5$ is chosen.

4.7. Our designed heat pipe parameters

Using the previous sections' authors' results, we designed the heat pipe to work in WWTP. The selected the working fluid does not freeze when the heat pipe it is installed outside of digester in cold climates regions. The wick material is selected to have high conductivity and the wall material is stainless steel to be hard enough when the heat pipe is exposed to the flows at high temperature or high velocity. The working temperature range is from the ambient temperature to a temperature less than the estimated exhaust gas temperature in a methane gas burner (we estimated exhaust gas temperature as 444 °C). To select the length, we think of running heat pipes in the heat exchanger system to recover heat from the effluent of digesters or raising the temperature of the influent, then L_t is estimated from the distance between the influent and effluent pipes. To select other parameters such as N, t_w and d_w, it has been consulted with a heat pipe manufacturer. The dimension and other parameters of the designed heat pipe are shown in Table 4-4 and Table 4-5 below. We used this design to insert in the systems of CHAPTER 7.

Table 4-4: Our designed heat pipe working condition

Heat pipe wall material	Wick type	Wick material	Working temperature	Working fluid	L_t (m)
SS304	Wrapped screen	Copper	20 - 232 °C	Methanol	1.07

Table 4-5: Our designed heat pipe parameters

d_v (m)	d_o (m)	t_w (m)	N (1/in)	t_{sw} (m)	L_e=L_c (m)	q_{limit} (W)	U_{HP} ($W/m^2.K$)
0.0198	0.0243	1×10^{-3}	200	1×10^{-3}	0.51	798	14,335

As Table 4-4 indicates, we selected stainless steel material for the heat pipe wall for three reasons:

1. By inspection we found that thermal resistance at the wall of heat pipe is small compared to other thermal resistances inside the heat pipe, and if we change the wall material from copper to stainless steel (which has smaller conductivity than copper), it does not significantly affect the total resistance inside the heat pipe.
2. The second reason was to strengthen the heat pipe and increase its lifetime to even be able to withstand high velocity and high temperatures of the external flows.
3. Moreover we selected SS304 which is not costly compared to other types of stainless steel alloys available in the market.

CHAPTER 5

5. Heat pipe heat exchangers

In this part of my work, the governing equations from the literatures are used to design a heat pipe heat exchangers and then my design approach is validated with the literatures. To do the optimized design for HPHE, the results from Matos et al. (2004) work and heat pipes are arranged in equilateral triangle staggering configuration in HPHE. Then I validated my design with the literatures. Finally I calculated the overall NTU for a system of HPHE.

Heat pipe heat exchangers (HPHE) are a number of heat pipe tubes installed in a sealed channel (see Figure 5-1). The hot flow passes over the evaporator side of the heat pipes and the cold flow passes over the condenser side and these two counter-flows in the channel are unmixed. The heat pipes are installed perpendicular to the flows.

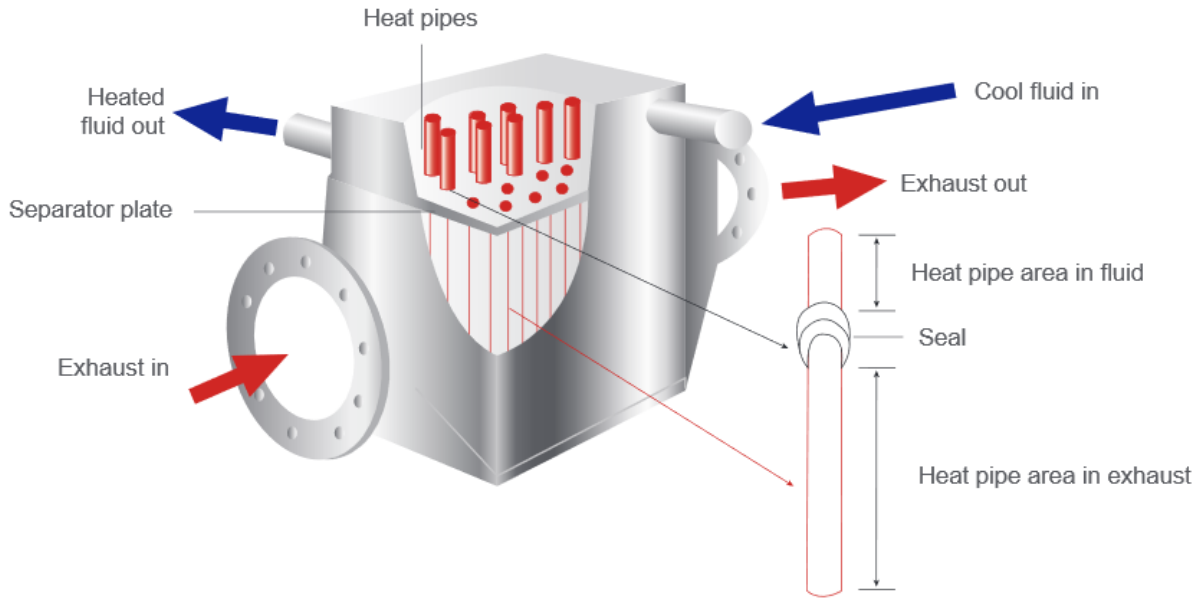

Figure 5-1: Schematic of HPHE, Spirax Sarco Inc.

The main concerns about using conventional heat exchangers in WWTPs is maintenance caused by clogging. Other concerns are heat exchanger weight and space requirements which are often limiting factors.

A better alternative to a conventional heat exchanger with less maintenance requirements and less construction restriction is highly desired and proposed here. Figure 5-2 shows a table which is generated by Spirax Sarco Inc., listing some of the applications they worked on.

Customer	Heat source	Application	Energy recovered	Payback period
Steel casting company in the Czech Republic	Exhaust at 450ºC from melting furnaces	Heating HVAC services water	560kW	6 months
Ceramic tile manufacturing company in India	Exhaust at 316ºC from tile kilns	Pre-heating the air entering the tile kilns	610 kW	16 months
Automotive parts manufacturer in the USA	Exhaust at 400ºC from an aluminium furnace	Pre-heating the air entering the aluminium furnace	530kW	16 months
Portable power provider in Botswana	Exhaust at 325ºC from heavy fuel oil boilers	Pre-heating heavy fuel oil	120kW	3 months
Oil & gas well head thermal oxidiser manufacturer in Canada	Exhaust gas at 350ºC from a diesel oil fuelled burner	Pre-heating burner combustion air	1,840kW	5 months

Figure 5-2: Spirax Sarco Inc., examples of heat pipes based energy recovery systems

5.1. Governing equations for a HPHE

To understand how to analyze a HPHE, we have to understand the configuration of a HPHE. The HPHE looks like a bank of tubes heat exchanger with two different and unmixed counter flows

over the tubes. In this section, we present the solutions of the energy equation for the two flows that shows coupling the thermal energy equations in hot and cold sides of a HPHE system.

Similar to heat exchangers, knowing NTU and effectiveness of the HPHE are important and as one knows their relationship, then can plot the effectiveness-NTU similar to what has been done for different configurations of heat exchangers.

In Tan & Liu et al.'s 1990 paper, the authors used the ε-NTU (effectiveness-NTU) method. The effectiveness-NTU method is based on the ratio of the maximum heat transfer rate in a heat exchanger $\varepsilon = \frac{q}{q_{max}}$ which is the solution of thermal energy equation when the two streams exchange heat through the wall.

Tan & Liu et al. considered a heat pipe heat exchanger as two flows coupled indirectly where heat pipes provide the coupling. The overall effectiveness of a HPHE was expressed as a function of two separate heat exchangers: one heat exchanger between the hot fluid stream and the evaporating working fluid (inside the heat pipes), and the other between the condensing working fluid (inside the heat pipes) and the cold fluid stream. Therefore two different effectiveness values were introduced for the evaporator and the condenser sections of the HPHE. In this thermal model, they first started with modeling of one row of heat pipes, and then extended the model to n rows of heat pipes (also see Chaudourne, 1984). A row is defined as sets of heat pipes which are perpendicular to the flow direction (Figure 5-3).

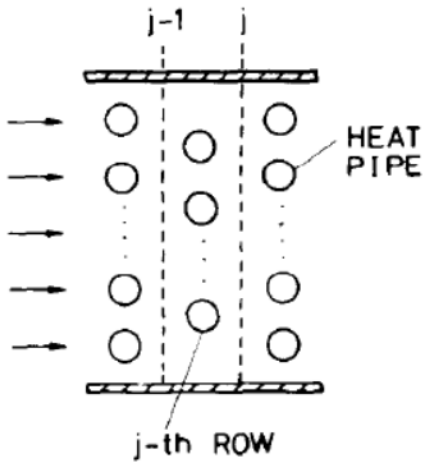

Figure 5-3: Huang et al. (1984) paper- illustration of a row in the staggered arrangement of heat pipes in a HPHE system

As shown in Tan & Liu et al. (1990), the Reynolds number and Nusselt number correlation for a HPHE are as follows:

$$\mathrm{Re} = \frac{\rho D_p v_{max}}{\mu}\left(\frac{\varepsilon_v}{1-\varepsilon_v}\right) \tag{5-1}$$

$$\mathrm{Nu} = f\left\{\left(0.5\,\mathrm{Re}^{1/2}\right)+\left(0.2\,\mathrm{Re}^{.21/.3}\right)\right\}\left(\mathrm{Pr}^{1/3}\right)\left(\frac{\mu}{\mu_w}\right) \tag{5-2}$$

Also

$$\mathrm{Nu} = \left(\frac{hD_p}{k}\right)\left(\frac{\varepsilon_v}{1-\varepsilon_v}\right) \tag{5-3}$$

where D_p is $1.5d_o$ (d_o is heat pipe outside diameter), v_{max} is the maximum possible velocity in HPHE (refer to banks of tubes section in Bergman, Lavine, et al., textbook), ε_v is void fraction, μ and k are dynamic viscosity and thermal conductivity of the external fluids flow in the HPHE system, h is convective heat transfer coefficient, f is a parameter that depends on the number of

rows in the HPHE and the geometrical arrangement of the heat pipes, Re is Reynolds number and Pr is Prandtl number. In the same literature, the thermal conductance in evaporator and condenser regions are as follows:

$$(UA)_e = \left(\frac{1}{(UA)_{HP,1\,Row}} + \frac{1}{(hA)_e} \right)^{-1} \tag{5-4}$$

$$(UA)_c = \left(\frac{1}{(UA)_{HP,1\,Row}} + \frac{1}{(hA)_c} \right)^{-1} \tag{5-5}$$

where $(UA)_{HP,1\,Row}$ refers to a row of heat pipes in a system of HPHE and its area is the heat pipes *cross-sectional area* for 1 row of heat pipes. Also $(hA)_e$ and $(hA)_c$ are thermal conductance of the flow in the evaporator and condenser regions respectively and their area are the heat pipe *surface area* for 1 row of the heat pipes in HPHE. The total thermal conductance in HPHE is

$$(UA)_{HPHE} = \left(\frac{1}{(UA)_{HP,1\,Row}} + \frac{1}{(hA)_e} + \frac{1}{(hA)_c} \right)^{-1} (N_L)^{-1} \tag{5-6}$$

where N_L is the number of rows in the HPHE system.

Note that A in $(UA)_{HP}$ is cross-sectional area of the heat pipe, but in $(hA)_e$ and $(hA)_c$, A is the heat transfer area (surface area) of the heat pipes.

To show the correlation for NTU in the evaporator and condenser sides of the HPHE, first we analyze one row of heat pipes in a HPHE. By definition, in the evaporator side of the HPHE:

$$NTU_e = \frac{(UA)_e}{(\dot{m}c_p)_e} = \frac{(UA)_e}{C_e} \tag{5-7}$$

and in the condenser side of the HPHE:

$$NTU_c = \frac{(UA)_c}{(\dot{m}c_p)_c} = \frac{(UA)_c}{C_c} \tag{5-8}$$

where U is the thermal conductance. Subscripts ‘e’ and ‘c’ are for evaporator and condenser sections. C_e and C_c are thermal capacity of the fluid passing through the evaporator and condenser sections respectively.

The corresponding effectiveness of the evaporator and condenser sides are the solutions of the thermal energy equation under the condition that the temperature of the evaporating or condensing fluid is uniform throughout the HPHE:

$$\varepsilon_e = 1 - e^{-NTU_e} \tag{5-9}$$

$$\varepsilon_c = 1 - e^{-NTU_c} \tag{5-10}$$

According to Chaudourne (1984), the effectiveness of a single row of heat pipes in a heat exchanger system (ε_p) results from coupling the evaporator and condenser sides for one row of heat pipes:

$$\varepsilon_p = \left(\frac{1}{\varepsilon_e} + \frac{C_e}{C_c \times \varepsilon_c} \right)^{-1} = \left(\frac{1}{\varepsilon_e} + \frac{C_r}{\varepsilon_c} \right)^{-1} \qquad \text{if } C_e < C_c \tag{5-11}$$

$$\varepsilon_p = \left(\frac{1}{\varepsilon_c} + \frac{C_c}{C_e \times \varepsilon_e} \right)^{-1} = \left(\frac{1}{\varepsilon_c} + \frac{C_r}{\varepsilon_e} \right)^{-1} \qquad \text{if } C_c < C_e \tag{5-12}$$

where C_r is the capacity ratio (C_{min}/C_{max}).

The HPHE has n number of rows, therefore with expanding the model for n rows of heat pipes, meaning n heat exchangers connected in series, we can obtain the overall effectiveness of the HPHE:

$$\varepsilon = \frac{1 - \left(\frac{1 - C_r \varepsilon_p}{1 - \varepsilon_p} \right)^n}{C_r - \left(\frac{1 - C_r \varepsilon_p}{1 - \varepsilon_p} \right)^n} \tag{5-13}$$

5.2. Heat pipe heat exchanger design validation for a sample WWTP

In this part, we show our heat pipe design validation with literature. Unfortunately the authors usually do not provide all of the details of the heat pipes they used or designed, but we used one of these papers which provided more details on their designed heat pipes that they used in their experimental apparatus.

5.2.1. Validation with Huang et al. (1984) results and using Tan & Liu et al. (1990) equations

In Huang et al. (1984) paper there is a curve for total energy versus flow rate that we thought it is worthy to regenerate it. To clarify the model to design the heat pipe heat exchanger, we used Tan & Liu et al., 1990 paper who validated their heat pipe design (heat pipe mean conductance reported as 3.36 W/°C in Huang et al.) with Huang et al.'s (1984) reported value.

To wrap up the validation, I checked my design with Chaudourne's (1984) effectiveness versus overall NTU solutions which shows the behavior of the heat pipe heat exchangers when $0 \leq C_r \leq 1$ and its effect on NTU. In my HPHE design to validate with Chaudorne's graph, I considered to arrange heat pipes in equilateral triangle staggering configuration refer to Matos et al. (2004) results.

To validate my design approach, I modeled a HPHE based on the specifications in Table 5-1 from Huang et al. (1984) paper:

Table 5-1: Huang et al. HPHE specifications

Number of rows, N	4
Number of heat pipes in each row, n_j	8
Total number of heat pipes	32
Condenser length of heat pipes, L_c	305 mm
Evaporator length of heat pipes, L_e	305 mm
Pipe arrangement	staggered
Pipe pitch : longitudinal	44.7 mm
transverse	38.7 mm
Cross-section : for hot flow	305×380 mm^2
for cold flow	305×380 mm^2

The Huang et al. (1984) HPHE operated under counter-flow conditions with air flowing in the condenser and evaporator sections. In the experimental set-up, to provide a hot air flow at the temperature up to 300°C, the authors installed a 30 kW electric heater in the rectangular hot air duct.

In Fig. 8 of Huang et al. (1984), the flow rate is given as SCMM which means in Standard Cubic Meter per Minute. By inspection and efforts to generate the graph, we suspect the reported values in the graph are regular flow rate (m^3/min) not Standard flow rate.

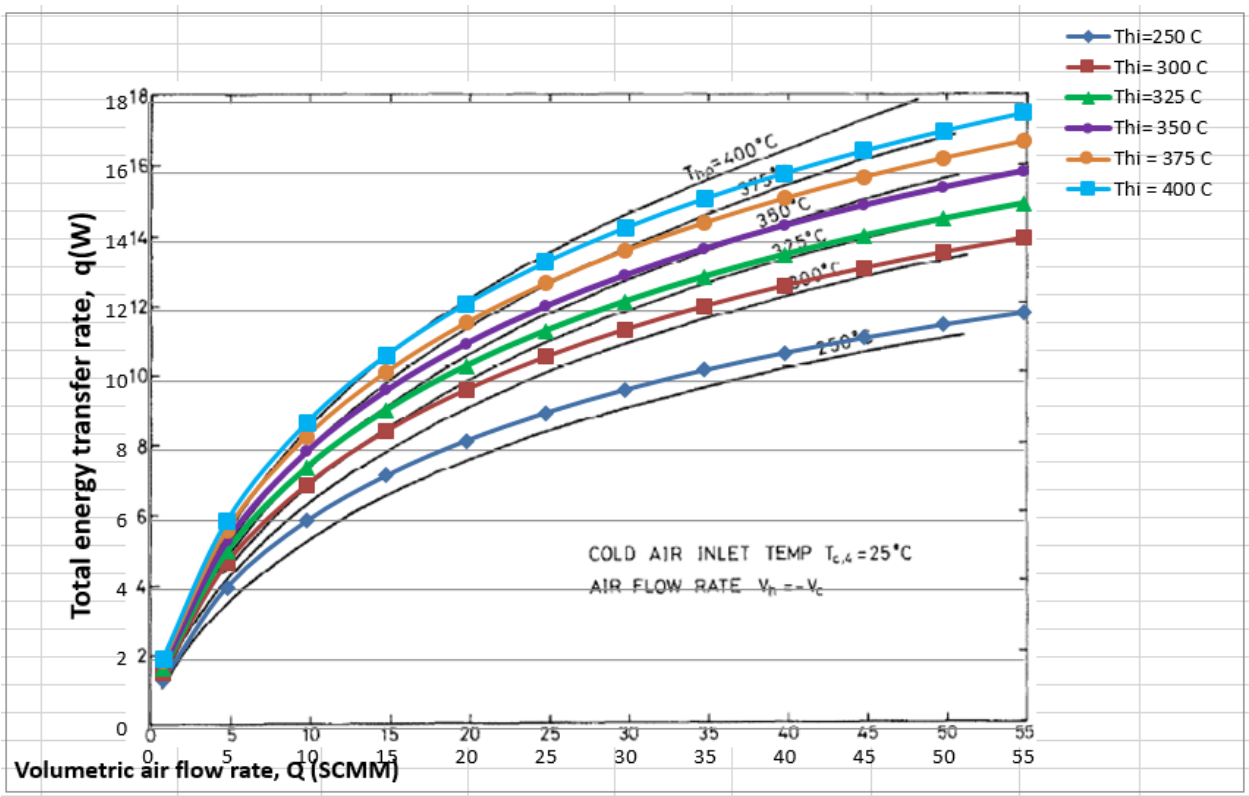

Figure 5-4: Validation of Fig. 8 of Huang et al. (1984) results. Total heat transfer rate (W) versus volumetric flow rate of air (m^3/min)

As shown in Figure 5-4, the colorful lines which are our model are close to the model based on the finite difference equations of Huang et al. (1984) results. A small deviation could be because of the difference between the finite difference approach and our approach.

5.2.2. Validation with Chaudourne (1984) model

In another effort, I validated the design with regenerating the curves provided in HPHE model by Chaudourne (1984) and I considered to arrange heat pipes in equilateral triangle staggering configuration refer to Matos et al. (2004) results.

In Fig. 4 of Chaudourne's work, HPHE effectiveness versus overall number of transfer units (NTU) for 10 rows of heat pipes is shown. Since both effectiveness and NTU are dimensionless,

they are independent of the flow rates, temperatures in evaporator and condenser side, number of heat pipes in a row, etc. Therefore we could validate our HPHE designs, using the sample WWTP data for 10 rows of heat pipes in HPHE.

Chaudourne (1984) starts with coupling evaporator and condenser sides for a row of heat pipes then expands the concept to all of the rows in the HPHE system (as we discussed previously in governing equations for HPHE).

In Chaudourne (1984) paper, they made the HPHE thermally balanced, meaning $NTU_e = NTU_c = NTU_{overall}$. Under this condition, the author plotted overall effectiveness versus overall NTU of the heat exchanger system. To validate Fig. 4 of the paper, I varied number of heat pipes in each row, as well as the mass flow rate in either condenser or evaporator to obtain C_r ranging from 0 to 0.9999 (as C_r=1 makes some values in our calculations indefinite). The number of rows kept constant similar to the paper. Then I checked my solution to be the same as Chaudourne (1984) solution (the author's solutions are shown in Figure 6-2 of CHAPTER 6 of this dissertation).

5.2.3. Calculating overall NTU for a HPHE system

In part of the process to validate with Chaudourne (1984), I needed to relate overall HPHE system NTU to NTU of one row of heat pipes. Therefore I correlated the heat pipe equations to obtain the overall NTU in a system which uses rows and columns of the heat pipes.

From earlier discussion, it is known that for one row of heat pipes in a HPHE,

$$NTU_e = NTU_{e,1Row} == \frac{(UA)_{e,1Row}}{C_e} \tag{5-14}$$

therefore we can conclude that

$$NTU_{e,tot} = N_L \times NTU_{e,1Row} \tag{5-15}$$

Similarly for the condenser side of HPHE:

$$NTU_c = NTU_{c,1Row} = \frac{(UA)_{c,1Row}}{C_c} \tag{5-16}$$

$$NTU_{c,tot} = N_L \times NTU_{c,1Row} \tag{5-17}$$

Now overall UA for the heat exchanger system is obtainable:

$$(UA)_{overall} = \frac{1}{\left[\frac{1}{(UA)_{e,1Row}} \times \frac{1}{N_L}\right] + \left[\frac{1}{(UA)_{c,1Row}} \times \frac{1}{N_L}\right]} = N_L \times \frac{1}{\frac{1}{(C_e \times NTU_{e,1Row})} + \frac{1}{(C_c \times NTU_{c,1Row})}}$$

or

$$(UA)_{overall} = \frac{1}{\left(\frac{1}{C_e \times NTU_{e,tot}}\right) + \left(\frac{1}{C_c \times NTU_{c,tot}}\right)}$$

Finally the overall NTU is as follows

$$NTU_{overall} = \frac{(UA)_{overall}}{(\dot{m}C_p)_{min}} = \left\{\left(\frac{1}{C_e \times NTU_{e,tot}}\right) + \left(\frac{1}{C_c \times NTU_{c,tot}}\right)\right\}^{-1} / C_{min} \tag{5-18}$$

If $C_e = C_c$ then $C_e = C_c = C_{min}$ and then the corresponding overall NTU is

$$(NTU)_{overall} = \left(\frac{1}{NTU_e} + \frac{1}{NTU_c}\right)^{-1} \tag{5-19}$$

CHAPTER 6

6. Heat exchanger comparisons

All of the comparison ideas and results of this chapter are my work under Dr. Adrienne Lavine's guidance. To begin, first I refer to the theory behind the HPHE design and I talk about the significant parameters in HPHE design and remind the correlations from the literatures.

In heat exchanger design and application, thermal resistance has a very important role in making one type be preferable to another type of heat exchanger. The thermal resistances depend on flow rates, flow types, fluid properties and geometry of the HPHE.

The thermal resistances affect the effectiveness of heat exchangers and the effectiveness also depends on the type of the exchangers, flow rates, heat transfer area and other flow characteristics of the flow as well as the fluid properties.

Another parameter that affects the thermal resistance is NTU (number of transfer units, see Eq. (5-7) and (5-8) in CHAPTER 5 or Eq. (6-1) and (6-2) of this chapter). NTU is a function of fluid properties (i.e. density), volumetric flow rate and heat transfer area.

As shown in Figure 6-1, as the heat capacity ratio ($C_r = C_{min} / C_{max}$) decreases, the effectiveness of the counter flow heat exchanger increases. Typically, one fluid flow rate (of the "target" fluid) is fixed by the requirements of the application, and C_r can be decreased by increasing the flow rate of the other fluid (the "working" fluid, which becomes C_{max}). However, there is a limit to how small C_r can be made, because in practice the working fluid flow rate is restricted and there is an energy cost to run the flow. Thus increasing NTU is a key to achieve better effectiveness in a counter flow heat exchanger. Higher value of NTU is obtainable by increasing surface area and overall heat transfer coefficient (given that C_{min} is fixed by the requirement of the application). In

a counter flow heat exchanger, as effectiveness correlation indicates ($\varepsilon = \frac{1-\exp\left[-\mathrm{NTU}(1-C_r)\right]}{1-C_r\exp\left[-\mathrm{NTU}(1-C_r)\right]}$), for large enough value of C_r ($\varepsilon = \frac{\mathrm{NTU}}{1+\mathrm{NTU}}$ when $C_r = 1$) even when NTU is a big value, effectiveness equals to unity is not obtainable in theory.

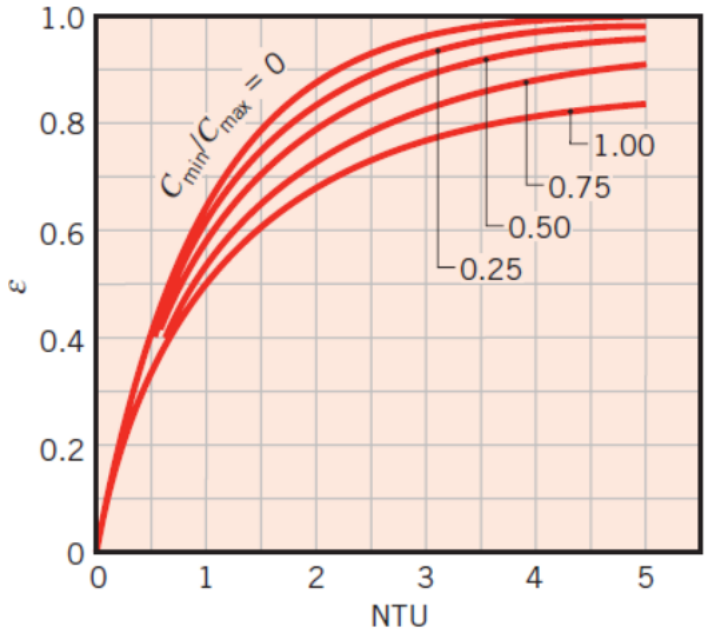

Figure 6-1: Effectiveness of a counter flow heat exchanger (Bergman, Lavine et al., textbook, 7th edition)

Similar to the counter flow heat exchanger, Figure 6-2 shows the effectiveness of HPHE versus the overall number of transfer units (NTU) which has been generated by Chaudourne (1984) for 10 rows of heat pipes under NTU_h=NTU_c condition. By investigating ε correlation for the HPHE system, effectiveness equal to unity is obtainable in theory when NTU is large enough.

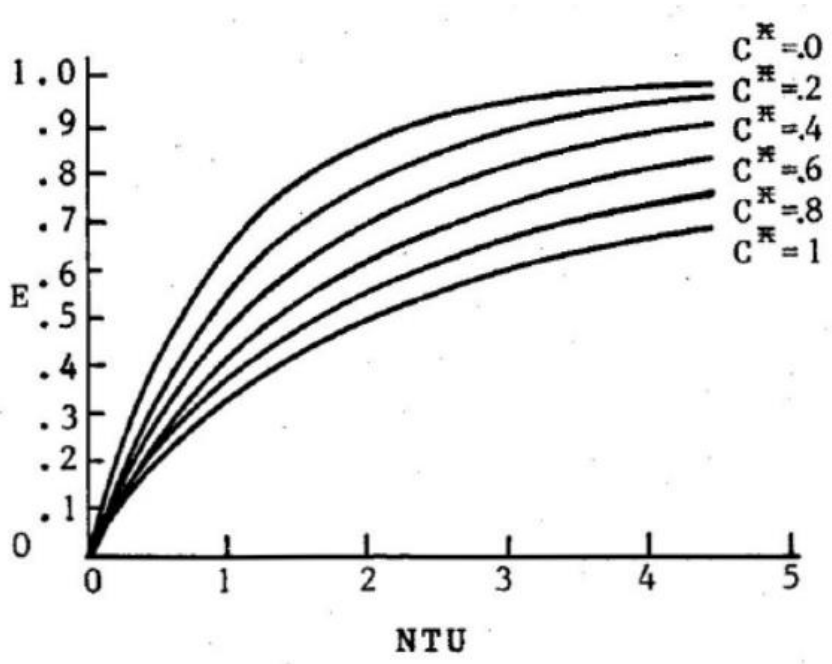

Figure 6-2: Effectiveness of a HPHE versus the overall NTU, Chaudourne (1984)

The equations for the NTU and effectiveness of the HPHE are given in HPHE chapter but we repeat them here again. Number of transfer units in the evaporator and condenser sides of the HPHE are as follows:

$$NTU_e = \frac{U_e A_e}{(\dot{m} c_p)_e} = \frac{U_e A_e}{C_e} \tag{6-1}$$

$$NTU_c = \frac{U_c A_c}{(\dot{m} c_p)_c} = \frac{U_c A_c}{C_c} \tag{6-2}$$

where according to Tan and Liu, (1990),

$$(UA)_e = \frac{1}{\frac{1/2}{(UA)_{HP,1Row}} + \frac{1}{(hA)_e}} \tag{6-3}$$

$$(UA)_c = \frac{1}{\frac{1/2}{(UA)_{HP,1Row}} + \frac{1}{(hA)_c}} \tag{6-4}$$

In Eq. (6-3) and (6-4) in the term $(UA)_{HP,1Row}$, A is the heat pipe cross-sectional area A in the terms $(hA)_h$ and $(hA)_c$ is the heat pipes surface area.

The corresponding effectiveness of the evaporator and condenser sides which are the solutions of the thermal energy equation are:

$$\varepsilon_e = 1 - e^{-NTU_e} \tag{6-5}$$

$$\varepsilon_c = 1 - e^{-NTU_c} \tag{6-6}$$

Then according to Chaudourne (1984), the effectiveness of a single row of heat pipes in a heat exchanger system (ε_p) results from coupling the evaporator and condenser sides for one row of heat pipes:

$$\varepsilon_p = \left(\frac{1}{\varepsilon_e} + \frac{C_e}{C_c \times \varepsilon_c} \right)^{-1} = \left(\frac{1}{\varepsilon_e} + \frac{C_r}{\varepsilon_c} \right)^{-1} \quad \text{if } C_e < C_c \tag{6-7}$$

$$\varepsilon_p = \left(\frac{1}{\varepsilon_c} + \frac{C_c}{C_e \times \varepsilon_e} \right)^{-1} = \left(\frac{1}{\varepsilon_c} + \frac{C_r}{\varepsilon_e} \right)^{-1} \quad \text{if } C_c < C_e \tag{6-8}$$

where C_r is the capacity ratio (C_{min}/C_{max}) and subscripts “c” and “e” are for the condenser and evaporator sides.

Expanding the model for n rows of heat pipes, meaning n heat exchangers connected in series, we obtain the overall effectiveness of the HPHE:

$$\varepsilon = \frac{1 - \left(\frac{1 - C_r \varepsilon_p}{1 - \varepsilon_p} \right)^n}{C_r - \left(\frac{1 - C_r \varepsilon_p}{1 - \varepsilon_p} \right)^n} \tag{6-9}$$

As shown in Figure 6-2, to achieve the highest effectiveness, we have to achieve the highest possible NTU. For an example from Eq. (6-5), for a large value of NTU, ε_e would be unity. Then in Eq. (6-9), ε for a HPHE can reach to 1 at the highest values of NTU as C_r goes to zero.

In all cases of the comparisons in this chapter, the inlet temperatures and the flow rates are based on the data from a sample WWTP, except that in the water-air and air-air comparisons the air temperature is estimated as the exhaust air temperature from burning methane in a digester and the liquid inlet temperature is the sludge temperature entering into a digester without any preheating. We also fix the width and the height of the exchangers based on the width and height of the operating spiral heat exchanger.

In the existing spiral heat exchanger in Oceanside WWTP, the hot fluid is water and the cold fluid is sludge and in water-water comparisons we keep this order. In water-air HPHE system cold fluid is also the sludge water with the reported flow rate from a sample WWTP.

Generally we followed these rules for the comparisons:

1. The HPHE design is based on the preliminary heat pipe design from CHAPTER 4, with the following dimensions and properties that are taken from Table 4-5:

Table 6-1: The designed heat pipe parameters which has been inserted in HPHE

d_v (m)	t_w (m)	d_o (m)	N (1/in)	d_{sw} (m)	t_{sw} (m)	$L_e=L_c$ (m)	L_a (m)
0.0198	0.0010	0.0243	200	6.35e-05	0.001	0.51	0.05

2. When one of the flow pair is water, we used the real values for flow rate of a spiral heat exchanger which is operating in a sample WWTP (Oceanside). If both flows are water then the flow rate and the temperatures are from real data of the sample WWTP ($C_r \approx 1$ case).

3. In the HPHE we changed the length of the heat pipe heat exchanger to achieve the same outlet temperatures (meaning the same effectiveness) that the spiral heat exchanger achieves (other dimensions are the same as reported for the operating spiral heat exchanger in Oceanside WWTP) with different fluid pairs. This way we can see which type of heat exchanger works better (requires shorter length) under the same operating temperature, width and height.
4. In all cases we kept the cold flow as the minimum flow (flow rate which has minimum $\dot{m}c_p$).

6.1. Comparisons basis

In the following comparisons we investigate the fluid type effects on the thermal resistances, on the effectiveness of the spiral heat exchanger and the heat pipe heat exchanger (HPHE), and then we will see under the same temperatures and flow rates which heat exchanger can achieve the desired performance with shorter length. To do this, different pairs of fluids have been investigated: water-water, air-air and water-air.

6.2. Water-water heat exchanger comparisons

In this section we show the comparisons between spiral heat exchanger and HPHE under the same conditions. According to Eq. (6-1) and (6-2), the higher NTU in each flow section is possible by decreasing $(\dot{m}c_p)$, which affects effectiveness of the HPHE. Therefore we kept the cold flow rate the same as the data and adjusted the hot flow rate to see how different ranges of C_r impact the heat exchanger performance and which heat exchanger would have shorter length. According

to the data provided by the sample WWTP, the volumetric flow rate of sludge and fresh water are the same, therefore we automatically have $C_r \approx 1$ for water-water comparison case.

In Table 6-2 we summarized the fixed and the calculated values for spiral heat exchanger and HPHE when both flows are water. As shown, the comparisons of heat exchangers are based on two extremes for C_r ($C_r \ll 1$ and $C_r \approx 1$). The fixed parameters are the controllable ones (T_{hi}, T_{ci}, T_{ho}, T_{co}, Q_c, Q_h, width and height) and only HPHE length is changed to get the effectiveness similar to spiral heat exchanger.

Table 6-2: Water-water spiral heat exchanger and HPHE comparisons under $C_r << 1$ and $C_r \approx 1$ conditions

	$C_r \approx 1$		**$C_r << 1$**	
	Spiral HX	**HPHE**	**Spiral HX**	**HPHE**
T_{ci} (°C)	55		55	
T_{hi} (°C)	61.2		61.2	
T_{co} (°C)	58.08		60.07	
T_{ho} (°C)	58.01		61.17	
ε	0.52		0.810	
Q_c (m^3/s)	0.035		0.035	
$\dot{m}_c$ (kg/s)	34.2		34.2	
Q_h (m^3/s)	0.033		2.28	
$\dot{m}_h$ (kg/s)	32.0		2,242.6	
HE Width (m)	0.7		0.7	
Height (m)	-	1.07	Height (m)	-
Re_h	355,000	61,000	24,877,594	4,241,816
Nu_h	711	490	21,285	7,121
h_h ($W/m^2.K$)	12,500	4,455	375,250	64,730
$(UA)_e$ (W/K)	-	236.0	-	258
NTU_h (1 row)	-	2.2	-	0.000028
Re_c	288,000	50,000	288,434	49,580
Nu_c	700	475	699	475
h_c ($W/m^2.K$)	9,200	4,300	9,203	4,272
$(UA)_c$ (W/K)	-	235	-	235
NTU_c (1 row)	-	1.97	-	0.002
UA_{tot}	140,500	140,600	237,851	238,149
NTU_{tot}	1.1	-	1.7	-
q_{HE}(kW)	823.4	823.4	878.8	878.8
Length (m)	17.4	**46.1**	17.4	**74.8**
$A_{s,tot}$ (m^2)	27	1,390	26.5	2,251.4
$(A_{s,tot}/L)$ (m^2/m)	1.5	30.1	1.5	30.1
N_L	-	1,193	-	1,935
N_T	-	15	-	15
S_T(m)	-	0.046	-	0.046
S_L(m)	-	0.040	-	0.040

The Reynolds numbers, Nusselt numbers, and heat transfer coefficients in Table 6-2 have been calculated from the equations shown in CHAPTER 5 of this dissertation which are adopted from Tan and Liu et al. (1990) paper.

According to the results in Table 6-2:

- Considering that the height and width of the heat exchangers are fixed, the ($A_{s,tot}$/L) (m^2/m) values in Table 6-2 show that the HPHE offers more surface area in a fixed volume.
- Table 6-2 also shows the length comparisons of the heat exchangers. In the water-water heat exchangers, for both $C_r \approx 1$ and $C_r << 1$, using a HPHE is not favorable because with the same effectiveness, width and height for the heat exchangers, the HPHE requires a longer length.

It will later be shown that the HPHE system works better than the spiral heat exchanger under some circumstances. To understand the conditions that make the HPHE system work better, we have to go deep in thermal resistances analysis.

6.2.1. Thermal resistances in water-water HPHE comparisons

In this section we investigate why HPHE works better under certain conditions by analyzing the thermal resistances.

In a HPHE, the total thermal resistance is the sum of three individual thermal resistances, one inside each heat pipe ($R_{HP,1\ Row}$) and the other two for the hot (R_e) and cold fluids flow (R_c) outside the heat pipe.

According to Chi (1976) textbook, the thermal resistances inside a heat pipe are introduced as below:

$$(UA)_{HP} = \frac{1}{R_{HP}}\left(\frac{W}{K}\right)$$

$$(UA)_{HP} = \frac{1}{\left(R_{p,e} + R_{w,e} + R_v + R_{w,c} + R_{p,c}\right)}\left(\frac{W}{K}\right) \qquad (6\text{-}10)$$

When A is used as the heat pipe cross-sectional area, then Eq.(6-10) becomes

$$(UA)_{HP} = \frac{1}{\left(\frac{t_p}{2\pi L_e r_o k_p} + \frac{t_w}{2\pi L_e r_i k_{eff,e}} + \frac{T_v F_v \left(\frac{L_e}{6} + L_a + \frac{L_c}{6} \right)}{\rho\lambda} + \frac{t_w}{2\pi L_c r_i k_{eff,c}} + \frac{t_p}{2\pi L_c r_o k_p} \right)} \left(\frac{W}{K} \right) \quad (6\text{-}11)$$

When the heat pipe is exposed to the external hot and cold flows in the HPHE, the total resistance of one row of heat pipes would be as follow:

$$R_{HPHE,\,1Row} = \frac{1}{\frac{1}{(UA)_{HP,1Row}} + \frac{1}{(hA)_e} + \frac{1}{(hA)_c}} \left(\frac{K}{W} \right) \quad (6\text{-}12)$$

where h_e and h_c are the heat transfer coefficient of the external flow passing over the heat pipes in the evaporator and the condenser sides respectively. In Eq. (6-12), all areas are for ONE row of heat pipes.

Note that in Eq. (6-12), A associated with U_{HP} is the heat pipe cross-sectional area, but the A is associated with h_e and h_c is the heat pipe surface area.

In Table 6-3 and Table 6-4 thermal resistances comparison for the water-water HPHE when $C_r \approx 1$ and $C_r << 1$ are given. The order of magnitude comparisons clarifies when using the HPHE is favorable.

Table 6-3: Thermal resistances comparison for water-water HPHE (for the heat pipes designed with the specifications in Table 6-1), $C_r \approx 1$

$R_{HP,1\ Row}$ (K/W)	R_e (K/W)	R_c (K/W)	$R_{HPHE,\ 1\ Row}$ (K/W)	$(UA)_{HPHE,1\ Row}$ (W/K)
0.0077	0.0004	0.0004	0.0085	118

Table 6-4: Thermal resistances comparison for water-water HPHE (for the heat pipes designed with the specifications in Table 6-1), $C_r << 1$

$R_{HP,1\ Row}$ (K/W)	R_e (K/W)	R_c (K/W)	$R_{HPHE,\ 1\ Row}$ (K/W)	$(UA)_{HPHE,1\ Row}$ (W/K)
0.00770	0.000027	0.00040	0.0081	123.1

Based on the thermal resistances comparison shown in Table 6-3 and Table 6-4:

- The internal thermal resistance for a row of heat pipes in the HPHE is large relative to the external resistances for the flow over the heat pipes in the evaporator and condenser sections. Thus, the thermal resistance inside a heat pipe is a limiting factor which makes the HPHE system work poorly for liquid flows over heat pipes for both $C_r \approx 1$ and $C_r << 1$.
- The external flow's thermal resistance is a function of the flow (fluid type and flow rate which impact Re# and Nu#) and geometry (dimensions of heat pipes and HPHE system). In the case when the resistance of the heat pipe is *not* dominant, changing any of the mentioned parameters which would decrease the external flows' thermal resistances is beneficial to run the HPHE with better effectiveness.
- The overall conclusion is that if we would like to replace an existing heat exchanger with a HPHE, thermal resistance analysis would help a lot to determine the conditions for which it would work better than a conventional heat exchanger.

6.3. Air-air heat exchanger comparison

In this set of comparison, we choose the fluid pair as air-air. Similar to the previous comparison, all controllable parameters are fixed and only the HPHE length changed to get the same effectiveness as in spiral heat exchanger under the same conditions.

The exhaust gas of burning methane in a digester behavior is very close to air, then we model it as air, and then we are interested to study the behavior air-air HPHE.

Note: The flow rate of the cold air in Table 6-5 is from a realistic data from the sample WWTP, and its inlet temperature has been assumed the ambient temperature of the air. The inlet temperature of the hot air has been estimated from the burning methane gas leaving the digester stack but its flow rate has been adjusted to reach the $C_r \approx 1$ and $C_r << 1$. We fixed the heat exchangers' width based on the data from Spiral HE operating in Oceanside WWTP, as well as the effectiveness (exit temperatures of the flows) based on the effectiveness of the spiral heat exchanger under the fixed parameters in Table 6-5.

The fixed and calculated values for the two sets of comparisons for $C_r \approx 1$ and $C_r << 1$ when the running fluids are air-air, are summarized in Table 6-5.

Table 6-5: Air-air spiral heat exchanger and HPHE comparisons under $C_r << 1$ and $C_r \approx 1$ conditions

	$C_r \approx 1$		**$C_r << 1$**	
	Spiral HX	**HPHE**	**Spiral HX**	**HPHE**
T_{ci} (°C)	20		20	
T_{hi} (°C)	232		232	
T_{co} (°C)	35.88		58.33	
T_{ho} (°C)	216.35		224.64	
ε	0.075		0.18	
Q_c (m^3/s)	2.99		2.99	
$\dot{m}_c$ (kg/s)	0.314		3.61	
Q_h (m^3/s)	0.451		2.3	
$\dot{m}_h$ (kg/s)	0.314		1.6	
HE Width (m)	0.7		0.71	
Height (m)	-	1.07	-	1.1
Re_h	29,512	5,1110	149,442	25,726
Nu_h	76	82	278	219.5
h_h ($W/m^2.K$)	81	45	297	120
$(UA)_e$ (W/K)	-	23.6	-	55.05
NTU_h for 1 row	-	0.108	-	0.077
Re_c	505,983	88,252	505,983	87,845
Nu_c	726	482	726	480
h_c ($W/m^2.K$)	375	167	374.52	167
$(UA)_c$ (W/K)	-	70.7	-	70.84
NTU_c for 1 row	-	0.323	-	0.46
UA_{tot}	1,768	1,753	4,389	4,399
NTU_{tot}	0.082	-	0.203	-
q_{HE}(kW)	344.8	344.1	829.0	830.68
Length (m)	17.4	**3.87**	17.4	**5.53**
$A_{s,tot}$ (m^2)	26.5	57.0	26.5	165.2
$(A_{s,tot}/L)$ (m^2/m)	1.5	29.4	1.5	29.87
N_L	-	99	-	142
N_T	-	15	-	15
S_T(m)	-	0.046	-	0.046
S_L(m)	-	0.040	-	0.040

As Table 6-5 indicates, the HPHE length is shorter than spiral heat exchanger length under the same conditions (for both $C_r \approx 1$ and $C_r << 1$) and in this case using the HPHE is favorable.

6.3.1. Thermal resistances comparisons in air-air HPHE

In Table 6-6 and Table 6-7 the thermal resistances of a row of heat pipes in a HPHE system are shown for the two cases $C_r \approx 1$ and $C_r << 1$.

Table 6-6: Thermal resistances for air-air HPHE (for the heat pipes with the specifications in Table 6-1) $C_r \approx 1$

$R_{HP,1\ Row}$ (K/W)	R_e (K/W)	R_c (K/W)	$R_{HPHE,\ 1\ Row}$ (K/W)	$(UA)_{HPHE,1\ Row}$ (W/K)
0.0077	0.0385	0.0103	0.0565	17.70

Table 6-7: Thermal resistances for air-air HPHE (for the heat pipes with the specifications in Table 6-1) $C_r << 1$

$R_{HP,1\ Row}$ (K/W)	R_e (K/W)	R_c (K/W)	$R_{HPHE,\ 1\ Row}$ (K/W)	$(UA)_{HPHE,1\ Row}$ (W/K)
0.0077	0.0143	0.0103	0.0323	30.98

Above comparisons between thermal resistances inside a heat pipe heat exchanger in the case of air flow in the evaporator and condenser sides of HPHE are given. When $C_r \approx 1$ the thermal resistances of the flows passing over the heat pipes are one order of magnitude larger than the thermal resistance inside the heat pipe, and that is the reason HPHE works favorably when air flows in the evaporator and condenser sides. Compared to a similar case in water-water HPHE, the heat transfer coefficient for air is smaller than for water mainly because it has lower thermal conductivity, therefore the thermal resistance for air is larger.

The same behavior applies for $C_r << 1$ in Table 6-7, which the thermal resistances of the external flows are dominant and then the HPHE works well for this case too.

As a result using heat pipe heat exchanger when both flows are air is favorable in these examples because the external flow thermal resistances are dominant.

6.4. Water-air Heat exchangers' comparisons

In this last comparison we have air in the hot side of the exchangers and in the cold side we have the sludge (modeled as water) that needs to be raised to a higher temperature. The water flow rate is as reported from the sample WWTP, and in the air side, we adjusted the air flow rate to achieve $C_r \approx 1$ and $C_r << 1$.

The inlet temperature of the cold side (sludge water) has been assumed at the ambient temperature (similar to the entering sludge to a digester without preheating). The inlet temperature of the hot air has been estimated from the burning methane gas leaving the digester stack.

We fix the heat exchangers' width based on the data from Spiral heat exchanger operating in Oceanside WWTP, as well as the effectiveness (exit temperatures of the flows) based on the effectiveness that the spiral heat exchanger achieves under the conditions in Table 6-8.

Table 6-8: Water-air spiral heat exchanger and HPHE comparisons under $C_r << 1$ and $C_r \approx 1$ conditions

	$C_r \approx 1$		**$C_r << 1$**	
	Spiral HX	**HPHE**	**Spiral HX**	**HPHE**
T_{ci} (°C)	20		20	
T_{hi} (°C)	232		232	
T_{co} (°C)	103.8		140.3	
T_{ho} (°C)	143.2		207.6	
ε	0.41		0.57	
Q_c (m^3/s)	0.035		0.035	
$\dot{m}_c$ (kg/s)	34.6		34.6	
Q_h (m^3/s)	179.1		1,303	
$\dot{m}_h$ (kg/s)	124.9		627.6	
HE Width (m)	0.7		0.7	
Height (m)	-	1.07	-	1.07
Re_h	11,738,511	2,026,097	58,983,057	10,177,474
Nu_h	9,113	3,376	33,153.8	9,478
h_h ($W/m^2.K$)	9,760	1,750	35,509	4,915
$(UA)_e$ (W/K)	-	207	-	238
NTU_h for 1 row	-	0.0015	-	0.0003
Re_c	94,312	16,412	94,312	16,406
Nu_c	462.5	360.7	462.5	361
h_c ($W/m^2.K$)	5,682	2,812	5,682	2,812
$(UA)_c$ (W/K)	-	224	-	224
NTU_c for 1 row	-	0.002	-	0.0016
UA_{tot}	95,090	95,159	129,698	129,718
NTU_{tot}	0.68	-	0.897	-
q_{HE}(kW)	12,108	12,115	17,394.15	17,398
Length (m)	17.4	**35.0**	17.4	**44.5**
$A_{s,tot}$ (m^2)	26.5	1,029	26.5	1,307
$(A_{s,tot}/L)$ (m^2/m)	1.5	29.3	1.5	29.4
N_L	-	884	-	1,123
N_T	-	15	-	15
S_T(m)	-	0.046	-	0.046
S_L(m)	-	0.040	-	0.040

According to Table 6-8, for water-air HPHE at both $C_r << 1$ and $C_r \approx 1$, the length of HPHE is longer than the spiral heat exchanger at similar conditions. The reason for this behavior is explained in the following thermal resistance comparisons.

6.4.1. Thermal resistances comparisons in water–air HPHE

In Table 6-9 and Table 6-10 comparisons between thermal resistances of the HPHE in the case of air flow in the evaporator and the condenser sides of HPHE are given.

Table 6-9: Thermal resistances water-air HPHE (for the heat pipes with the specifications in Table 6-1) $C_r \approx 1$

$R_{HP,1\ Row}$ (K/W)	R_e (K/W)	R_c (K/W)	$R_{HPHE,\ 1\ Row}$ (K/W)	$(UA)_{HPHE,1\ Row}$ (W/K)
0.00770	0.0010	0.00061	0.009	107.6

Table 6-10: Thermal resistances for water-air HPHE (for the heat pipes with the specifications in Table 6-1) $C_r << 1$

$R_{HP,1\ Row}$ (K/W)	R_e (K/W)	R_c (K/W)	$R_{HPHE,\ 1\ Row}$ (K/W)	$(UA)_{HPHE,1\ Row}$ (W/K)
0.00770	0.00035	0.00061	0.009	115.5

As the above tables show, the thermal resistances of external flows over the heat pipes are smaller than the thermal resistances inside the heat pipes, and therefore the HPHE does not work favorably in this case. This means the thermal resistance inside the heat pipe is the limiting parameter and does not effectively transfer heat from the evaporator to the condenser side of the HPHE system.

6.5. Chapter Conclusions

- To understand if a HPHE works favorably in a specific application, we should analyze the thermal resistances for one row of heat pipes in the HPHE system.
- If the thermal resistances of external flows over the heat pipes are higher than the thermal resistance inside each heat pipe, then it means that the increased heat transfer area of a HPHE is beneficial. In such a case, using HPHE would be favorable.
- If the vice versa applies, then using heat pipes in a heat exchanger cannot improve heat exchange and we have to think of another alternative to the HPHE.
- In this set of comparisons we found that if both fluids are air, then the HPHE is beneficial, but it should not be misunderstood that is the only case HPHE is favorable. Since the external thermal resistances depend on the flow rates and dimensions, it is possible to have large external resistances no matter what the fluid is, and in that case the HPHE could be beneficial.

CHAPTER 7

7. Heat pipe design refinement to shorten HPHE length

All of the methods and calculations, curves and results presented in this chapter are my work under guidance of Professor Adrienne Lavine.

In CHAPTER 4 when I was designing heat pipe, I did optimizations based on the literatures that has been referred in the same chapter. Those optimizations were for the length of the heat pipe and we do not have any criteria to optimize other parameters. In this chapter first I investigate what key parameters are sensitive in maximum heat pipe transfer rate (q_{limit}) and heat transfer coefficient (U_{HP}), and then I perform parametric study to see their behaviors on U_{HP} and q_{limit}.

Since we are using our designed heat pipe in HPHE system, if we increase the heat transfer coefficient (U_{HP}) we can have lesser heat pipes in the heat exchanger system. While we improve U_{HP}, we have to consider that maximum heat transfer rate per heat pipe (q_{limit}) should satisfy the required heat transfer rate per heat pipe ($q_{max,1HP\ in\ HPHE}$) in HPHE. Finally a method to refine the heat pipe design which leads to shorten the length of HPHE is suggested.

In CHAPTER 6 when we designed a HPHE we did not consider the fact that the heat load imposed on each heat pipe in the HPHE system might be higher or lower than the designed heat load. In fact we need to satisfy this inequality:

$$q_{limit} \geq q_{max,1HP\ in\ HPHE} \tag{7-1}$$

where q_{limit} is the heat transfer rate limit in a heat pipe (the minimum heat transfer load among all heat transfer limitations in a heat pipe, refer to APPENDIX for heat transfer limits in a heat pipe), and $q_{max,1HP\ in\ HPHE}$ is the maximum possible heat transfer rate for one heat pipe in the HPHE system, which will occur at one of the ends of the HPHE with the larger temperature difference:

$$q_{max1HP\ in\ HPHE} = \max\left\{\left(\frac{T_{hi} - T_{co}}{R_{tot\,1HP}}\right), \left(\frac{T_{ho} - T_{ci}}{R_{tot\,1HP}}\right)\right\} \quad (7\text{-}2)$$

In a heat pipe design if $q_{limit} < q_{max,1HP\ in\ HPHE}$ then we have to increase q_{limit} by varying the key parameters. And if $q_{limit} \geq q_{max,1HP\ in\ HPHE}$ applies, then we can use this opportunity to have shorter HPHE by decreasing q_{limit} to achieve $q_{limit} \approx q_{max,1HP\ in\ HPHE}$. Because as q_{limit} decreases, it is possible to increase U_{HP} and if it happens then we can achieve the desired effectiveness in a HPHE by using fewer rows of heat pipes.

Based on the above reasons, the purpose of this chapter is to refine our heat pipe design by adjusting q_{limit} based on the demands for the heat transfer rate of each heat pipe in the HPHE system and achieve the benefit of a shorter HPHE.

We are splitting the above goal into two parts:

- Refining the design of the heat pipe to adjust its heat transfer limit according to the demands in the HPHE ($q_{limit} \approx q_{max,1HP\ in\ HPHE}$) which in our case since $q_{limit} > q_{max,1HP,inHPHE}$ as we decrease q_{limit} , we will be seen to also automatically improve (increase) U_{HP}.
- And then optimize the HPHE design to achieve the desired effectiveness in a shorter length of the HPHE system (CHAPTER 8).

7.1.Key parameters in q_{limit} and U_{HP}

In heat pipe design there are parameters that may have significant effects on U_{HP} and maximum hear transfer limit (q_{limit}). We would like to study which of these parameters are more sensitive in the heat pipe design. The parameters as listed are those we can control:

d_v: heat pipe core diameter $d_v = 2(r_i - t_w)$

t_w: Wrapped screen wick thickness (when using wrapped screen as wick)

d_{sw}: Wrapped screen wire diameter

t_{sw}: Screen wire thickness

t_p: Heat pipe wall thickness

N: Number of meshes per inch

L_e: Length of the evaporator

L_c: Length of the condenser

k_p: Heat pipe wall thermal conductivity

In the above list, t_p and k_p are associated with the choice of pipe size and material. It will be seen later that thin pipe wall and high pipe thermal conductivity are desirable, however these variables are not that important and in practice would be selected from commercially available options based on other considerations such as compatibility with the heat pipe fluid. Therefore we will not explore these variables in detail. Also we do not have information about the variation and ranges of t_{sw}, then we can use it as a fixed parameter (as manufacturer provided to us) in this study.

To the best of our knowledge, in wrapped screen wicks, d_{sw} and N are discrete values which are related to each other. The information in the table below is provided by a heat pipe manufacturer:

Table 7-1: Discrete values for mesh number per inch and screen wire diameter for wrapped screen wick

N (1/inch)	d_{sw} (inch)
50	0.0075
100	0.0045
150	0.0026
200	0.0021
325	0.0014

For simplicity and to reduce the number of variables, we decided to use continuous variables for N and d_{sw}; then we made a correlation between N and d_{sw} values in Table 7-1 by curve-fitting:

$$d_{sw} = 0.215\times (N^{-0.923}) \quad (7\text{-}3)$$

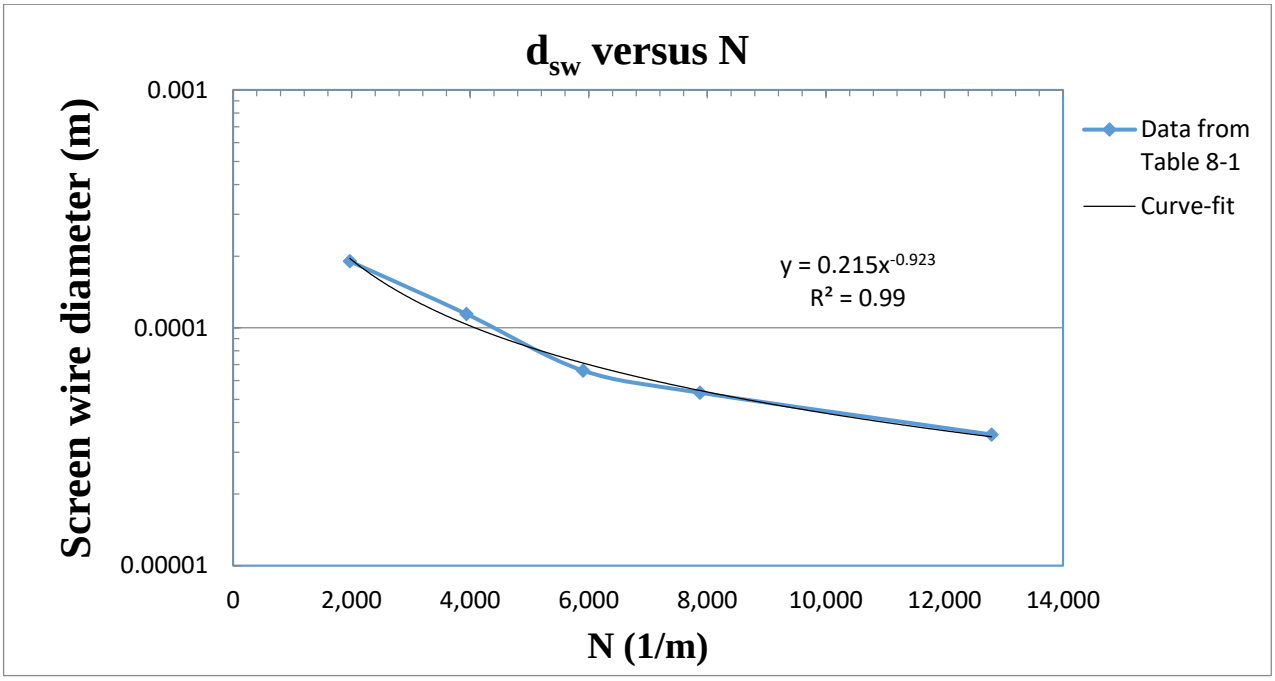

Figure 7-1: Screen wire diameter (d_{sw}) versus number of meshes per meter (N) for wrapped screen wick

Some results from the literature (as shown in CHAPTER 4) can help us to reduce the number of key parameters among those listed previously. Jafari, Shamsi, Filippeschi et al., (2017) ran an optimization algorithm as well as experimental analysis and found that the optimum L_e/L_c is around 1 which improves the heat transfer capability per heat pipe and decreases the thermal resistance inside a heat pipe. Also in another paper by Tan, Liu and Wong (1991), the authors found that the optimum ratio of a heat pipe evaporator length to the total length is 1/2. We used both of these results and let $L_e = L_c$ and $L_e/L_{total} = 0.5$.

By relating N to d_{sw} and also letting $L_e = L_c$, we reduce the key parameters to four: d_v, t_w, L_e, and N.

Before starting to refine the heat pipe design, we have to get a deeper understanding of how U_{HP} of a heat pipe changes with the variables d_v, t_w, L_e, and N.

7.2. Effects of the key parameters on the thermal resistances inside a heat pipe

In Chi (1976) textbook, the thermal resistances in a heat pipe are related to the conductance, $(UA)_{HP}$, as below:

$$(UA)_{HP} = \frac{1}{\left(R_{p,e} + R_{w,e} + R_v + R_{w,c} + R_{p,c}\right)} \left(\frac{W}{m^2K}\right) \tag{7-4}$$

The resistances are expressed as below

$$(UA)_{HP} = \frac{1}{\left(\frac{t_p}{2\pi L_e r_o k_p} + \frac{t_w}{2\pi L_e r_i k_{eff,e}} + \frac{T_v F_v \left(\frac{L_e}{6} + L_a + \frac{L_c}{6} \right)}{\rho\lambda} + \frac{t_w}{2\pi L_c r_i k_{eff,c}} + \frac{t_p}{2\pi L_c r_o k_p} \right)} \left(\frac{W}{K} \right) \tag{7-5}$$

The objective of our design in CHAPTER 6 was to reduce the length of the HPHE system while achieving a certain effectiveness. If we think of the flow rates as fixed (so C_r is fixed), then to achieve a certain effectiveness we need a certain value for NTU, which means that there is a required value of conductance $(UA)_{HP}$. In order to reduce the cost of the system, we want to reduce the number of heat pipes and hence their total surface area. Therefore, it is desirable for U_s (the overall heat transfer coefficient per unit surface area) to be as large as possible, where:

$$U_s = \frac{(UA)_{HP}}{A_s} = \frac{(UA)_{HP}}{2\pi r_o L_e} \tag{7-6}$$

In calculating U_s, $(L_e r_o)$ cancels out of every term (see Eq. (7-5) except in R_v (leaving r_o/r_i as a parameter discussed below). Based on preliminary design of a heat pipe R_v is negligibly small compared to other resistances. Therefore we found that U_s is approximately independent of L_e:

$$U_s = \frac{1}{\left(\frac{t_p}{k_p} + \frac{r_o t_w}{r_i k_{eff,e}} + \frac{2\pi r_o L_e T_v F_v \left(\frac{L_e}{6} + L_a + \frac{L_c}{6} \right)}{\rho\lambda} + \frac{r_o t_w}{r_i k_{eff,c}} + \frac{t_p}{k_p} \right)} \tag{7-7}$$

As shown in above equation for U_s,

- As either t_p (heat pipe wall thickness) or t_w (wick thickness) increase, U_s decreases.

- $\frac{r_o}{r_i} = 1 + \frac{t_p}{r_i}$ is a function of t_p and r_i, where $r_i = d_v/2 + t_w$. Then if t_p increases, then r_o/r_i increases which leads to decreasing U_s. Similarly if r_i increases then r_o/r_i decreases and then U_s increases. Later, the effects of d_v and t_w on U_s will be shown graphically.
- For a wrapped screen wick, k_{eff} is defined as

$$k_{eff} = \frac{k_l\left[(k_l + k_w) - (1 - \epsilon)(k_l - k_w)\right]}{(k_l + k_w) + (1 - \epsilon)(k_l - k_w)}$$

  As the equation for k_{eff} shows, with $k_w > k_l$, k_{eff} increases with increasing screen porosity, ϵ. The porosity is related to the number of meshes per inch, N, according to $\epsilon = 1 - \frac{1.05\pi N d_{sw}}{4}$. From Eq. (7-3) we can see that as N increases, Nd_{sw} increases. Therefore, as N increases, ϵ decreases, k_{eff} increases, and U_s increases.
- The length (L_e or L_c) does not have an effect on U_s because the thermal resistance of the vapor flow is very small compared to other resistances inside the heat pipe.

From the above discussion, in order to maximize U_s, we want thin heat pipe wall, thin wick, small r_o/r_i and high effective thermal conductivity in order to minimize the resistance.

7.3. Parametric study of the effect of key parameters in heat pipe thermal resistance and heat transfer limit

In parametric study, we used U_s (overall heat transfer coefficient per unit surface area of heat pipe) to see the effects of parameters on overall heat transfer coefficient in a heat pipe. The results below confirm the previous discussion and show the magnitude of the effects. We also show their behavior on q_{limit}.

To confirm the above results on behavior of U_s when other key parameters change, we used Eq. (7-7) (programmed in a MATLAB code) to see the effect of all key parameters on U_s. Figure 7-2 to Figure 7-5 shows these behaviors.

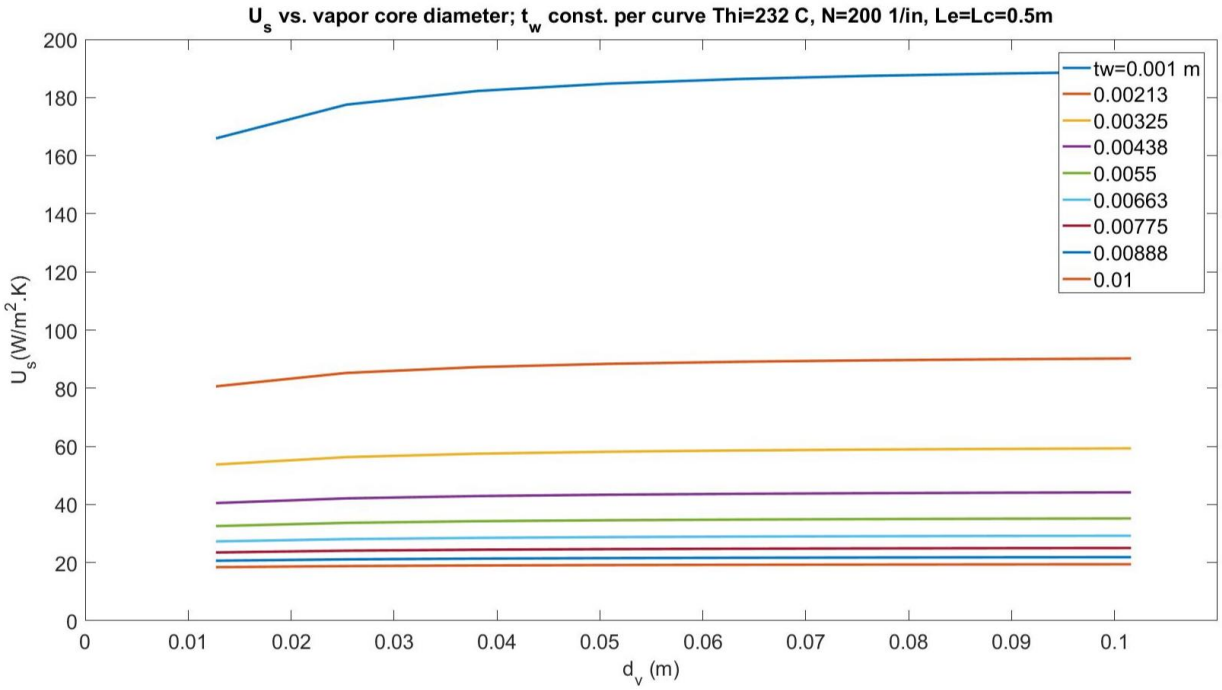

Figure 7-2: Heat transfer coefficient of a heat pipe versus the vapor core diameter (d_v)

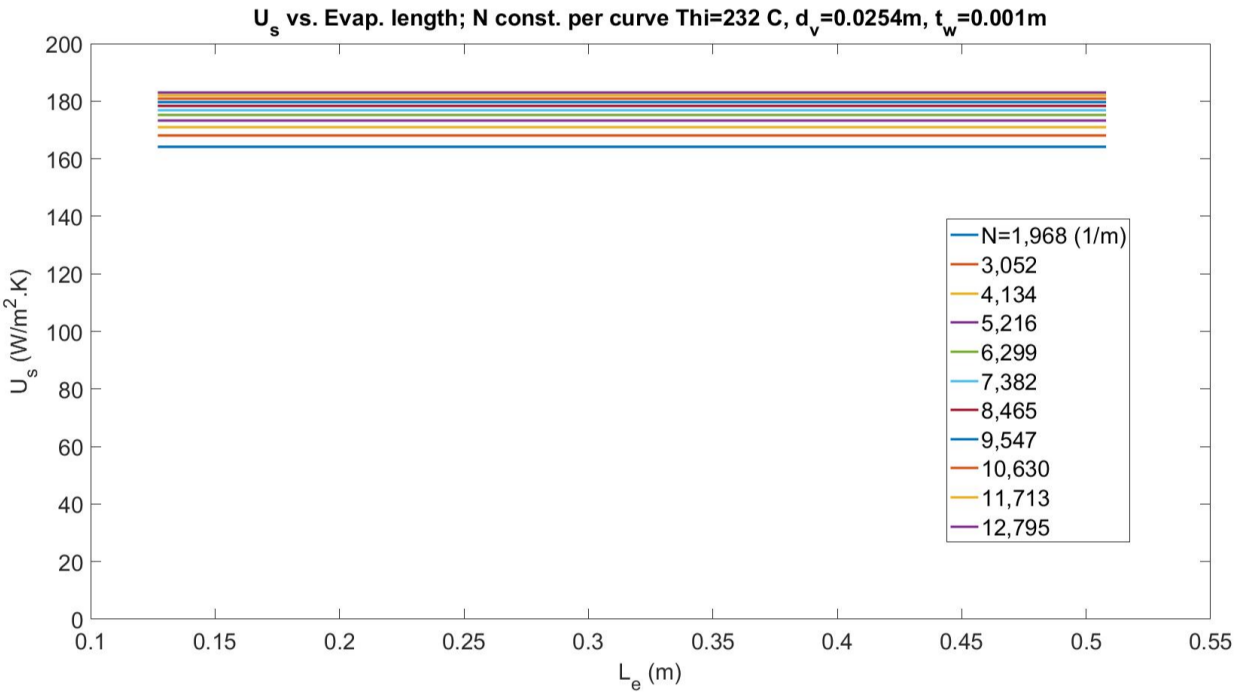

Figure 7-3: Heat transfer coefficient of a heat pipe versus the evaporator length (L_e)

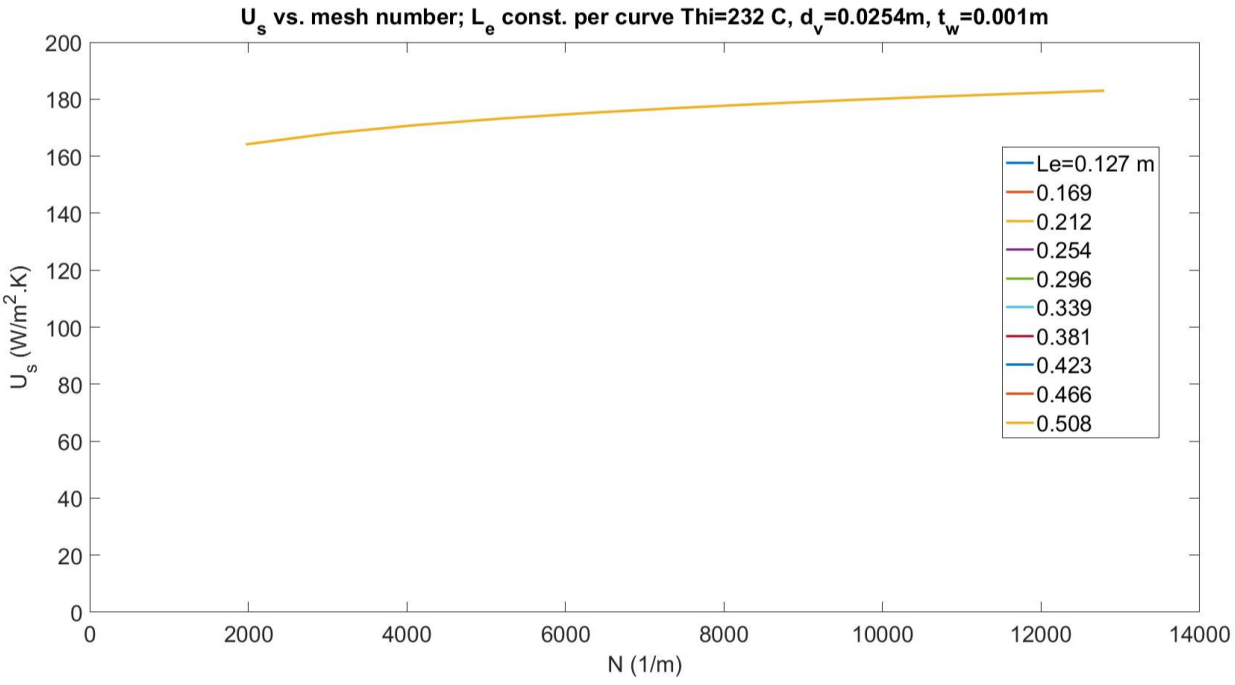

Figure 7-4: Heat transfer coefficient of a heat pipe versus the number of meshes per meter (N)

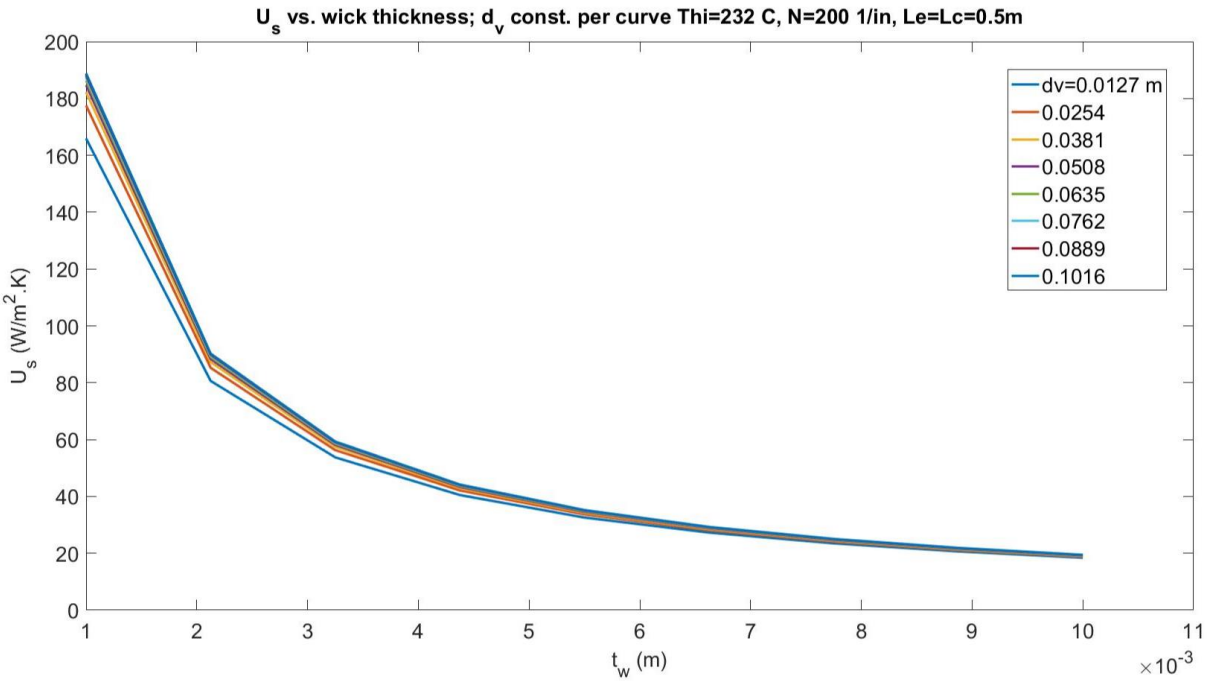

Figure 7-5: Heat transfer coefficient of a heat pipe versus the wick thickness (t_w)

From parametric study, above curves confirm that $\mathbf{U_s}$ decreases with increasing $\mathbf{t_w}$ and varying d_v and N changes U_s only slightly. But $\mathbf{U_s}$ *does not change* with varying $\mathbf{L_e}$.

Similarly the parametric study on the maximum heat transfer rate (q_{limit}) of the heat pipe are presented as below.

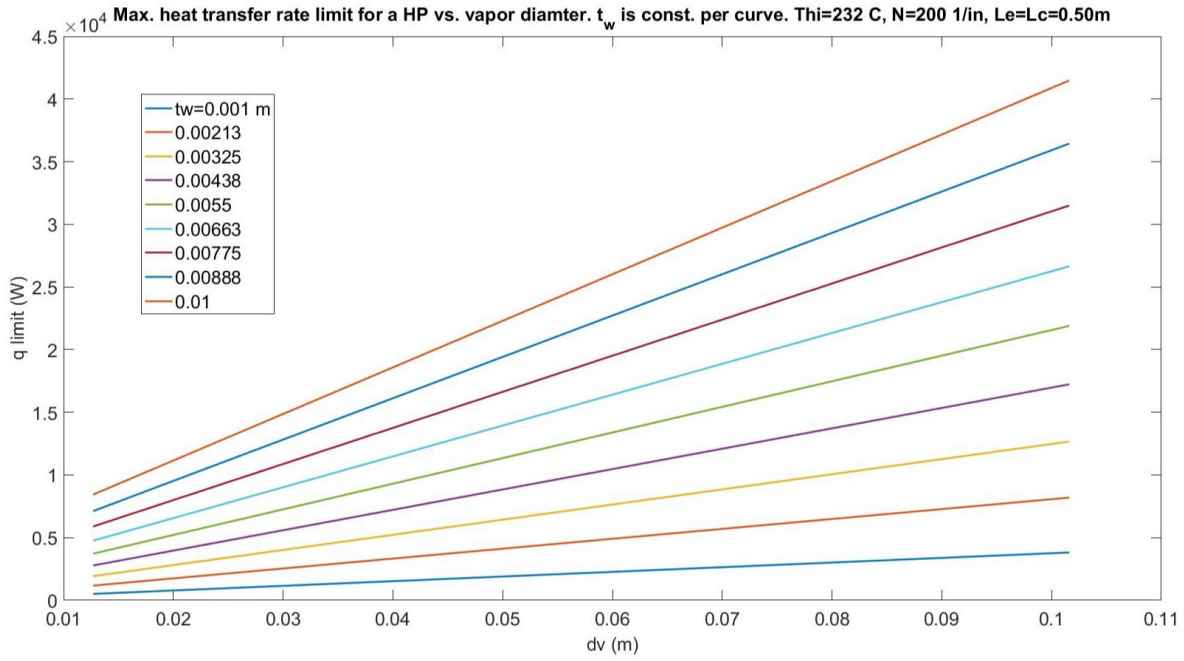

Figure 7-6: q_{limit} (maximum heat transfer rate in a heat pipe) versus vapor core diameter (d_v)

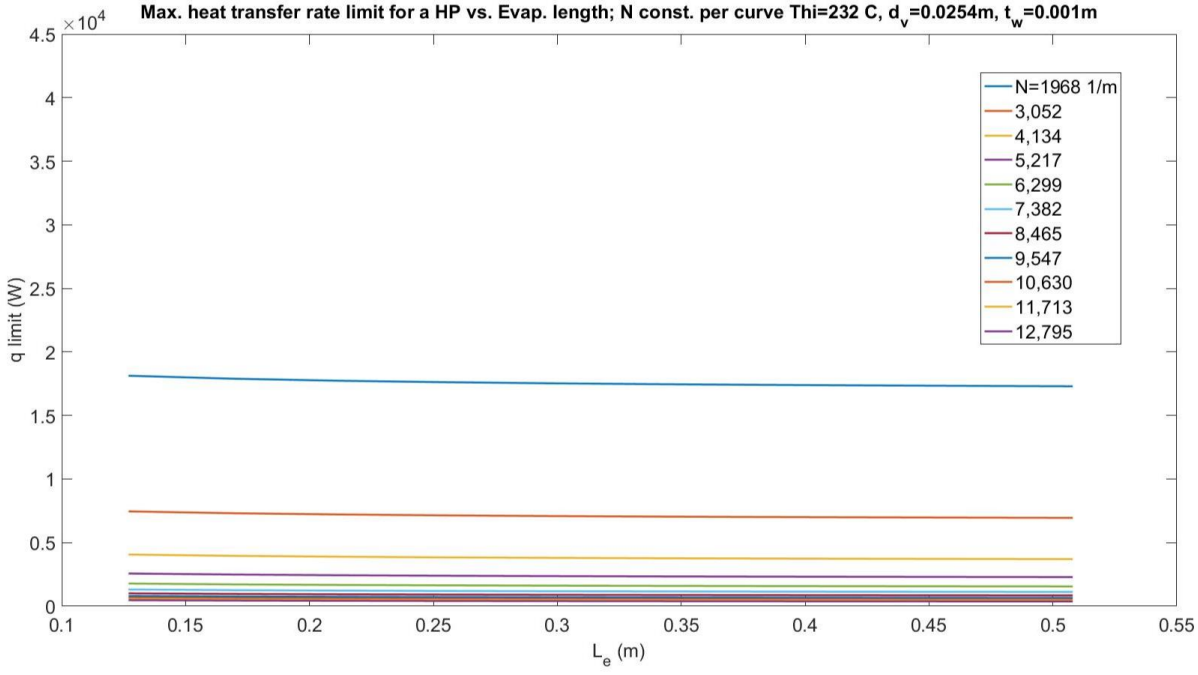

Figure 7-7: q_{limit} (maximum heat transfer rate in a heat pipe) versus the evaporator length (L_e)

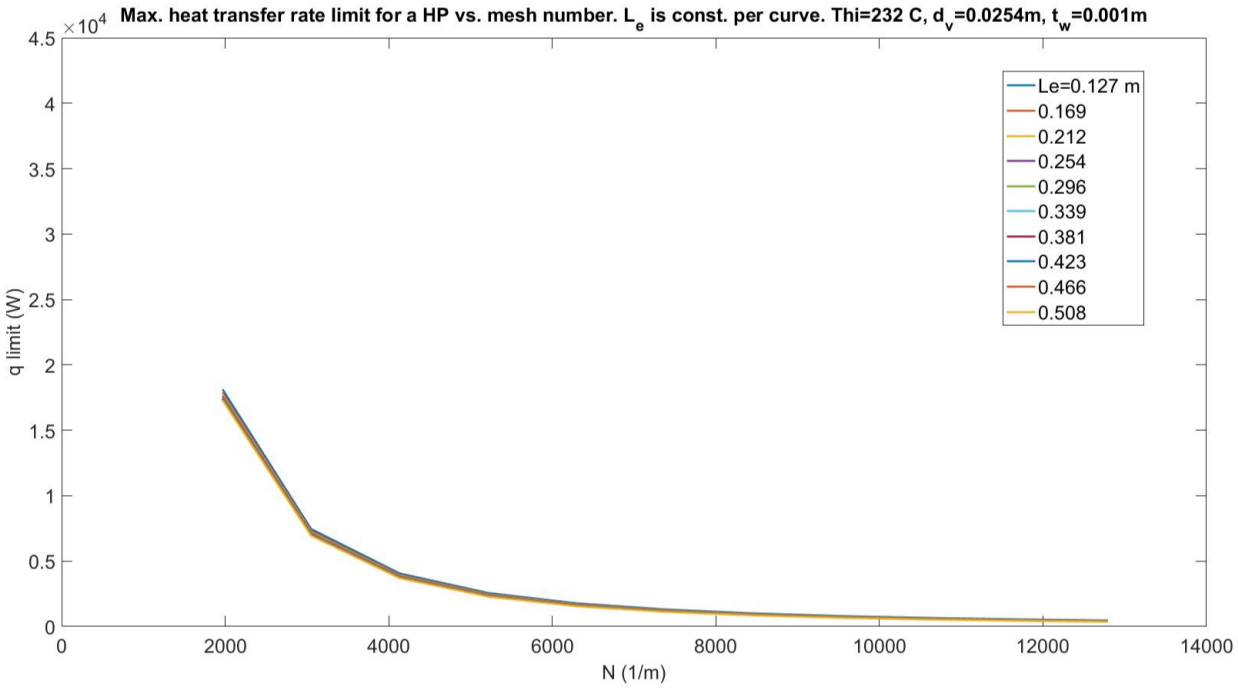

Figure 7-8: q_{limit} (maximum heat transfer rate in a heat pipe) versus the number of meshes per meter (N)

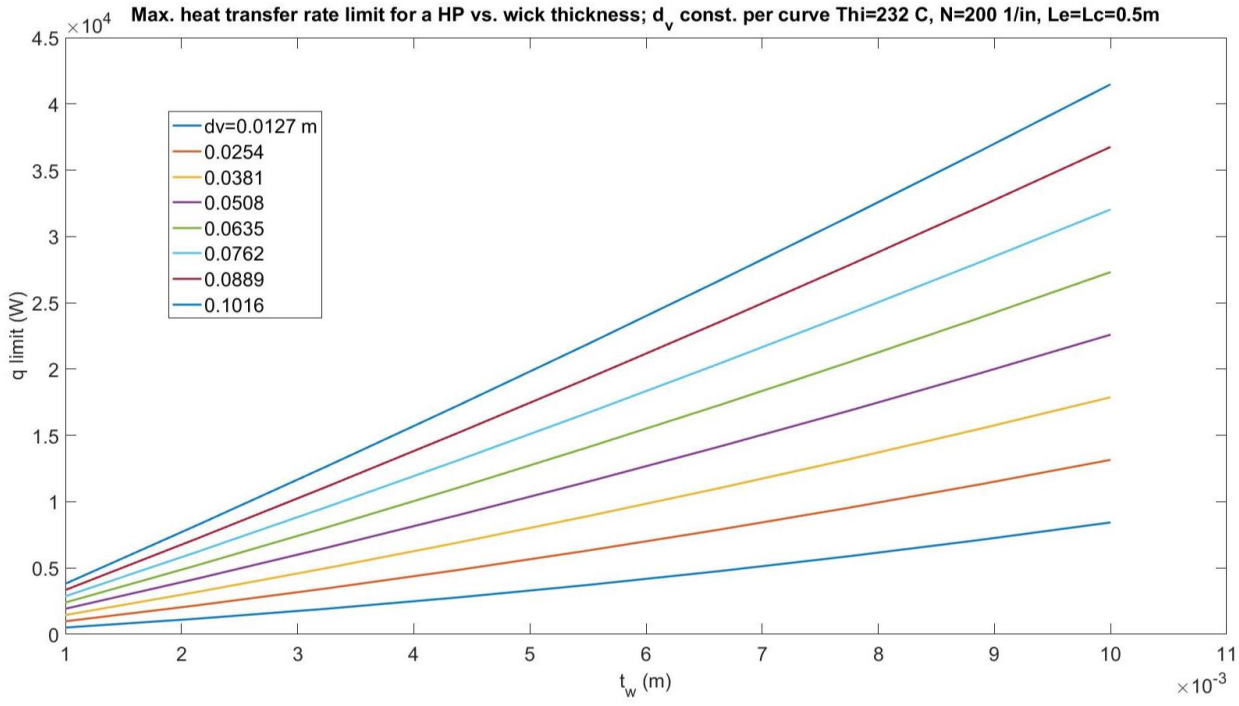

Figure 7-9: q_{limit} (maximum heat transfer rate in a heat pipe) versus the wick thickness (t_w)

As above curves show, $\mathbf{q_{limit}}$ is mainly a function of $\mathbf{d_v}$, $\mathbf{t_w}$ and **N** but *not* L_e, where $\mathbf{q_{limit}}$ increases with increasing t_w and d_v and decreases as N increases.

From the parametric study results, the best way to increase U_s is to decrease t_w, but that also decreases q_{limit}. As discussed in the beginning of this chapter, if we have $q_{limit} > q_{max,1HP\ in\ HPHE}$, then to have shorter HPHE we would want to decrease q_{limit} as much as possible and that's why we try to achieve $q_{limit} \approx q_{max,1HP\ in\ HPHE}$. We are also interested to make N small and d_v large because these parameters tend to make q_{limit} bigger, so we could then make t_w even smaller and still have $q_{limit} \approx q_{max,1HP\ in\ HPHE}$.

7.4. Adjusting the key parameters to shorten the HPHE length

As discussed in the previous section and in Figure 7-2 to Figure 7-9, we have three parameters that can be adjusted to satisfy $q_{limit} \approx q_{max,1HP\ in\ HPHE}$. And also in the air-air HPHE at $C_r \approx 1$ (which worked favorably as reported in CHAPTER 6), we find the design for the heat pipe which satisfies the above criterion which improves U_s. From now on we call U_s as U_{HP} to be more clear about what parameter we are talking about.

To satisfy $q_{limit} \approx q_{max,1HP\ in\ HPHE}$ for the heat pipe we designed in CHAPTER 4, we were curious to know if we could improve each parameter (t_w, N, d_v) that we found has significant effects on U_{HP} and q_{limit} to decrease the length of the system. To start, first we prioritized the key parameters based on their effect (curve slopes shown previously in Figure 7-2 to Figure 7-9) on U_{HP} and q_{limit}:

- Wick thickness t_w is most important since it affects both U_{HP} and q_{limit}, but in opposite directions.

- Number of meshes N per unit length is another important parameter, since it has a sharp slope in q_{limit} versus N curve.
- Vapor core diameter d_v is the last one and affects q_{limit}.

Before starting the procedure, we have to know what kind of behavior from HPHE is desirable. For an instance in this study these parameters are fixed: N_T (width), T_{hi}, T_{co}, T_{ci}, T_{co}, Q_h, Q_c, and the height of the HPHE. Therefore after finding a new value for each key parameter (where $q_{limit} = q_{max,1HP\ in\ HPHE}$ applies), T_{co} and T_{ho} will change. Then before finding the new value for the next parameter (as prioritized above), we first have to change the number of rows along the length of the HPHE (N_L) to achieve the desired temperatures at the exit of the HPHE system (to have the desired effectiveness). We acknowledg that it is one way to get a reasonable design which satisfies both the inequality and shortens the HPHE length.

Now we apply the following approach based on priority of the key parameters:

1. Wick thickness (t_w): Since t_w is a common parameter in both U_{HP} and q_{limit}, then it has the first priority. I found the value of t_w that achieves $q_{limit} = q_{max,1HP\ in\ HPHE}$. (This value of t_w might not be feasible regarding manufacturing or might be costly, so we have to consider applicability.) When t_w changes, T_{ho} and T_{co} (and clearly the effectiveness) of the HPHE will change and I then adjust N_L to achieve the desired effectiveness prior to varying the next parameter. Note that when N_L is changed, $q_{max,1HP\ in\ HPHE}$ changes and the q_{limit} requirement may no longer be met.
2. Similarly for N, I keep t_w the same value I found in the previous step and adjust N to achieve $q_{limit} \approx q_{max,1HP\ in\ HPHE}$. Then I adjust N_L to get the desired effectiveness.

3. About d_v, which has the least importance, I repeat the above procedures using t_w and N I found in the previous steps, and I change d_v to achieve $q_{limit} \approx q_{max,1HP\ in\ HPHE}$. Then I have to adjust N_L to get the desired effectiveness.

After completing these steps if q_{limit} becomes less than $q_{max,1HP\ in\ HPHE}$, I iterate d_v again, if not, the parameters are left as they are. Since N_L is integer, I might not get exact $q_{limit} = q_{max,1HP\ in\ HPHE}$ in the last step, therefore as long as $q_{limit} > q_{max,1HP}$ in the HPHE the process can be stopped.

As mentioned in the introduction of this chapter, in my design I have $q_{limit} > q_{max,1HP\ in\ HPHE}$ then I adjusted q_{limit} according to HPHE demands. The final result of improving the heat pipe design is to achieve $q_{limit} \approx q_{max,1HP\ in\ HPHE}$ which results in decreasing the length of the HPHE with the same effectiveness, because U_{HP} improved in each heat pipe.

In Table 7-2 the original designed heat pipe parameters as it has been explained in CHAPTER 4 is shown. Then the refined design to $q_{limit} \approx q_{max,1HP\ in\ HPHE}$ is shown in Table 7-3.

Table 7-2: The original heat pipe has been designed for HPHE with T_{hi}= 232°C, T_{ci}=20°C, $\dot{m}_h$ (adjusted combusted exhaust gas mass flow rate to reach $C_r \approx 1$), $\dot{m}_c$ (realistic air mass flow rate)

d_v (m)	d_o (m)	t_w (m)	N (1/in)	L_e=L_c (m)	q_{limit} (W)	U_{hp} (W/m^2.K)
0.0198	0.0243	1×10^{-3}	200	0.51	798	14,335

Table 7-3: The refined heat pipe design for HPHE with T_{hi}= 232°C, T_{ci}=20°C, $\dot{m}_h$ (adjusted combusted exhaust gas mass flow rate to reach $C_r \approx 1$), $\dot{m}_c$ (realistic air mass flow rate)

d_v (m)	d_o (m)	t_w (m)	N (1/in)	L_e=L_c (m)	q_{limit} (W)	U_{hp} (W/m^2.K)
0.0198	0.0229	0.306×10^{-3}	200	0.51	240.1	46,584

As shown above, the preliminary heat pipe design dimensions and parameters were reasonable to be inserted into the air-air HPHE and the inequality was valid ($q_{limit} \geq q_{max,1HP\ in\ HPHE}$). We acknowledged that we can get a reasonable design which satisfies the inequality and shorten the length of the HPHE simultaneously. As shown U_{HP} has been improved from Table 7-2 to Table 7-3 which leads to decrease of the length of the system.

In Table 7-4 and Table 7-5 the same comparisons are shown for the HPHE system which use the heat pipes parameters of Table 7-2 and Table 7-3 respectively.

Table 7-4: The inserted heat pipes from Table 7-2 in air-air HPHE; T_{hi}= 232°C, T_{ci}=20°C, $\dot{m}_h$ (adjusted combusted exhaust gas mass flow rate to reach $C_r \approx 1$), $\dot{m}_c$ (realistic air mass flow rate)

N_L	N_T	# of HPS	W (m)	L (m)	T_{co} (°C)	T_{ho} (°C)	ε	$q_{max,1\ HP\ in\ HPHE}$ (W)
99	15	1,485	0.71	3.87	35.88	216.35	0.075	231.7

Table 7-5: The refined designed heat pipes from Table 7-3 in air-air HPHE; T_{hi}= 232°C, T_{ci}=20°C, $\dot{m}_h$ (adjusted exhaust gas mass flow rate to reach $C_r \approx 1$), $\dot{m}_c$ (realistic air mass flow rate)

N_L	N_T	# of HPS	W (m)	L (m)	T_{co} (°C)	T_{ho} (°C)	ε	$q_{max,1\ HP\ in\ HPHE}$ (W)
97	15	1,455	0.69	3.67	35.84	216.38	0.075	235.9

Notice in Table 7-5 q_{limit} is not exactly equal to $q_{max,1HP\ in\ HPHE}$ because N_L is an integer number.

Comparing Table 7-3 to Table 7-4 shows that both the HPHE length and width decreased due to improvement in U_{HP}. Improvement in U_{HP} results in using less number of heat pipes in the HPHE system which is economically beneficial.

CHAPTER 8

8. HPHE Optimization

In this chapter, an approach from a literature is selected, then it is utilized for optimizing HPHE system and a new correlation is obtained for the optimum dimensionless parameter in a system of HPHE. Then it is shown what will be the real optimum S/d_o for a system of HPHE.

Optimization of HPHE system is not a single step. In an ideal optimization, one have to first optimize the heat pipe design, then apply the optimized heat pipes dimensions and the heat transfer coefficient (U_{HP}) in the HPHE system and do another optimization of the HPHE system while $q_{max,1HP\ in\ HPHE}$ does not exceed q_{limit}.

Our objectives to optimize the HPHE system are:

- Raising temperature of the cold flow from 20 ˚C to about 36°C in the shorter length of the HPHE when effectiveness is fixed
- Satisfy this equation : $q_{max,1HP\ in\ HPHE} \approx q_{\ limit}$

The key parameters for designing a system of HPHE are:

- Number of rows N_L
- Number of columns N_T
- Spacing between heat pipes (heat pipe diameter is not included, meaning when S=0, then heat pipes touch each other)
- Flow rates in cold and hot sides of the system Q_h and Q_c

Within the parametric study I did, I found that not all of the above parameters could be optimized, because they depend on the application of HPHE (i.e flow rates) and the input

information (such as space limitations, number of columns and rows, etc.). Then the only parameter which worth optimizing, is *spacing* between the heat pipes in system.

Refer to Stanescu, Fowler and Bejan (1995) paper, the authors' objective was to maximize the overall thermal conductance between the cylinders and external flow in a fixed volume by optimizing the cylinder-to-cylinder spacing (S). We have common goal with the authors; we would like to have shorter length of HPHE (~3 meters) with highest possible overall HPHE heat conductance. To do this, I fix the width and height of the system (width ~0.7 meters, height ~1 meters).

In the Stanescu et al., (1995) work, the staggered cylinders configuration (which gives higher performance compared to in line configuration of heat pipes in a system of HPHE) are in an equilateral triangular shape for simplicity and we considered the same in our preliminary design.

One interesting fact we learned from the authors (Stanescu et al., 1995) is how to derive a correlation for $\left(\frac{S}{d_o}\right)$. In their paper they introduced an equation for optimum (spacing/do) ratio when Reynolds number was small (laminar flow) and Nusselt number was Zukaskas' equation for small Reynolds number.

In my work, Reynolds number does not fall into laminar region, therefore I repeated their approach with an appropriate Nusselt number to achieve equations for $(S/d_o)_{optimum}$ for the system of HPHE with high Reynolds number (turbulent flow). Note that as Reynolds number is increased and moves to turbulent region, the flow thermal behavior completely changes.

II tried two different Nusselt number correlation, one from bank of tubes theory and the other one for the HPHE system. Then I calculated $\left(\frac{S}{d_o}\right)_{opt}$ for both correlations and finally I preferred to use the one which looks simpler and easier to compute.

Fixed parameters in my optimization method are:

- Width and height of the HPHE
- T_{hi}, T_{ci}, T_{co}, T_{ho}
- Flow rates in the evaporator and in the condenser sides

8.1.Spacing (S)

I would like to clarify what we mean by "spacing". In the Stanescu et al., (1995) paper, the authors mentioned S is cylinder-to-cylinder spacing which it is not explicitly defined the spacing direction in staggered tubes configuration; longitudinal, transverse or diagonal. But since their cylinders arrangements are staggered with equilateral triangular arrangement which S_T=S_D, then we believe that they mean $S = S_D - d_o$. Therefore we use the same concept and define the *spacing* for the staggered tubes arrangements as below:

$$\text{spacing} = S_D - d_o \tag{8-1}$$

where d_o is the outside diameter of the heat pipe. Since I use the staggered equilateral triangular heat pipe arrangements in the HPHE system, then

$$S = S_D - d_o = S_T - d_o \tag{8-2}$$

According to Bergman, Lavine et al. textbook, for the staggered tubes configurations when we have equilateral arrangement ($S_T = S_D$), the longitudinal spacing is defined as

$$S_L = \frac{\sqrt{3}}{2} S_T \tag{8-3}$$

8.2. $\left(\frac{S}{d_o}\right)_{opt}$ based on Nusselt number in bank of tubes theory

I am looking forward to find an optimum $\left(\frac{S}{d_o}\right)_{opt}$ which applies to a wider range of Reynolds and Prandtl numbers. In Bergman, Lavine, Incropera and DeWitt textbook (7th edition), a general equation for bank of tubes which offers average heat transfer coefficient for the entire bank regardless of tubes arrangement (aligned and staggered arrangements) and fluid regime (laminar and turbulent) is offered. This experimental equation has been proposed by A. Zukauskas in 1972,

$$Nu_D = C_1 \left(Re_{d,max}^m\right) Pr^{0.36} \left(\frac{Pr}{Pr_s}\right)^{\frac{1}{4}} \tag{8-4}$$

$$N_L \geq 20$$
$$0.7 \leq Pr \leq 500$$
$$10 \leq Re_{d,max} \leq 2\times10^6$$

where constants m and C_1 are given in a table in the same reference (Table 8-1) and depend on the tubes configurations and Reynolds number.

Table 8-1: Constants C_1 and m for Eq. (8-4) (Bergman, Lavine, Incropera and DeWitt textbook, 2011)

Conguration	$Re_{D,\max}$	C_1	m
Aligned	$10–10^2$	0.80	0.40
Staggered	$10–10^2$	0.90	0.40
Aligned	$10^2–10^3$	Approximate as a single (isolated) cylinder	
Staggered	$10^2–10^3$		
Aligned $(S_T/S_L > 0.7)^a$	$10^3–2 \times 10^5$	0.27	0.63
Staggered $(S_T/S_L < 2)$	$10^3–2 \times 10^5$	$0.35(S_T/S_L)^{1/5}$	0.60
Staggered $(S_T/S_L > 2)$	$10^3–2 \times 10^5$	0.40	0.60
Aligned	$2 \times 10^5–2 \times 10^6$	0.021	0.84
Staggered	$2 \times 10^5–2 \times 10^6$	0.022	0.84

[a]For $S_T/S_L < 0.7$, heat transfer is inefficient and aligned tubes should not be used.

Now I follow the steps similar to Stanescu et al., 1995 work.

Similar to Stanescu et al. I consider two cases, S << d_o and S << d_o where S is cylinder-to-cylinder spacing (in banks of tube model) and d_o is the outside diameter of the heat pipe. Then I write the total heat transfer rate in the HPHE system for each case between the volume and the fluid and let S/d_o <<1 and in another case S/d_o >>1. Using Darcy law for the average longitudinal velocity and then Carman-Kozeny model (see Stanescu et al., 1995) for the permeability of the equilateral triangle array, a correlation for q is obtainable. And then I apply the two cases in the equation for q.

8.2.1. Case 1: S << d_o

The equation for q when S << d_o is similar to the equation offered in Stanescu et al., 1995. Similar to the authors work, we start with $q_{S<<do} \cong \dot{m} c_p (T_w - T_\infty)$ between the volume and the fluid. Then using Darcy law for the average longitudinal velocity, stagnation excess pressure at the channel entrance $\left(\Delta p \cong \frac{1}{2}\rho U_\infty^2\right)$ and then Carman-Kozeny model (see Stanescu et al., 1995) for the permeability of the equilateral triangle array, a correlation for $q_{S<<do}$ is obtainable. The next step is to let $\tilde{S} = \frac{S}{d_o} << 1$ to achieve a neat equation for heat transfer based on dimensionless parameters $\tilde{S}$ and Reynolds number:

$$q_{S<<do} \cong \frac{1}{25}\rho C_p \nu \frac{WH}{L}\left(Re_{d,max}^2\right)\tilde{S}^3 (T_w - T_\infty) \tag{8-5}$$

$$\left(\frac{q}{T_w - T_\infty}\right)_{S<<do} \cong \frac{1}{25}\rho C_p \nu \frac{WH}{L}\left(Re_{d,max}^2\right)\tilde{S}^3 \tag{8-6}$$

8.2.2. Case 2: S >> do

While $\tilde{S} = \frac{S}{d_o} >> 1$ is considered, it means each cylinder (heat pipe in this research) is bathed by free stream velocity and temperature, then according to the paper (Stanescu et al., 1995), the heat transfer rate from each cylinder is

$$q_1 = Nu_d \frac{k}{d_o}\pi d_o L (T_w - T_\infty) \tag{8-7}$$

By replacing Eq. (8-4) (experimental equation has been proposed by Zukauskas for Nusselt number) in Eq. (8-7) and then knowing that $q = nq_1$ (n is total number of heat pipes) results in:

$$q_{S>>do} = \frac{LW}{(S+D)^2}\ \frac{1}{\cos 30} C_1\ \left(Re_{d,max}^{m}\right) Pr^{0.36}\ \left(\frac{Pr}{Pr_s}\right)^{\frac{1}{4}} k\,\pi\,H\,(T_w - T_\infty)$$

or

$$q_{S>>do} = 3.63\, C_1\, k\, \frac{HLW}{d_o^2}\ \left(1+\tilde{S}\right)^{-2}\ \left(Re_{d,max}^{m}\right) Pr^{0.36}\ \left(\frac{Pr}{Pr_s}\right)^{\frac{1}{4}} (T_w - T_\infty) \qquad (8\text{-}8)$$

Then letting $\tilde{S} = \frac{S}{d_o} >> 1$ gives a simplified correlation for the total heat transfer rate in HPHE system:

$$q_{S>>do} = 3.63\, C_1\, k\, \frac{HLW}{d_o^2}\ \left(\tilde{S}\right)^{-2}\ \left(Re_{d,max}^{m}\right) Pr^{0.36}\ \left(\frac{Pr}{Pr_s}\right)^{\frac{1}{4}} (T_w - T_\infty)$$

and when replace q in above equation, the correlation for the case S>>d_o becomes

$$\left(\frac{q}{T_w - T_\infty}\right)_{S>>do} = 3.63\, C_1\, k\, \frac{HLW}{d_o^2}\ \left(\tilde{S}\right)^{-2}\ \left(Re_{d,max}^{m}\right) Pr^{0.36}\ \left(\frac{Pr}{Pr_s}\right)^{\frac{1}{4}} \qquad (8\text{-}9)$$

8.2.3. Intersections of case 1 and case 2 results

According to Stanescu, Bejan (1995), in case 1 where S<<do, the thermal conductance increases as $\tilde{S}$ increases and in case 2 where S>>do, the thermal conductance increases as $\tilde{S}$ decreases. Therefore it would mean that the optimal spacing for maximum thermal conductance can approximately be evaluated by intersecting Eq. (8-6) and (8-9):

$$\frac{1}{25}\rho\, C_p\, \nu\, \frac{WH}{L}\ \left(Re_{d,max}^{2}\right) \tilde{S}^3 = 3.63\, C_1\, k\, \frac{HLW}{d_o^2}\ \left(\tilde{S}\right)^{-2}\ \left(Re_{d,max}^{m}\right) Pr^{0.36}\ \left(\frac{Pr}{Pr_s}\right)^{\frac{1}{4}}$$

$$\tilde{S}^5 = 90.69\, C_1\, \left(\frac{L}{d_o}\right)^2\ \left(Re_{d,max}\right)^{m-2}\ Pr^{-0.64}\ \left(\frac{Pr}{Pr_s}\right)^{\frac{1}{4}}$$

or

$$\left(\frac{S}{d_o}\right)_{opt}^{5} = 90.69\,C_1 \left(\frac{L}{d_o}\right)^{2} \left(Re_{d,max}\right)^{m-2} Pr^{-0.64} \left(\frac{Pr}{Pr_s}\right)^{\frac{1}{4}}$$

and then the optimum dimensionless spacing is obtainable

$$\left(\frac{S}{d_o}\right)_{opt} = 2.46\left(C_1\right)^{\frac{1}{5}} \left(\frac{L}{d_o}\right)^{0.4} \left(Re_{d,max}\right)^{\frac{(m-2)}{5}} Pr^{-0.128} \left(\frac{Pr}{Pr_s}\right)^{0.05} \qquad (8\text{-}10)$$

In this study for HPHE systems, the above equation derived as an optimum spacing between the heat pipes should be tried in both evaporator and condenser sections, then it will be seen that there will be two optimum spacing. For one value of $\left(\frac{S}{d_o}\right)_{opt}$, the inequality $q_{1HP\ in\ HPHE} < q_{limit}$ is valid. The optimum spacing is between the two values are calculated for the evaporator and the condenser sides where $q_{1HP\ in\ HPHE} \approx q_{limit}$.

8.3. $\left(\frac{S}{d_o}\right)_{opt}$ based on Nusselt number correlation for the HPHE

The Nusselt number equation from Tan and Liu (1990) paper which is specifically for the heat pipe heat exchanger is different from Zukauskas's,

$$Nu = f\left(0.5Re^{\frac{1}{2}} + 0.2Re^{\frac{2}{3}}\right)^{\frac{1}{5}} Pr^{\frac{1}{3}} \left(\frac{\mu}{\mu_w}\right) \qquad (8\text{-}11)$$

where $Re = \left(\frac{\rho v d_o}{\mu}\right)\left(\frac{\varepsilon}{1-\varepsilon}\right)$. Following above steps, then the optimal value for (spacing/d_o) is obtainable:

$$\left(\frac{S}{d_o}\right)_{opt} = 2.46\left(\frac{L}{d_0}\right)^{0.4} \left(0.5Re^{-\frac{3}{2}} + 0.2Re^{-\frac{4}{3}}\right)^{\frac{1}{5}} \left(\frac{\varepsilon}{1-\varepsilon}\right)^{\frac{2}{5}} Pr^{-0.133} \left(\frac{\mu}{\mu_w}\right)^{0.2} \qquad (8\text{-}12)$$

The instruction of how to use the derived equation is similar to the explanations in section 8.2.3.

8.4. Results

As shown using the HPHE Nusselt number equation from Tan and Liu (1990) paper in section 8.3, and comparing to the results was obtained in section 8.2, I prefer to use the results from bank of tubes theory in section 8.2 and Eq. (8-10) which looks simpler and it does not change the ultimate results.

Table 8-2 to Table 8-4 show the parameters in air-air HPHE system before and after applying Stanescu et al. (1995) optimization method.

Note: The air-HPHE design which is optimized here uses the refined heat pipe deign from CHAPTER 7.

Table 8-2: air-air HPHE parameters before applying HPHE optimization method; T_{hi}= 232°C, T_{ci}=20°C, $\dot{m}_h$ (adjusted combusted exhaust gas mass flow rate to reach $C_r \approx 1$), $\dot{m}_c$ (realistic mass flow rate of air)

S/do (m)	S_T (m)	S_L (m)	Re_h	Re_c	T_{co} (°C)	T_{ho} (°C)	ε	$q_{max1\ HP\ in\ HPHE}$ (W)	HPHE length (m)	Width (m)
0.89	0.043	0.037	5,179	89,439	35.84	216.38	0.075	235.9	3.67	0.69

Table 8-3: $(S/d_o)_{opt}$ for the evaporator and the condenser sides of air-air HPHE $C_r \approx 1$, T_{hi}= 232°C, T_{ci}=20°C

	S/d_o optimum	S_T optimum (m)	S_L optimum (m)	ε	$q_{max1\ HP\ in\ HPHE}$ (W)
Evaporator	1.47	0.057	0.049	0.045	143.8
Condenser	0.66	0.038	0.033	0.97	306.7

As shown in Table 8-2 , we need to have $q_{max1\ HP\ in\ HPHE}$ = 235.9 watts which satisfies the inequality $q_{max,1HP\ in\ HPHE} \approx q_{limit}$ (as discussed in CHAPTER 7), then for this reason the optimum spacing is between the two calculated values for the evaporator and the condenser sides to satisfy $q_{1HP,inHPHE} \approx q_{limit}$:

$$0.66 < \left(\frac{S}{d_o}\right)_{opt} < 1.47 \tag{8-13}$$

Table 8-4 shows the iterated values of $\left(\frac{S}{d_o}\right)_{opt}$ in the range of Eq. (8-13) which satisfies

$$q_{max,1HP\ in\ HPHE} \approx q_{limit}$$

Table 8-4: air-air HPHE $C_r \approx 1$ parameters after applying the optimized value for S/d_o

	$(S/d_o)_{opt}$ (m)	S_T (m)	S_L (m)	T_{co} (°C)	T_{ho} (°C)	ε	$q_{max,1\ HP\ in\ HPHE}$ (W)	HPHE length (m)	Width (m)
Air-air HPHE	0.87	0.043	0.037	36.12	216.10	0.075	240	3.64	0.69

Comparing Table 8-2 and Table 8-4, it is shown that the HPHE length and effectiveness improved. The improvement is not much which confirms we chose good values for S in our preliminary design of the HPHE.

CHAPTER 9

9. Economical Overview

In this dissertation, an approach to the economical savings will be considered. All of the correlations are based on the air-air HPHE $C_r \approx 1$ design. To relate the energy recovery payback by using HPHE, new correlations are offered which are based on the refined heat pipe design in CHAPTER 7 which has been inserted in air-air- HPHE ($C_r \approx 1$) and then the system has been optimized in CHAPTER 8. For any new design of heat pipe and then HPHE, the correlations should be obtained the same way that will be explained in this chapter.

As it has shown in CHAPTER 6 when we compared spiral heat exchanger with HPHE for different fluid pair and at $C_r << 1$ and $C_r \approx 1$, it has been found that air-air HPHE works favorable in the application which is the interest of this study. We use the same design in this chapter for the air-air HPHE $C_r \approx 1$ that has been optimized in CHAPTER 8.

Generally we know the cost of electricity in California per kWh (kilowatt-hour), therefore we are able to obtain value of the energy recovered by burning CH_4 and predict the possible savings.

The average price that people in the U.S. pay for the electricity is about $0.12 cents per kilowatt-hour (www.npr.org/blogs/money/2011/10/27/141766341/the-price-of-electricity-in-your-state , March 2018). The price of electricity in the greater Los Angles is $0.16 per kW.h.

For an instance, the heat production by burning Methane gas (CH_4) in each digester in Hyperion waste water Treatment Plant (HTP) in Los Angeles, California is approximately of 4,500 kW (15.8 million Btu/hr). Even if we can recover 10% of the heat by pre-heating the inlet to the gas-engine, we can save $1,700 per day.

We do calculations for the cost of the designed HPHE as well as pay back per year for the refined design of heat pipe in CHAPTER 7 and the optimize HPHE design as in CHAPTER 8 (air-air with $C_r \approx 1$). The hot air temperature assumed to be 232 °C to heat the cold air at ambient temperature of 20 °C.

In generating Figure 9-3 as shown below, we assume HPHE works 24 hours a day in a whole year period. Knowing the price of electricity for an instance in Los Angeles ($0.16 per kW.h), we can calculate the pay back by recovering heat from combusted methane gas per year.

To estimate the cost of HPHE, we have a quote from Advanced Cooling Technology Inc. (www.1-ACT.com) provided on April 2016 for the prelilinary designed heat pipe with outside diameter of 0.0243 m, and heat pipe material of copper (see Table 9-1). Although we changed the heat pipe wall material from copper to stainless steel (SS304) and refined the d_o size in CHAPTER 7, but we still used the quote as an estimation. For a SS304 heat pipe, with copper wick and d_o=0.0229 m, the heat conductance capacity is 19.2 W/K.

Table 9-1: Heat pipe quote provided by a heat pipe manufacturer (on April 2016, ACT-1 Inc.)

Item	Description	Quantity	Price	Price unit	Value
001	NRE	1 Lot	$1,600	Each	$1,600.00
002	Custom Copper/Methanol Heat Pipe	1	$4,350	Each	$4,350.00
003	Custom Copper/Methanol Heat Pipe	5	$1,070	Each	$5,350.00
004	Custom Copper/Methanol Heat Pipe	10	$700	Each	$7,000.00

As mentioned earlier in this chapter, we assume HPHE works 24 hours a day in a whole year period. The price of electricity in Los Angeles is $0.16 per kW.h , then by calculating the amount of heat recovery in the HPHE, we can calculate the investment back by recovering the heat from the combusted methane gas (in air-air HPHE, $C_r \approx 1$) per year. As shown in Eq. (9-1), we convert q (kW) to q (kW.h) for a year period as below:

$$q\left(\text{kW.h}\right) = q\left(\text{kW}\right) \times 52.143\left(\frac{\text{week}}{\text{year}}\right) \times 7\left(\frac{\text{days}}{\text{week}}\right) \times 24\left(\frac{\text{hr}}{\text{day}}\right) \tag{9-1}$$

And then we can calculate the value of the heat recovery in U.S dollars:

$$\$q = q\left(\text{kW.h}\right) \times \$\,0.16 \tag{9-2}$$

From Table 9-1, we know that we have to use numerous heat pipes in our system, therefore we assumed $700 per heat pipe added to $1,600 NRE (Non-recurring engineering) fee. In the equation below N_L is the variable (N_T is fixed) and this equation is valid only for the quote was provided by the manufacturer:

$$\$ \text{ HPHE cost} = (N_L \times N_T \times 700) + \text{NRE} \tag{9-3}$$

To relate the length of the heat pipe heat exchanger to the cost of heat pipes, we made a curve-fit correlation for total price of HPHE and the length of HPHE by changing number of rows (Figure 9-1) and the correlation is as below:

$$\$ \text{ HPHE} = 282{,}304 \times L \tag{9-4}$$

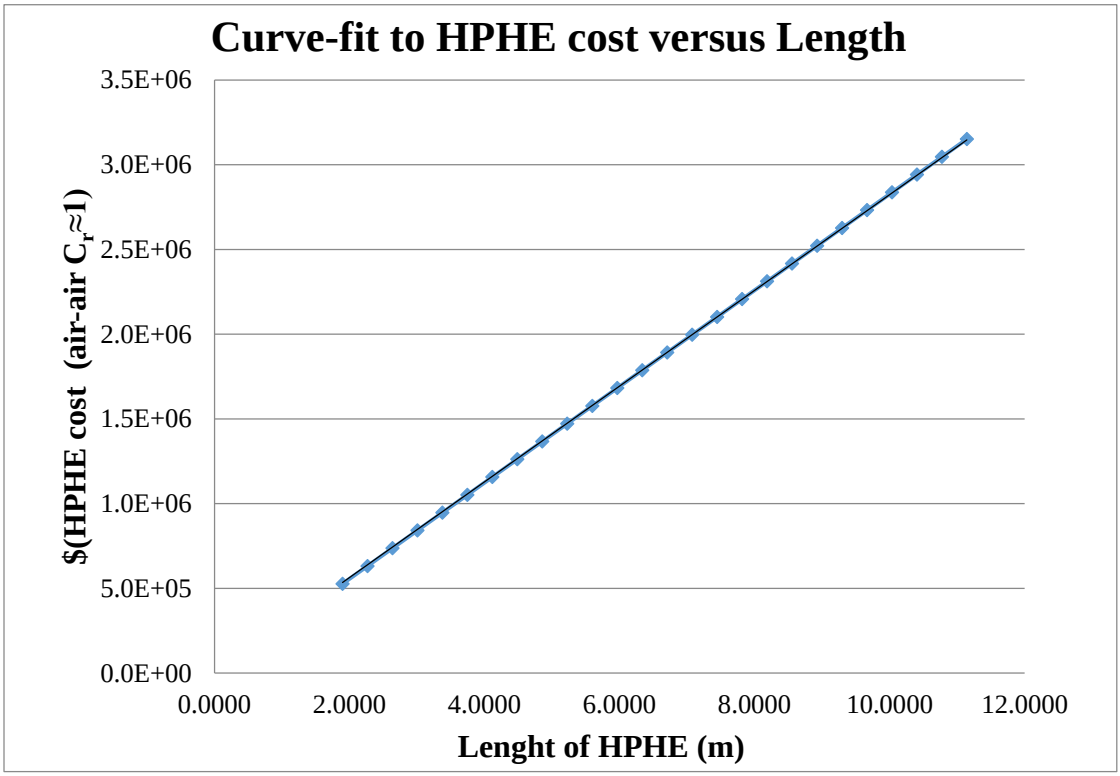

Figure 9-1: Curve-fit correlation for HPHE cost versus HPHE length for air-air HPHE ($C_r \approx 1$) has been designed in CHAPTER 8

I also fixed the number of heat pipes per row (number of columns) to 15 (we assumed the width of the HPHE as an input) and the optimized spacing for the HPHE in CHAPTER 8 is used. Then I obtained another curve-fit correlation as shown in Figure 9-2 and Eq. (9-5) between the HPHE length and the number of rows N_L:

$$L = 0.0372 \times N_L \tag{9-5}$$

Again note that Eq. (9-4) and Eq. (9-5) are good only for this design of air-air HPHE ($C_r \approx 1$), the quote in Table 9-1 and the assumptions are used. If the design parameters and/or assumptions change (based on the application and/or restrictions) then one should obtain a new correlations as described above.

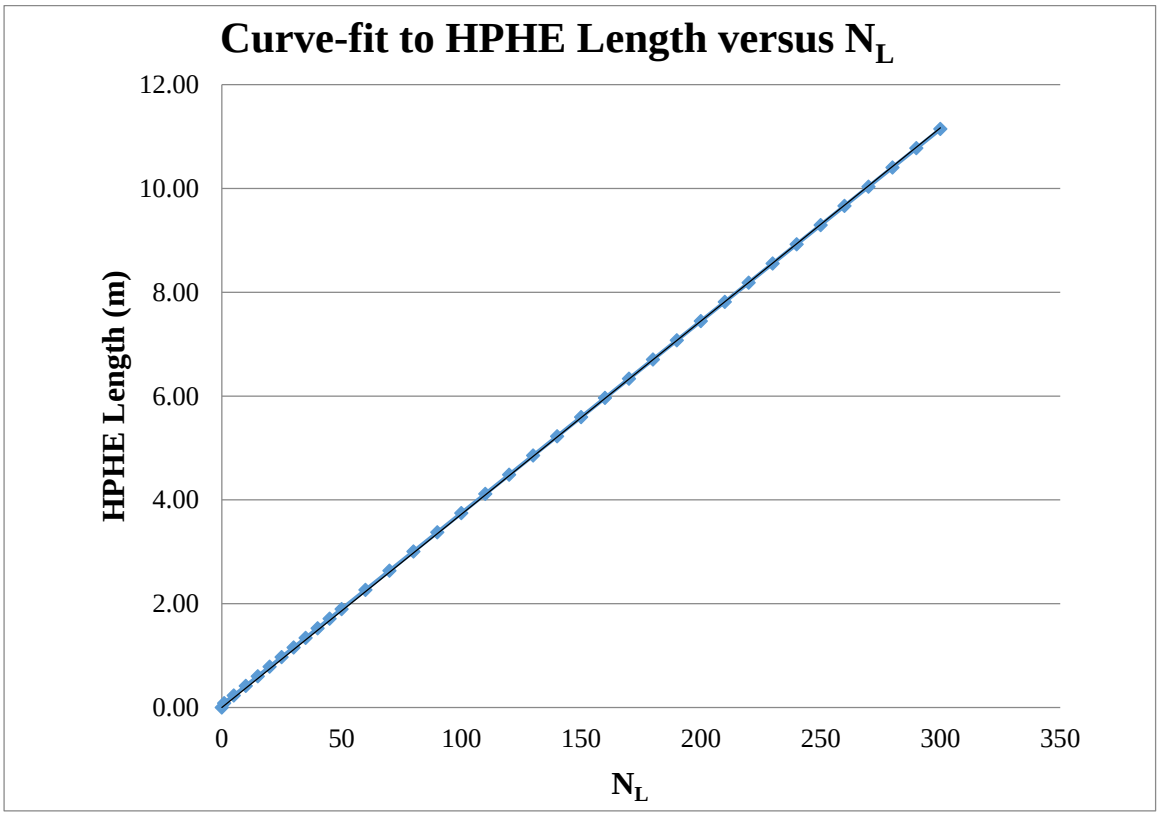

Figure 9-2: Curve-fit correlation for HPHE

Now we have all information to set in our MATLAB code. Both HPHE money back per year and the total cost of HPHE are depending on heat pipe length and we can plot them for different entering exhaust temperatures (T_{hi}). Figure 9-3 shows this plot.

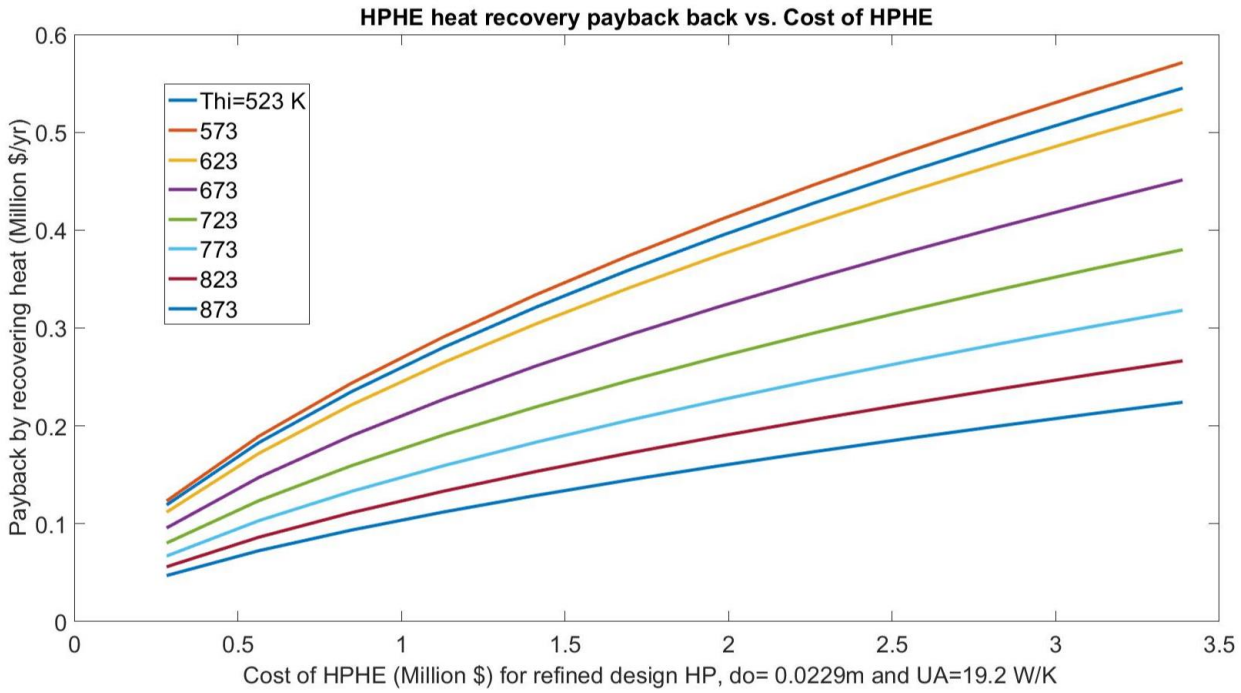

Figure 9-3: HPHE pay back by recovering heat from combusted methane gas versus cost of HPHE at different entering hot exhaust temperatures in the evaporator side of our optimized HPHE

In the code I made for the above figure, the lenghts of HPHE are integer numbers from 1 to 12 meters. As Figure 9-3 shows, if I choose to have longer HPHE the cost of HPHE increases but we can have the earlier payback period.

Based on Figure 9-3 and the design in CHAPTER 8, where the HPHE length is 3.64 m for the effectiveness=0.076, the total number of heat pipes used are 1,455. The cost of HPHE is $1,020,100. Then refer to Figure 9-3 , the pack back is $0.1 million per year and it takes ten years to compensate the investment. If T_{hi} be higher than 232°C, for an instance 450°C, then we can halve the payback period.

In an effort to estimate to released gas from the burner of a digester, we found T_{hi} = 444 °C, then based on the prediction of this chapter for this specific design of the HPHE, we can have the investment back in less than five years.

9.1. Net energy saving

In addition to the cost savings, there is also the potential to reduce the environmental impact of the plant by saving energy and reducing CO_2 emissions. In the favorable air-air HPHE ($C_r \approx 1$) design as presented in CHAPTER 8, the total amount of heat recovery is 349,000 watts. This value is the energy *saving* only and there also would be an energy requirement to manufacture the HPHE. Therefore,

Net energy saving = (energy recovery in HPHE) – (energy used to manufacture HPHE)

The net energy savings corresponds to a reduction in CO_2 emissions. Determining the net energy savings and corresponding CO_2 emission reduction could be a topic for future research.

CHAPTER 10

10. Conclusions

This dissertation has investigated the opportunities for heat recovery at treatment plants. There are opportunities at different places in the plant, specifically in anaerobic digesters and our focus is the digester.

There are some points regarding the heat recovery in a WWTP as follows:

1. Heat exchangers in treatment plants are troublesome (clogging) and costly (maintenance difficulties).
2. Since sludge flow is abrasive, in conventional heat exchangers corrosion and erosion occurs. This problem could be fixed but not completely, by selecting other metallurgies such as stainless steel.
3. In spiral heat exchangers engineers use materials that resist abrasion but still there is another issue remaining which is clogging that makes this type of heat exchanger undesirable.

By designing the heat pipes and then inserting them in the HPHE, we could gather useful results about the heat pipe and the HPHE design and the conditions under which their use is favorable:

1. As the order of magnitude comparisons of the thermal resistances inside a heat pipe clarifies, the thermal resistance of the heat pipe wall is not a limiting factor and then we can select a corrosion and erosion resistant material for the heat pipe wall, even if it is not a good conductor as copper. Chi 1976 provides some data for metals which are compatible with methanol (working fluid inside our heat pipe) and the information

given is a good start to the heat pipe design. Among those variety of metals, stainless steel 304 is an optimum selection.

2. Regarding the maintenance of HPHE, heat pipes usually have long life-time and they do not break easily during the operation. Also HPHE box could be designed somehow that the heat pipe can be removed and replaced from top of the heat exchanger box with removing some screws and light weighted flanges (that hold heat pipes vertical in heat exchanger); compared to heavy inaccessible flanges in other conventional heat exchangers. That is the reason HPHE maintenance is expected to be easier.
3. The heat pipe damages rarely happen and non-working pipes could be left in the box, because few damaged heat pipes in quite large number of them do not have a noticeable effect on the performance of HPHE.
4. To understand if a HPHE works favorably in a specific application, we should analyze the thermal resistances for the heat pipes exposed to the external flows in the HPHE system.
5. If the thermal resistances of external flows over the heat pipes are higher than the thermal resistance inside the heat pipe, then it means that the increased heat transfer area of a HPHE by using heat pipes is beneficial. In such a case, using HPHE would be favorable.
6. If the vice versa applies, then using heat pipes in a heat exchanger cannot improve the heat exchange between the hot and the cold streams.
7. For the particular conditions investigated in this work, we found that if both fluids are air, then the HPHE is beneficial, but it should not be misunderstood that is the only case HPHE is favorable. Since the external thermal resistances depend on the flow rates and

dimensions, it is possible to have large external resistances no matter what the fluid is, and in that case the HPHE could be beneficial.

8. Heat pipe heat exchangers represent a new opportunity to recover energy from the effluent of digesters without any moving parts. Although in this study water-water HPHE is not comparable to spiral heat exchanger with similar effectiveness and width (numerous heat pipes needed in HPHE box that makes it long) but at least HPHE is a less troublesome way to recover energy and this substitute method can be used to recover part of the energy from the digested sludge.
9. In HPHE system if heat is expected to be recovered from gas, instead of liquid for both condenser and evaporator sides (Table 6-5), then HPHE competes with spiral heat exchanger and can deliver the same amount of heat within considerably shorter length.

10.1. Applications of gas-gas HPHE in the WWTP

1. Air-air (gas-gas) HPHE has plenty of applications in WWTP namely in aeration tank to recirculate the gas and pre-heat the entering gas to aeration system.
2. In another application in an aeration tank, the gas inside the tank has 100% relative humidity, the exhausted gas flowing to HPHE not only circulates and pre-heats the entering gas to the tank, but also condenses simultaneously in HPHE.
3. In another application in digesters, methane gas is burning to run gas engines, but the exhaust gas of the engine is too hot, noisy and pollutant. HPHE could be installed in the hot exhaust gas line to recover energy (cool down) and then pre-heat the inlet to the gas-engine to save electricity. On the other hand the energy recovered by the hot exhaust gas can run a turbine to generate electricity or to provide heat inside the

buildings; the latter method is practiced in some large treatment plants, by using conventional heat exchangers.

4. HPHEs can pay back the invested capital in few years (in the case which was studied in this dissertation, it is about five years) with saving electricity and even providing energy for turbines or gas engines to generate electricity.

APPENDIX

A. Heat pipe design literature

The materials in this appendix are all from the literatures (Chi, 1976, Peterson, 1994, etc.) and the details on the design of a heat pipe are explained.

A.1. Surface Tension and Wettability

To analyze and understand the operation of a heat pipe, first it is necessary to understand the liquid-surface interface behavior. Figure A-1 schematically shows how the densities of liquid and vapor are varied at the interface.

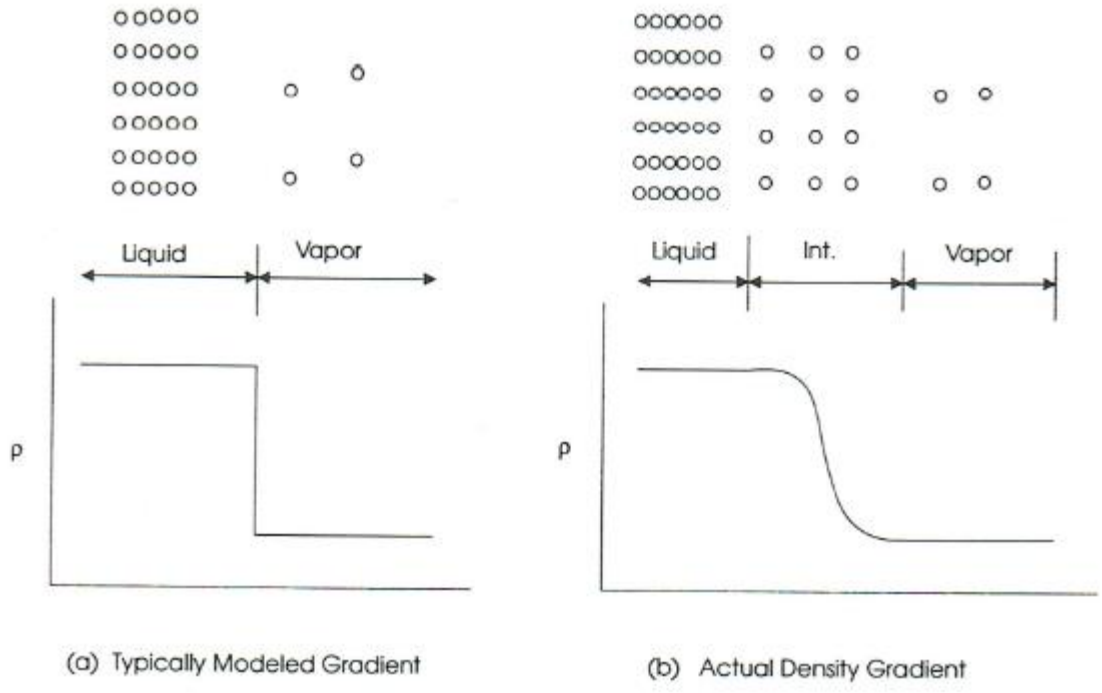

Figure A-1: Density variation at the liquid-vapor interface (Peterson, 1994)

The non-equilibrium conditions between the evaporator and condenser liquid-vapor interfaces are responsible for the operation of heat pipes. As shown in Figure A-2, vaporization from a liquid-

vapor interface causes the liquid meniscus to recede into the wicking structure. In the other side of a heat pipe, the condensation results in a liquid meniscus which has significantly greater radius of curvature than the curvature of the interface when it is in equilibrium. This difference in the radius of curvature in evaporator and condenser interfaces provides the capillary pumping pressure necessary for the heat pipe operation. These phenomena are shown in Figure A-2 below.

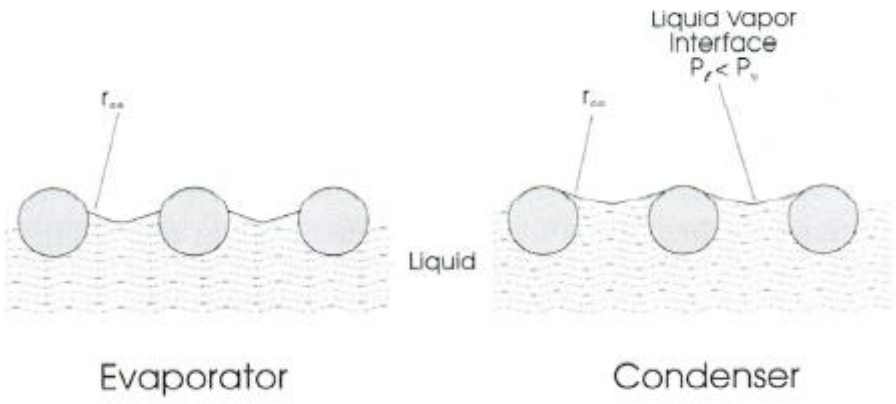

Figure A-2: Non- equilibrium conditions occurring in the evaporator and condenser of a heat pipe (Peterson, 1994).

A.1.1. One-dimensional Vapor pressure drop

As was shown the details and correlations for vapor flow pressure drop in CHAPTER 4, the theory behind liquid flow pressure drop is explained in this appendix.

A.1.2. Liquid pressure drop ΔP_l

Similar to the vapor pressure drop, the liquid pressure gradient is also the result of the combined effects of both viscous and inertial forces. The viscous forces in the liquid results in a pressure drop dP_l/dx and this phenomena resists the capillary flow through the porous wick. Because the liquid pressure gradient may vary along the longitudinal axis of the heat pipe, the total

liquid pressure drop is the integrate of the pressure gradient over the length of the flow passage, or

$$\Delta P_l(x) = -\int_0^x \frac{dP_l}{dx} dx \tag{A-1}$$

and the pressure gradient is resulting from frictional drag (Chi, 1976). The frictional drag is due to the shear stress

$$\frac{dP_l}{dx} = -\frac{2\tau_l}{r_{h,l}} \tag{A-2}$$

where τ_l is the frictional shear stress at liquid-solid interface and $r_{h,l}$ is the liquid hydraulic radius.

Now the Reynolds number and drag coefficient in the liquid flow in the heat pipe can be defined as below

$$Re_l = \frac{2r_{h,l}\,\rho_l v_l}{\mu_l} \tag{A-3}$$

$$f_l = \frac{2\tau_l}{\rho_l v_l^2} \tag{A-4}$$

where v_l is the local liquid velocity and is related to local heat flow rate and is defined as :

$$v_l = \frac{q}{\epsilon A_w \rho_l \lambda} \tag{A-5}$$

In Eq. (A-5) A_w is the wick cross-sectional area and ϵ is the wick porosity.

Replacing the previous equations into the liquid pressure drop, yields:

$$\frac{dP_l}{dx} = \left(\frac{(fRe)_l\,\mu_l}{2\epsilon A_w (r_{h,l})^2 \lambda \rho_l} \right) q \tag{A-6}$$

or it could be written as

$$\frac{dP_l}{dx} = \left(\frac{\mu_l}{KA_w \lambda \rho_l} \right) q \tag{A-7}$$

In Eq. (A-7), K is Permeability (see Table 4-1) and is defined as the property of the porous material (wick) which shows the ability of the material to transfer the liquid under some applied pressure gradient. Permeability is a function of the shape of the flow path and is expressed as

$$K = \frac{2 \in (r_{h,l})^2}{(fRe)_l} \tag{A-8}$$

For constant heat addition and removal, Eq. (A-7) could be written as

$$\Delta P_l = \left(\frac{\mu_l}{KA_w \lambda \rho_l} \right) q \, L_{eff} \tag{A-9}$$

where L_{eff} is the effective length of the heat pipe.

A.2. Heat pipe operating limits

There are several limitations that control the axial heat transport capacity of a heat pipe. These limits are called viscous, sonic, entrainment and boiling limits.

To evaluate the maximum heat transfer capacity, we have to choose the smallest heat transfer rate among all heat transport limits and call it q_{limit}.

A.2.1. Viscous limitation

At very low operating temperature of a heat pipe or a thermosyphon, the vapor pressure difference between the evaporator and the condenser regions may be too small. In some cases, the viscous forces within the vapor region are much larger than the pressure gradients due to temperature field. In such conditions, the pressure gradients within the vapor region may not be

sufficient to push the vapor flow forward and results in vapor stagnation. The stagnation of vapor flow is called the viscous limitation.

The viscous limit might happen in cryogenic heat pipes, or heat pipes with long condenser region, or heat pipes undergoing start up from a frozen state.

To formulate viscous limitation, let's assume an isothermal vapor and ideal gas behavior of the vapor in two-dimensional model of the vapor flow. Then the radial velocity component is a significant factor in determining the maximum axial heat transfer to reach the viscous limit:

$$q_v = \frac{A_v r_o^2 \lambda \rho_v P_v}{16 \mu_v L_e} \tag{A-10}$$

where r_o is the outer radius of heat pipe, ρ_v and P_v are the vapor density and pressure at the evaporator end respectively.

A.2.2. Sonic limitation

Modeling sonic limitation in a heat pipe is similar to a compressible flow in a duct of constant cross-section with mass addition and removal, and a constant mass flow in a duct with variable cross-section. Figure A-3 shows the mass flow rate and pressure distribution as a function of axial position of a heat pipe.

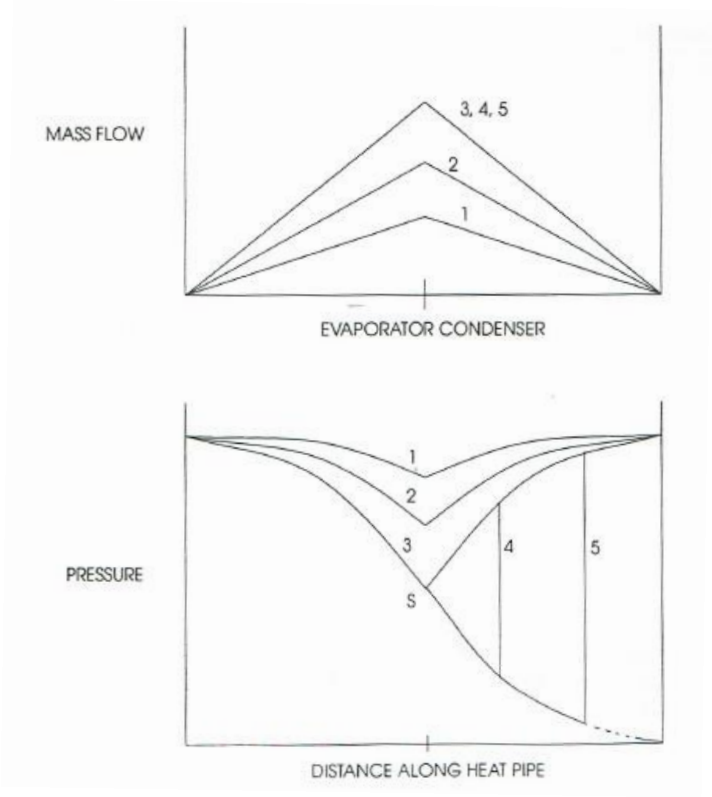

Figure A-3: Axial pressure distribution and mass flow in a heat pipe (Peterson, 1994)

As shown in Figure A-3, if the thermal load is increased more and more, the vapor velocity at the end of evaporator reaches the velocity of the sound (point S on the curve 3). Then further reduction of the condenser pressure will not result in any increase in the mass flow rate, and this is the condition that the shock wave will form (curve 4).

Curve 5 shows wave forming during the startup phase of a heat pipe and then the wave slowly progresses upstream and gets weaker until it eventually disappears.

Similar to above situation might happen in a heat pipe. The sonic limitation is an upper bound to the axial heat transport capacity and does not necessarily result in dry-out of the evaporator wick or total heat pipe failure but it should be considered.

A.2.3. One-dimensional gas flow sonic model

Similar to ideal behavior of gas flow in a duct, let's assume that the frictional effects in a heat pipe are negligible, then we use conservation of energy and momentum to evaluate the temperature and the pressure ratios of stagnation to static states,

$$\frac{T_o}{T_v} = 1 + \frac{v_v^2}{2c_p T_v} \tag{A-11}$$

$$\frac{P_o}{P_v} = 1 + \frac{\rho_v v_v^2}{2P_v} \tag{A-12}$$

where "o" and "v" indicate the stagnation and static states. The velocity of vapor flow is

$$v_v = \sqrt{\gamma_v R_v T_v} \tag{A-13}$$

If we combine the above equations and relate them to the axial heat load, it yields an expression for the axial heat transfer in terms of physical properties. At sonic velocities, Mach number is 1, and then the maximum axial heat transport prior to onset of the choked flow is obtainable:

$$q_{s,max} = A_v \rho_o \lambda \sqrt{\frac{\gamma_v R_v T_o}{2(\gamma_v + 1)}} \tag{A-14}$$

Although this expression intended for use at the end of the evaporator region, but it is still valid for the condenser section of the heat pipe.

For the vapor-flow at high Mach numbers, the temperature distribution of liquid-vapor interface along the entire length of a heat pipe is obtainable from Eq. (A-11) and (A-14).

A.2.4. Entrainment limitation

Because in a heat pipe, the liquid and vapor move in the opposite directions, there is a shear force at the liquid-vapor interface. If heat input in evaporator increases, then the vapor velocity

becomes high enough to tear the liquid from the surface of the wick and the liquid entrains in the vapor. The entrainment results in dry-out of the evaporator wicking structure.

Entrainment equations developed for heat pipes and thermosyphons are different and the completed details are given in Peterson's textbook (Peterson, 1994).

A method had been offered to determine the entrainment limitation in a heat pipe (refer to Peterson, 1994 for more details) utilizes the Weber number and then related the vapor velocity and the heat transport capacity to the heat flux:

$$We = \frac{2 r_{h,w} \rho_v v_v^2}{\sigma} \tag{A-15}$$

where v_v in Eq. (A-15) is vapor velocity that could be also defined as

$$v_v = \frac{q}{A_v \rho_v \lambda} \tag{A-16}$$

To prevent entrainment of liquid droplets into the vapor flow, the Weber number must be less than unity, and then the maximum transport capacity of the entrainment is obtainable

$$q_{e,max} = A_v \lambda \sqrt{\frac{\sigma \rho_v}{2 r_{h,w}}} \tag{A-17}$$

where $r_{h,w}$ is the hydraulic radius of the wick surface pores. For the screen mesh wick, $r_{h,w}$ is half of the wire spacing, for groove wicks it is equal to the width of the groove and for packed spheres it is 0.41 of the sphere radius (Chi, 1976).

A.2.5. Boiling limitation

In an operating heat pipe, for high enough heat flux in the evaporator section, nucleate boiling may occur in the wicking structure which makes the bubbles be trapped in the wick. These bubbles block the liquid to return to condenser and result in evaporator dry-out. This pheromone is called boiling limitation.

In spite of other limitations studied previously that all depend on the axial heat transfer rate, the boiling limitation depends on the radial or circumferential heat flux applied to the evaporator.

The boiling limit could be formulated based on nucleate boiling theory which consists of two phenomena: bubble formation and growth or collapse of the bubble. Bubble formation depends on the number and size of nucleation sites on a solid surface as well as the temperature difference between the heat pipe wall and the working fluid. This temperature difference which is superheat temperature, controls the bubbles formation and can be defined in terms of the maximum heat transfer rate

$$q_{max} = \left(\frac{k_{eff}}{T_w} \right) \Delta T_{cr} \tag{A-18}$$

where k_{eff} is the effective thermal conductivity of the liquid-wick combination, T_w is heat pipe wall temperature and ΔT_{cr} is the critical superheat temperature

$$\Delta T_{cr} = \left(\frac{T_{sat}}{\lambda \rho_v} \right) \left(\frac{2\sigma}{r_n} - \Delta P_{cm} \right) \tag{A-19}$$

In Eq. (A-19) T_{sat} is the saturation temperature of the fluid and r_n is the critical nucleation site radius. According to Dunn and Reay (1982), for a conventional metallic heat pipe case material, r_n can be in the order of 10^{-6} to 10^{-5} inches (2.54×10^{-8} to 2.54×10^{-7} meter) (Peterson, 1994).

The growth or collapse of a bubble on a flat or planar surface is directly dependent on the corresponding temperature and pressure difference of the liquid across the liquid-vapor interface. This pressure difference is caused by the vapor pressure and surface tension of the liquid.

By performing a pressure balance on any given bubble and using Clausius-Claperyon equation $\left(\frac{dP}{dT} = \frac{\lambda \rho_v}{T_v} \right)$ to relate the temperature and pressure, we can obtain an expression for the boiling heat transfer limit for bubble growth. This expression is a function of the fluid properties:

$$q_{b,max} = \left(\frac{2\pi L_e k_{eff} T_v}{\lambda \rho_v \ln\left(\frac{r_i}{r_v}\right)} \right) \left(\frac{2\sigma}{r_n} - \Delta P_{cm} \right) \tag{A-20}$$

where r_i is the inner radius of the heat pipe wall and r_n is the nucleation site radius. The appropriate correlations for k_{eff} could be found in Table A-1.

Table A-1: Effective thermal conductivity (k_{eff}) for liquid-saturated wick (Chi, 1976)

Wick Structures	k_e
Wick and liquid in series	$\frac{k_l k_2}{\epsilon k_w + k_l(1-\epsilon)}$
Wick and liquid in parallel	$\epsilon k_l + k_w(1-\epsilon)$
Wrapped screen	$\frac{k_l[(k_l+k_w)-(1-\epsilon)(k_l-k_w)]}{(k_l+k_w)+(1-\epsilon)(k_l-k_w)]}$
Packed spheres	$\frac{k_l[(2k_l+k_w)-2(1-\epsilon)(k_l-k_w)]}{(2k_l+k_w)+(1-\epsilon)(k_l-k_w)}$
Rectangular grooves	$\frac{(w_f k_l k_w \delta)+wk_l(0.185w_f k_w+\delta k_l)}{(w+w_f)(0.185w_f k_w+\delta k_l)}$

A.2.6. Iteration of $q_{c,max}$ for turbulent vapor flow ($Re_v > 2300$) and $M_v \leq 0.2$

When the vapor flow is turbulent and $M_v \leq 0.2$, calculating the maximum capillary limit is not straightforward and it needs to solve a non-linear equation. According to (Chi, 1976), the pressure gradients in vapor and liquid phases are derived as

$$\frac{dP_v}{dx} = +F_v q - D_v \frac{dq^2}{dx} \tag{A-21}$$

$$\frac{dP_l}{dx} = -F_l q \pm \rho_l g \sin \Psi \tag{A-22}$$

which in Eq. (A-22), the second term $\left(\pm \rho_l g \sin\psi\right)$ sign should be selected carefully:

- '+' sign is for when the liquid flows in a direction with gravity
- '-' sign is for the case when the liquid flows in a direction against gravity

Based on Figure A 4, for the liquid and vapor pressure distributions in a heat pipe, the maximum effective capillary pressure can be written as:

$$P_{cm,eff} = \int_0^{L_{tot}} \left(\frac{dP_v}{dx} - \frac{dP_l}{dx} \right) dx \tag{A-23}$$

Now replace the appropriate correlations for $\frac{dP_l}{dx}$ and $\frac{dP_v}{dx}$ from Eq. (A-21) and (A-23) in the above equation:

$$P_{cm,eff} = \int_0^{L_{tot}} \left\{ \left(+ F_v q - D_v \frac{dq^2}{dx} \right) - \left(- F_l q \pm \rho_l g \sin \Psi \right) \right\} dx \tag{A-24}$$

Note: For the gravity aided heat pipes design $\left(+ \rho_l g \sin \Psi\right)$ is used, as it has been done in this study.

The second term in Eq. (A-24) is simplified (refer to Chi, 1976 for more details),

$$\int_0^{L_{tot}} \left(D_v \frac{dq^2}{dx} \right) dx = 0$$

And Eq. (A-24) will be simplified as follows:

$$P_{cm,eff} = \int_0^{L_{tot}} \left\{ \left(F_v + F_l \right) q - \left(\pm \rho_l g \sin \Psi \right) \right\} dx \tag{A-25}$$

Within the preliminary calculations, it is found that $Re_v > 2300$ and $M_v \le 0.2$, then for *incompressible turbulent* flow of vapor, vapor frictional coefficient should be used (refer to Kraus and Bar-Cohen, 1983 results in CHAPTER 4),

$$F_v = \frac{0.019\,\mu_v}{A_v r_{h,v}^2 \rho_v \lambda}\left(\frac{2 r_{h,v} q}{A_v \lambda \mu_v}\right)^{3/4} \tag{A-26}$$

The above equation could be rewritten as

$$F_v = A \times (B)^{3/4} \times (q)^{3/4}$$

where $A = \dfrac{0.019\,\mu_v}{A_v\, r_{h,v}^2\, \rho_v\, \lambda}$ and $B = \dfrac{2\, r_{h,v}}{A_v \lambda\, \mu_v}$.

Now each term of Eq. (A-25) is integrated separately. Assuming that properties of fluids and liquid are constant and are independent of the length of the condenser and the evaporator, the first term of Eq. (A-25) becomes

$$P_{cm,eff} = \int_0^{L_{tot}} F_v q\, dx = A \times (B)^{3/4} \int_0^{L_{tot}} (q)^{7/4}\, dx$$

Assuming that the heat transfer rate distribution (q) along the heat pipe is uniform and is independent of the x (location), then

$$\int_0^{L_{tot}} F_v q\, dx = F_v q\, L_{tot}$$

similarly in the second term of Eq. (A-25)

$$\int_0^{L_{tot}} F_l q\, dx = F_l q\, L_{tot}$$

and the third term becomes

$$\int_0^{L_{tot}} -(\pm \rho_l g \sin\psi) dx = -(\pm \rho_l g \sin\psi)\, L_{tot}$$

Finally all of the terms in the Eq. (A-25) are replaced,

$$P_{cm,eff} = \left\{\left(F_v + F_l\right)q - \left(\pm \rho_l g \sin \Psi\right)\right\} L_{tot} \tag{A-27}$$

If a heat pipe is operating in a gravitational field where the circumferential communication of liquid within the liquid is possible, the maximum effective capillary pressure $P_{cm,eff}$ available for axial transport of fluid will be smaller than the maximum capillary pressure from equation $P_c = \frac{2\sigma}{r_c}$. This decrease is due to the gravitational force in the direction perpendicular to the heat pipe axis that is

$$P_{cm,eff} = \frac{2\sigma}{r_c} - \Delta P_{\perp}$$

Note: If a heat pipe is gravity assisted, then we will have positive value for $\rho_l g \sin\psi$ as we have in this study. Now we can rewrite Eq. (A-27)

$$\frac{P_{cm,eff}}{L_{tot}} + \left(\pm \rho_l g \sin \Psi\right) = \left(F_v + F_l\right)q \tag{A-28}$$

Then we can calculate the q from Eq. (A-28):

$$q = \left\{\frac{\frac{2\sigma}{r_c} - \Delta P_{\perp}}{L_{tot}} + \left(\pm \rho_l g \sin \Psi\right)\right\} \frac{1}{\left(F_v + F_l\right)}$$

or

$$q = \left\{\frac{\frac{2\sigma}{r_c} - \Delta P_{\perp}}{\frac{L_{tot}}{\left(A \times (B)^{3/4} \times (q)^{3/4}\right) + F_l}} + \left(\pm \rho_l g \sin \Psi\right)\right\} \tag{A-29}$$

where in the non-linear Eq. (A-29), q is the only unknown and note that it is assumed that q is uniform through the length of the heat pipe. This q is called $q_{c,max}$ and if this is the smallest value

among all heat pipe heat transfer limitations, it is called q_{limit} (maximum heat capacity of the heat pipe).

In this study the heat pipe is designed to be oriented vertically, therefore $\psi = 90$. In Eq. (A-29), $q_{c,max}$ is obtained *iteratively*. After iteration with known total length of the heat pipe that in this study is L_{tot}=1.07 (m), then $q_{c,max}$ is evaluated as 798 (W) (refer to Table 4-5). In the heat pipe designed in this dissertation, $q_{c,max}$ is q_{limit}.

REFERENCES

1. Abdel-Aal, M., Smits, R., Mohamed, M., De Gussem, K., Schellart, A. and Tait, S., '*Modeling the viability of heat recovery form combined sewers'*, School of Engineering Design and Technology, University of Bradford & Sheffield, UK and Department of Research, Belgium. Water Science and Technology, 2014
2. Baek, N.C., Shin, U. C., and Yoon, J. H., '*A study on the design and analysis of a heat pump heating system using wastewater as a heat source'*. Solar Thermal Research Center, Korea Institute of Energy. Solar Energy, 2004
3. Bergman, T., Lavine, A.S. , Incropera, F., and DeWitt, D., textbook, '*Fundamentals of heat and mass transfer*', 7th edition, John Wiley & Sons, Inc.
4. Bruno, J.C., Lopez, V.O., and Coronas, A., *'Integration of absorption cooling systems into micro gas turbine trigeneration systems using biogas: Case study of a sewage treatment plant'*, Journal of Applied Energy, 2008
5. Cakira, F.Y., Stenstrom, M.K., *'Greenhouse gas production: A comparison between aerobic and anaerobic wastewater treatment technology'*, University of Florida and University of California Los Angeles, Water Research 39, pp.4197–4203, 2005
6. Chaudourne, S. , '*Modeling and optimization of heat pipe heat exchangers*', France, 1984
7. Chi, S. W., '*Heat Pipe Theory and Practice'*, A sourcebook. Series in thermal and fluids engineering. The George Washington University, McGraw-Hill Book Company, 1976
8. Dunn, P. D., and Reay, D. A., '*Heat pipes*', 3rd edition, Pergamon, New York, USA, 1982
9. Dürrenmatt, D.J. and Wanner, O., '*A mathematical model to predict the effect of heat recovery on the wastewater temperature in sewers'*, Swiss Federal Institute of Aquatic Science and Technology. Water Research 48, pp.548-558, 2014
10. Dürrenmatt D.J. and Wanner, O., '*Simulation of the wastewater temperature in sewers with TEMPEST',* Water Science Technology, 2008
11. Huang, B.J., Tsuei, J.T, , '*A method of analysis for heat pipe heat exchangers*', International Journal of Heat and Mass Transfer, Vol. 28, No.3, pp.553-562, 1985
12. Hyperion Treatment Plant Monthly Report, Operations Section, February 2014

13. Jafari, D., Shamsi, H., Filippeschi, S., Marco, P.D., Franco, A, '*An experimental investigation and optimization of screen mesh heat pipes for low-mid temperature applications*', Experimental Thermal and Fluid Science 84, pp.120 –133, 2017
14. Kraus, A.D., Bar-Cohen, A, '*Thermal Analysis and Control of Electronic Equipment*', Hemisphere Publishing Corporation, 1983
15. Matos, R.S., Vargas, J.V.C., Laursen, T.A., Bejan, A., '*Optimally staggered finned circular and elliptic tubes in forced convection*', International Journal of Heat and Mass Transfer, 47,pp. 1347–1359, 2004
16. Metcalf and Eddy, '*Wastewater Engineering, Treatment and Reuse'*, 4th edition, 2003
17. Peterson, G. P., '*An introduction to heat pipes, Modeling, Testing and Applications'*, Wiley series in thermal management of microelectronic and electronic systems. The Department of Mechanical Engineering, Texas A&M university College Station, John Wiley and Sons, INC, USA, 1994
18. Shukla, K. N., '*Heat Pipe for Aerospace Applications—An Overview'*, Journal of Electronics Cooling and Thermal Control, 2015
19. Stanescu, G., Fowler, A. J. and Bejan, A., '*The optimal spacing of cylinders in free-stream cross-flow forced convection*', International Journal of Heat and Mass Transfer. Vol. 39, No. 2, pp. 311-317, 1996
20. Tan, J.O., Liu, C.Y., , '*Predicting the performance of a Heat pipe heat exchanger, using the effectiveness- NTU method*', International Journal of Heat and Mass Transfer, Vol. 11, No.4, pp.376-379, 1990
21. Tan, J.O, Liu, C.Y., and Wong, Y.W., '*Heat Pipe Heat Exchanger Optimization*', Heat Recovery Systems and CHP, Vol. 11, No. 4, pp. 313-319, 1991